THE RELATIONSHIP BETWEEN NONENZYMATIC GLYCATION OF LENS CRYSTALLINS AND DIABETIC CATARACT FORMATION

by

Ronald E. Perry

Submitted to the Faculty of the School of Graduate Studies of the Medical College of Georgia in Partial Fulfillment of the Requirements for the Degree of

Doctor of Philosophy

March

1986

THE RELATIONSHIP BETWEEN NONENZYMATIC GLYCATION OF LENS CRYSTALLINS AND DIABETIC CATARACT FORMATION

This dissertation submitted by Ronald E. Perry has been examined and approved by an appointed committee of the faculty of the School of Graduate Studies of the Medical College of Georgia.

The signatures which appear below verify the fact that all required changes have been incorporated and that the dissertation has received final approval with reference to content, form and accuracy of presentation.

This dissertation is therefore accepted in partial fulfillment of the requirements for the degree of Doctor of Philosophy.

3/4/86
Date

[redacted]
Advisor

[redacted]
Department Chairman

[redacted]
Dean, School of Graduate Studies

ACKNOWLEDGEMENT

This work is dedicated to my parents Charles and Barbara, and to my sister Rhonda whose unwavering confidence and support made my achievement of a higher degree possible.

I would like to thank my major advisor, Dr. E. C. Abraham for the unique opportunity of pursuing my own research interests. His patience and guidance are greatly appreciated and I believe we have both benefited from our association. I would also like to express my appreciation to Dr. Alan Costoff for his generous gift of animals and supplies throughout my studies, and to Dr. Brooke Webber for his assistance in the amino acid analysis of the lens proteins and subunits.

TABLE OF CONTENTS

LIST OF FIGURES

LIST OF TABLES

LIST OF ABBREVIATIONS

HMW	High Molecular Weight
Glc	Glucose
Glc-Lys	Glycated Lysine
pCMB	para-Chloromercuric Benzoic Acid

Amino Acid Abbreviations

Ala	Alanine
Arg	Arginine
Asn	Asparagine
Asp	Aspartate
Cys	Cysteine
Gln	Glutamine
Glu	Glutamate
Gly	Glycine
His	Histidine
Ile	Isoleucine
Leu	Leucine
Lys	Lysine
Met	Methionine
Phe	Phenylalanine
Pro	Proline
Ser	Serine
Thr	Threonine
Trp	Tryptophan
Tyr	Tyrosine
Val	Valine

INTRODUCTION

Statement of the Problem

Prolonged elevation of blood glucose in diabetes mellitus results in a number of sequelae including peripheral nerve damage, kidney damage, arteriosclerosis, retinopathy, and cataracts (1). The complications of diabetes are all related directly or indirectly to insulin-independent tissues wherein cellular glucose levels reflect the increased blood glucose levels. This increased cellular glucose concentration results in an increase in non-enzymatically glycated proteins. This is a post-translational modification which results when the acyclic form of glucose reacts with the ε-amino group of lysines or the amino terminus of a protein. This reaction results in a Schiff-base intermediate which undergoes an Amadori rearrangement to form a stable and practically irreversible ketoamine structure. This modification is dependent on the glucose concentration and protein half-life (2). The proteins of the lens are extremely long lived and turn over very slowly or not at all, which provides for great opportunities for posttranslational modifications (3). The crystallins have been shown to undergo several types of posttranslational modifications, among which are C-terminal degradation, deamination, oxidation, aspartic acid racemization, and non-enzymatic glycation (4-8). It has been hypothesized that the lens proteins become water-insoluble and aggregate to form large high molecular weight particles that scatter light, producing lens opacities (cataracts) (9). It is not yet known which of the posttranslational modifications are normal and which are associated with the lens proteins becoming water-insoluble. This study was designed to determine the relationship between non-enzymatic glycation of lens crystallins and the formation of large

insoluble high molecular weight aggregates. The progressive changes in glycated protein levels, disulfide bond formation and the formation of HMW protein aggregates were studied in streptozotocin induced diabetic rats. Also, the extent of non-enzymatic glycation of the lens crystallins and their subunits were examined in both control and diabetic cataract lenses. Furthermore, the insoluble HMW components were identified and their extent of glycation was characterized.

Review of Related Literature

Diabetes and Its Sequelae

Diabetes, because of its frequency, is probably the most important metabolic disease. It affects every cell in the body, and the essential biochemical processes that go on there. Diabetes has been a medical problem since antiquity, and one which in the United States now ranks eighth as a cause of death (10). The name "diabetes" was originated by Aretaeus (30 to 90 A.D.) and comes from the Greek words meaning "siphon" and "to run through", and in medicine signifies the chronic excretion of an excessive volume of urine. The qualifying word, mellitus, is Latin meaning "honeyed" or "sweet." Hence, diabetes mellitus is a disease associated with copious sweet urine (1).

The fundamental problem of diabetes is a relative lack of functional insulin, the hormone produced in the islets of Langerhans of the pancreas. This lack of insulin is responsible for an inappropriate elevation in blood glucose levels due to the inability of glucose to enter insulin dependent tissues such as muscle and adipose.

Diabetes mellitus is a chronic disorder characterized by a number of sequelae. Diabetes is the leading cause of new blindness, and diabetics are twice as likely to develop heart disease. Other complications involve the kindeys, nervous system, and peripheral blood vessels all of which the severity is inversely proportional to the degree of diabetic glycemic control (10).

Diabetic retinopathy is the leading cause of permanent visual loss in the diabetic patient. Almost all diabetics will develop some form of retinopathy after having had diabetes for 20 years, with 95 percent affected after 30 years. Retinopathy is characterized by the appearance

of new blood vessels on the optic disc or on the surface of the retina. This neovascularization is seen in association with generalized retinal ischemia resulting from a thickening of the capillary basement membrane. These new blood vessels are extremely fragile and prone to hemorrhage and microaneurysms all of which result in scar tissue and retinal detachment (11).

Diabetic patients have an increased incidence, earlier onset, and increased severity of atherosclerosis in the intima and calcification in the media of the arterial wall. Peripheral vascular disease has been estimated to occur 11 times more frequently and to develop about 10 years earlier in diabetics than in nondiabetics. The vessels most likely to be involved are the arteries of the legs, resulting in a 50-fold increase in gangrene of the legs and feet (12).

The same capillary basement thickening found in the retina is also seen in the kidney and the major capillary beds of the skin and muscle. This microvascular disease in the kidney results in glomerular membrane thickening, hypertension, and eventually renal failure (13).

Diabetics also suffer segmental injury to nerves, associated with demyelination and Schwann cell degeneration, involving sensory and motor peripheral nerves and the autonomic nervous system. It is characterized by tremors, loss of coordinated motion, incontenence, and impotence. Affected nerves show basal lamina thickening similar to the capillary abnormalities (14).

The diabetic is four to six times more likely to develop cataracts at a younger age than the normal population. There are approximately 200,000 people with cataracts between the ages of 14 and 44 in the United States. These cataracts occur primarily in diabetics (15). A cataract

is described as any opacity of the crystallin lens that interferes with vision.

In studying the diabetic sequelae, it is of interest to note that tissues with the greatest incidence of diabetic complications (lens, retina, nerve, kidney, blood vessels, red blood cells) are insulin independent and therefore freely permeable to glucose.

The involvement of the insulin-independent tissue in diabetic sequelae has led researchers to examine the effect of increased intracellular glucose on tissue function. Biochemical changes may be responsible for alterations in vascular basement membranes that lead to diabetic microangiopathy (16). One of the first theories put forth involves the polyol (sorbitol) pathway (17). Glucose becomes sorbitol (a sugar alcohol) via the effect of the enzyme aldose reductase. Figure 1 depicts a Schwann cell and the pathways within the cell and shows a subsequent conversion from sorbitol to fructose, in which the enzyme sorbitol dehydrogenase plays a role. It is postulated that sorbitol accumulates and becomes trapped within the Schwann cell. The accumulated sorbitol may be toxic and lead to segmental demyelination and neuropathy. Gabbay et al. (18) has pursued the relationship in neurologic complications by studying the sciatic nerves of diabetic rats. Using enzyme assays they show localization of aldose reductase to the Schwann cell and sorbitol dehydrogenase to the axon. Weingrad and Clements (19) have shown sorbitol accumulation in the alloxan diabetic rabbit aorta and human aorta. Current research in this area involves the development of aldose reductase inhibitors and their effect on diabetic sequelae (20-21).

FIGURE 1. Sorbitol pathway and related metabolism within a Schwann cell.

Modified from Kozak, G. P.: Why treat diabetes? In Levine, R. (ed.), Individualizing Therapy in Maturity Onset Diabetes. New York Science and Medicine Publishing Co., Inc., 1979.

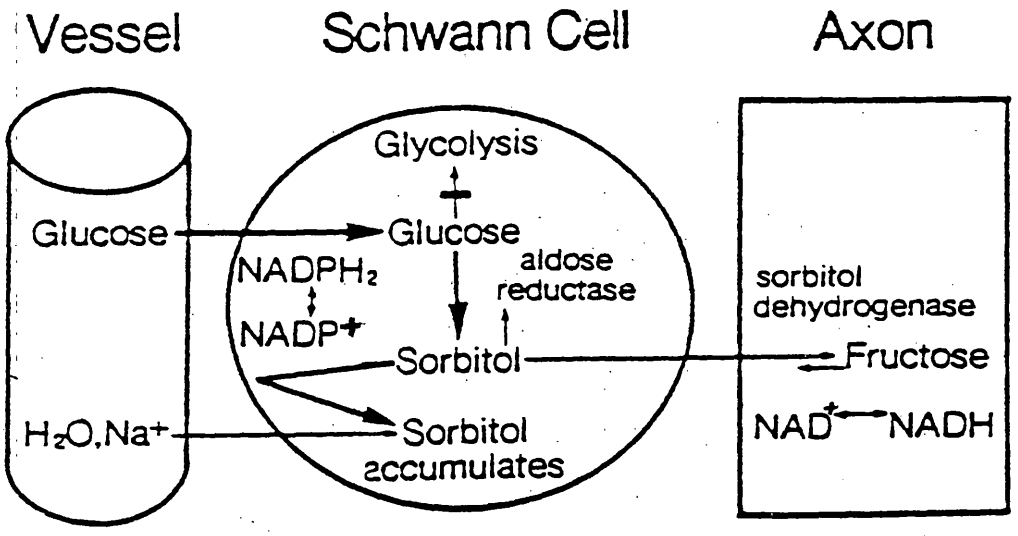
Vessel
Schwann Cell
Axon
Glycolysis
Glucose
Glucose
NADPH₂
NADP+
aldose reductase
sorbitol dehydrogenase
Sorbitol
Fructose
H₂O,Na+
Sorbitol accumulates
NAD+
NADH

FIGURE 2. Pathway from glucose to formation of glycoproteins

Modified from Kozak, G. P.: Why treat diabetes? In Levine, R. (ed.), Individualizing Therapy in Maturity Onset Diabetes. New York Science and Medicine Publishing Co., Inc., 1979.

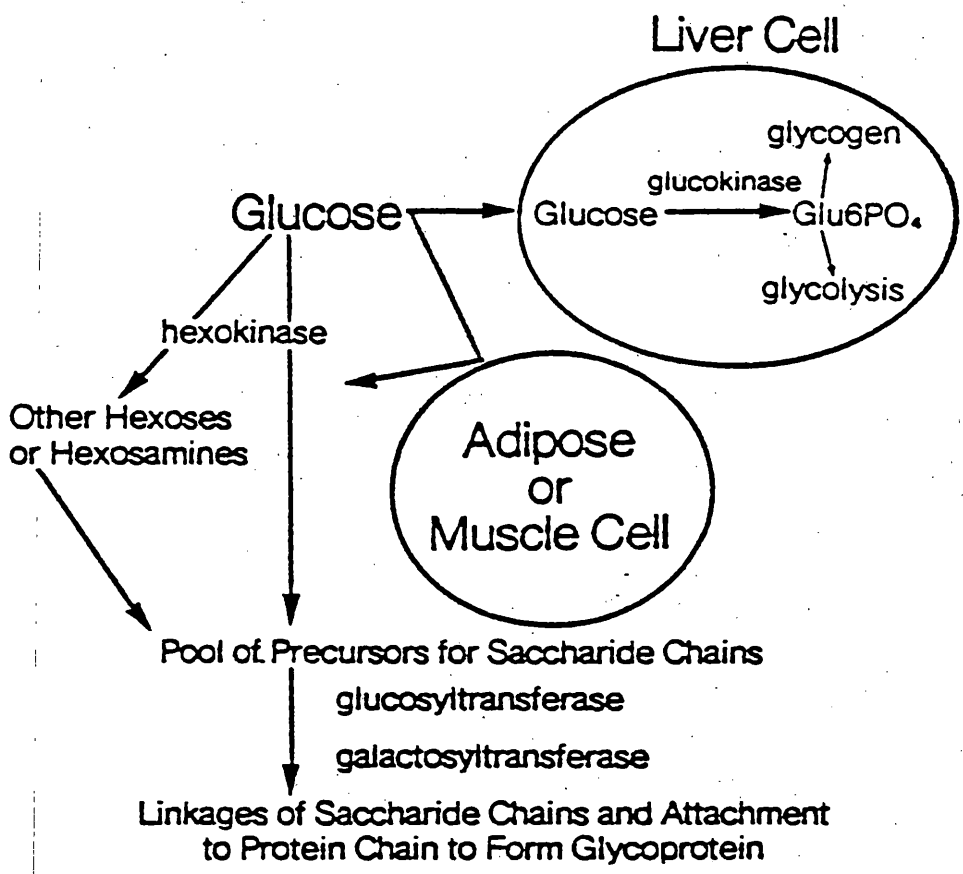
Liver Cell
glycogen
glucokinase
Glucose
Glucose
Glu6PO4
glycolysis
hexokinase
Other Hexoses
or Hexosamines
Adipose
or
Muscle Cell
Pool of Precursors for Saccharide Chains
glucosyltransferase
galactosyltransferase
Linkages of Saccharide Chains and Attachment
to Protein Chain to Form Glycoprotein

Another theory involves an increase in the formation of glycoproteins which are a major component of the basement membrane (22). Figure 2 depicts the pathway for the formation of glycoproteins from glucose and other sugars. These hexoses (or hexosamines or both) are subsequently linked and enzymatically attached to proteins to form glycoproteins. It has become evident that the fundamental morphologic alteration of diabetic microangiopathy involves the thickening of capillary basement membranes (23). The best studied tissue is that of the renal glomerulus. Spiro et al. (24) have studied the relationship of the renal glomerular basement membrane and glycoprotein formation in diabetes mellitus. Their investigations demonstrate an increase in the activity of the enzyme glucosyl transferase in the untreated diabetic kidney cortex. They interpreted this to result in an increase in the deposition of various glycoproteins in the kidney. When animals were treated with insulin at an early stage of diabetes, their glucosyl transferase activity could be returned to normal values.

Non-enzymatic Glycation

Prolonged elevation of blood glucose in diabetes results in an increased level of non-enzymatically glycated protein. This modification results when the ε-amino groups of lysine or the amino terminus of a protein reacts with the acyclic form of glucose to yield a Schiff-base intermediate (Figure 3) (2). This aldimine is readily reversible with the ratio of k_1 to k_{-1} close to one. As hyperglycemia is maintained this intermediate will undergo a practically irreversible Amadori rearrangement to a stable ketoamine derivative. The extent of modification is dependent on the glucose concentration and protein half-life. The insulin independent tissues are directly exposed to the increased ambient

FIGURE 3. Reaction scheme for non-enzymatic glycation

Briefly, glucose reacts with a free amino terminus or ε-amino group of lysine to form the reversible aldimine. As glucose concentrations are maintained the aldimine undergoes an Amadori rearrangement to the stable ketoamine structure.

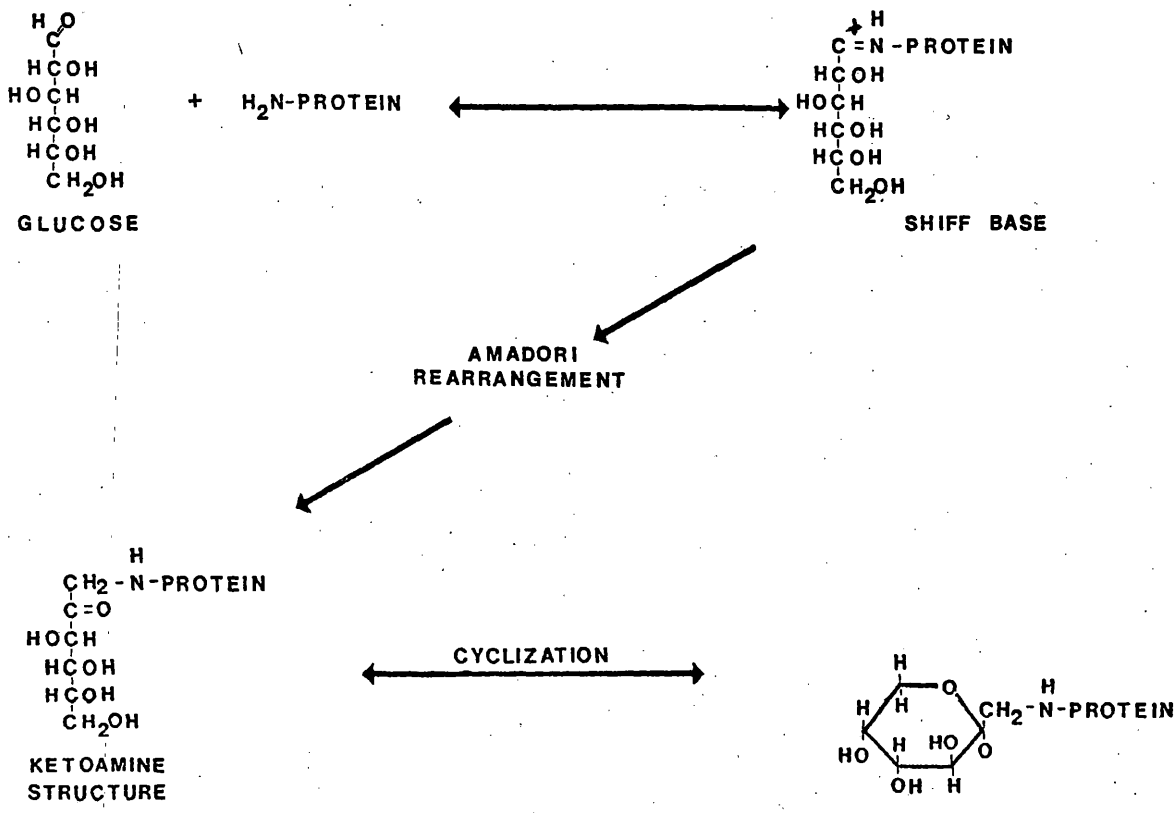
GLUCOSE
+ H2N-PROTEIN
SHIFF BASE
AMADORI
REARRANGEMENT
KETOAMINE
STRUCTURE
CYCLIZATION
CH2-N-PROTEIN

blood glucose levels resulting in an increase in non-enzymatically glycated proteins. Perhaps the detrimental effects are noted strictly by this relationship, either independently or in conjuction with other proposed mechanisms.

The glycated hemoglobin $A_{I(s)}$ (A_{Ia1}, A_{Ia2}, A_{Ib}, and A_{Ic}) are the best characterized of the non-enzymatically glycated proteins (25). The red blood cell is insulin independent and the hemoglobin within has a life span of about 120 days. Hemoglobin becomes non-enzymatically glycated in both normal and diabetic patients. Levels of Hb A_I are increased during hyperglycemia in diabetic patients in direct relationship to the degree of diabetic control (25). The process of glycation is relatively irreversible; therefore, once a hemoglobin molecule is glycated it remains in that form for the life of the red cell. Hemoglobin A_{Ic} takes approximately 60 days to reach a stable level (26). The level of glycated hemoglobin reflects the average glucose level that the red cell is exposed to during its life cycle. Levels of Hb A_I now provide an index of long-term blood glucose control in the diabetic patients (27). This post-translational modification is not completely benign, however, as hemoglobin oxygen affinity and sensitivity to the allosteric effector 2,3-diphosphoglycerate is altered (28).

Using glycated hemoglobin as a model it has been postulated that this type of post-translational modification could contribute to the morbidity and mortality associated with diabetes (29). Researchers have shown that the lipoproteins are non-enzymatically glycated in proportion to the degree of hyperglycemia (30-32). Atherosclerosis has been linked to low ratios of high density lipoproteins (HDL) to low density lipoproteins (LDL). Experiments have demonstrated that non-enzymatic

glycation affects the biologic activity of both HDL and LDL. Witztum et al. (31,32) demonstrated that glycated HDL is more rapidly catabolized and they have suggested that the glycated HDL has an increased affinity for its cell surface receptor. Conversely, glycated LDLs have a decreased affinity for its receptor and therefore are not taken in as rapidly as non-glycated LDL. This relationship has been theorized to result in decreased HDL to LDL rates which is associated with atherosclerosis.

The relationship between non-enzymatic glycation and diabetic neuropathy has been investigated by Cerami and coworkers (33). These investigators have suggested that since nervous tissue is also insulin-independent, non-enzymatic glycation of myelin or axonal proteins may contribute to this neuropathy. Their experiments using the sciatic nerve from diabetic dogs and rats showed an increased amount of non-enzymatically glycated lysine residues as opposed to normal controls. It was suggested that this glycation involves the myelin proteins or axonal proteins which could alter their turnover or nerve conduction.

The complications, retinopathy and nephropathy, are both believed to result in capillary basement membrane thickening (24). Histochemical studies reveal increased glycoproteins in diabetic basement membranes, but their exact nature has not been determined (34). It has been shown that the α-adrenergic receptor is non-enzymatically glycated in diabetic rats, leading others to propose that other structural and receptor proteins are subject to non-enzymatic glycation and may lead to basement membrane thickening (35).

The Lens Structure

The crystallin lens forms the second refracting unit of the vertebrate eye, adding 20 diopters of plus power to that created by the cornea (36). As such, it must remain perfectly clear or light will not reach the retinal sensory elements in an undisturbed state. The lens must also remain supple to produce the accomodative changes in refractive state necessary as one looks from a distant to a near target. For those not involved in lens research, there is often a tendency to look upon the lens as an inert "bag of proteins" that for some reason "coagulates" and therefore becomes opaque or cataractous as one grows old. This is far from reality. The lens is a highly ordered structure and depends upon active cellular metabolism to maintain this order.

The lens is surrounded by a typical basement membrane known as the lens capsule (Figure 4). The capsule is secreted anteriorly by the epithelial cells and posteriorly by the cortical fibers (37). The capsule itself is non-cellular, having a structure composed largely of glycoprotein-associated type IV collagen (38). Also present is a proteoglycan, heparan sulfate, which composes less than 1% of the lens capsule, yet is considered very important in determining the structure of the matrix (39). The structure of the capsule matrix appears to be critical in maintaining capsule clarity. However, when the capsule is separated from the underlying cells, it is found to be metabolically inert, lacking any enzymatic or metabolic properties (37).

Underlying and rather firmly attached to the basal lamina of the anterior capsule (38) is a single layer of cuboidal cells (Fig. 4). Except in pathologic conditions, no epithelial cells are found in the posterior lens. These cells have the metabolic activity to carry out

FIGURE 4. Schematic representation of the mammalian lens in cross section

Arrows indicate direction of cell migration from the epithelium to the cortex. From Jose, J. G.: The lens. In Anderson, R. E. (ed.), Biochemistry of the Eye.

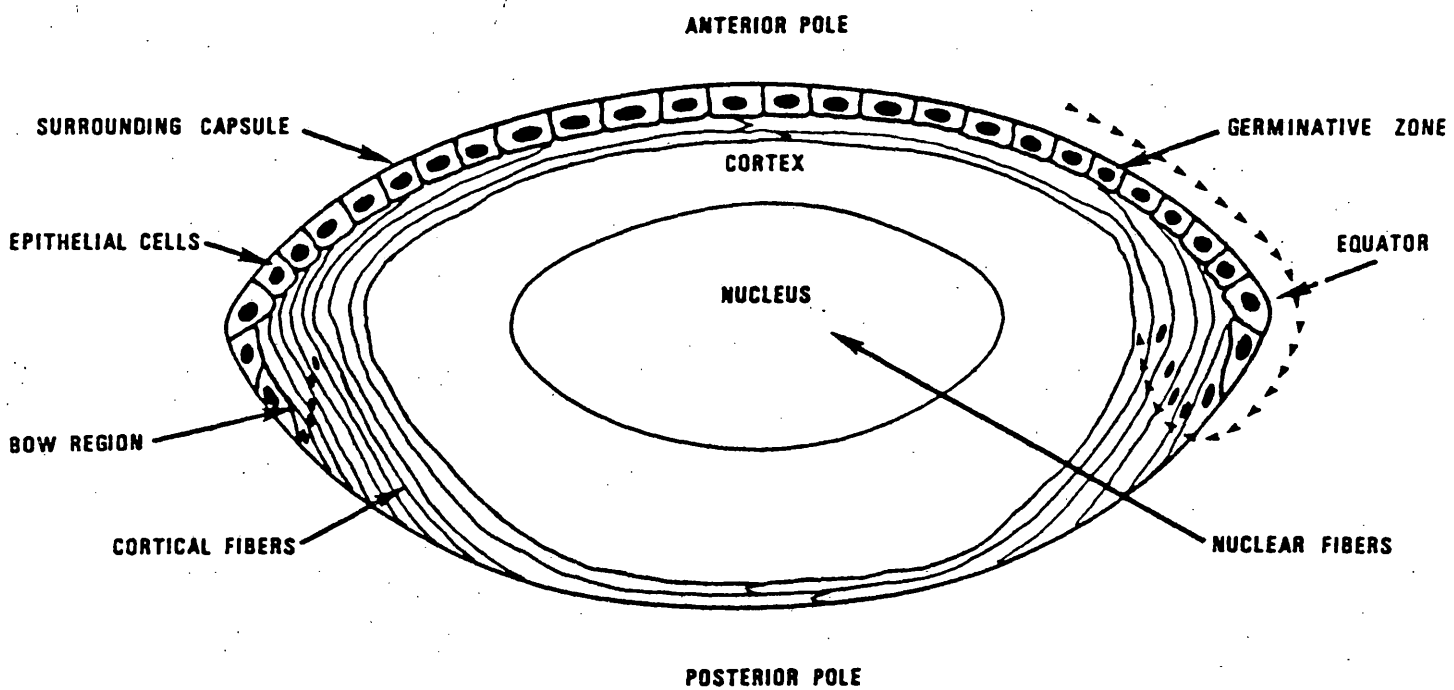
ANTERIOR POLE
SURROUNDING CAPSULE
GERMINATIVE ZONE
CORTEX
EPITHELIAL CELLS
EQUATOR
NUCLEUS
BOW REGION
CORTICAL FIBERS
NUCLEAR FIBERS
POSTERIOR POLE

FIGURE 5. Cross section of a rat lens showing the development of fibers of the equatorial region known as the "bow region." From Jose, J. G.: The lens. In Anderson, R. E. (ed.), Biochemistry of the Eye.

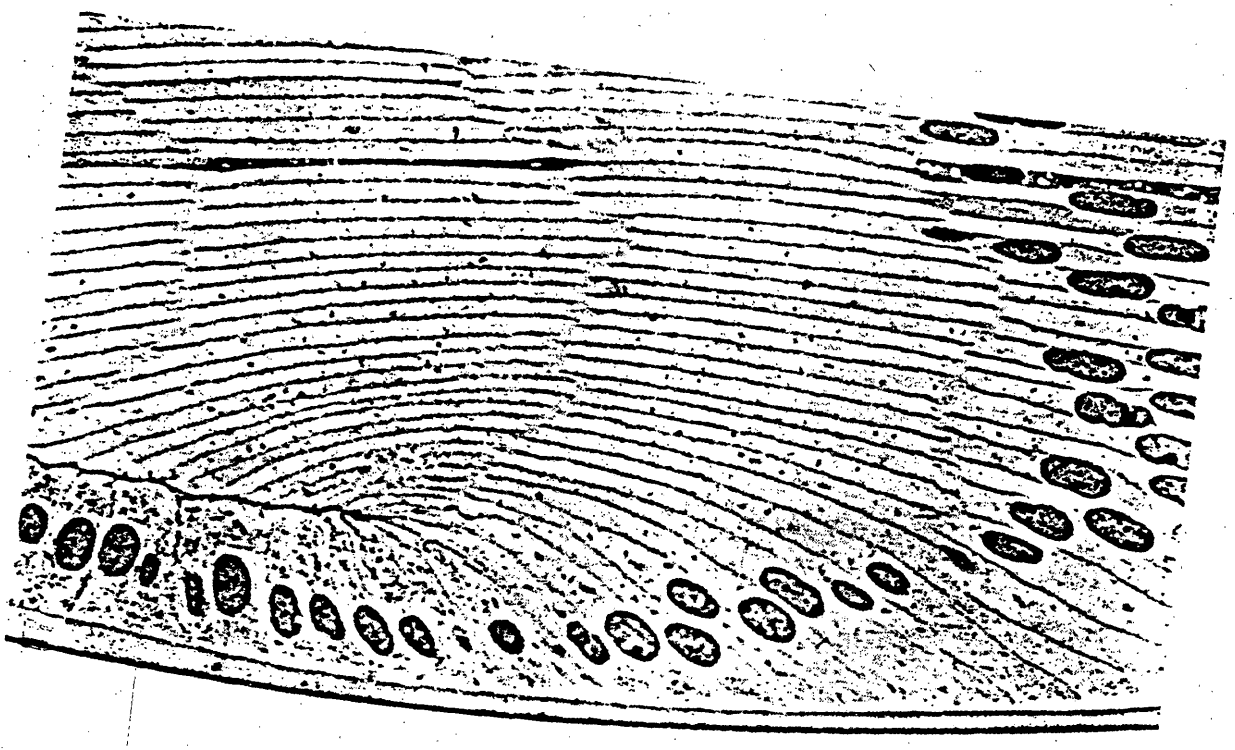

all normal cell activities including DNA, RNA, protein, and lipid biosynthesis, as well as to generate sufficient ATP to meet the energy needs of the lens (39). The epithelial cells are mitotic. The highest level of pre-mitotic (replicative or S-phase) DNA synthesis occurs in a ring around the anterior lens known as the germinative zone. These newly formed cells migrate equilaterally (follow arrows in Figure 4) where they differentiate into fibers in an area known as the bow region (Figures 4 and 5) (39).

As the epithelial cells progress to the bow region, they change in both morphology and in macromolecular synthetic activity. These cells have begun the process of terminal differentiation into lens fibers. Certain morphologic features immediately become apparent, the most striking of which is the increase in cell size, which is associated with a tremendous increase in the mass of cellular proteins and in the membranes of each individual fiber cells. As these two cell constiuents increase, most other cell organelles diminish and ultimately dissapear. It should be noted that as the epithelial cells move to the equator and there differentiate into the fibers, each new fiber is laid down upon an increasing bundle of previously formed fibers. The oldest of these fibers were produced in embryonic life and persist in the very center of the lens (the lens core or nucleus). The fibers in the outermost portion are the most recently formed and make up the cortex of the lens. No distinct morphological division differentiates the cortex from the nucleus of the lens; instead there is a gradual transition from one region to another. The overall structure is somewhat like an onion, with the oldest layers being more central (40). In addition the proteins within the fibers do not turn over or turn over very slowly so that the protein near the center of the lens are as old as the animal itself (41).

Lens Metabolism

The lens derives its energy from glucose present in the aqueous humor, the fluid within the anterior and posterior chambers which bathe the lens (42). The glucose levels within the aqueous humor are approximately ½ those of the plasma glucose levels (43). Sugars gain access to the internal lens via only one carrier system which does not require any expenditure of energy. As a consequence, the system does not transport sugars against a concentration gradient. However, because the sugar is metabolized, the carrier mechanism (known as facilitated diffusion) continually brings additional sugar into the lens so that in effect the concentration gradient is directed inward. Nonetheless, this inward flow is not entirely controlled by the external sugar concentration since within limits the carrier mechanism does not bring excess sugar into the lens if external sugar is increased. By as yet unknown mechanisms, the internal lens sugar concentration is kept at a constant 10 mg/100 g, independent of external concentration. However, when the external concentration exceeds about 175 mg/dl the control breaks down and the internal concentration increases accordingly (43). Therefore, in uncontrolled diabetes the internal lens glucose concentration would be increased in proportion to the increased plasma glucose levels.

Most of the glucose that is transported into the lens is phosphorylated by forming glucose-6-phosphate (Glc 6-P) by hexokinase (Fig. 6). This reaction is rate-limiting in the lens, being 70 to 100 times slower than that of the other enzymes involved in lens glycolysis (44). Once formed, glucose-6-phosphate enters either of two metabolic pathways. The most active pathway is anaerobic glycolysis which provides most of the high energy phosphate bonds required for lens metabolism. Due to

FIGURE 6. Pathways of sugar metabolism in the lens

From Jose, J. G.: The lens. In Anderson, R. E. (ed.), Biochemistry of the Eye.

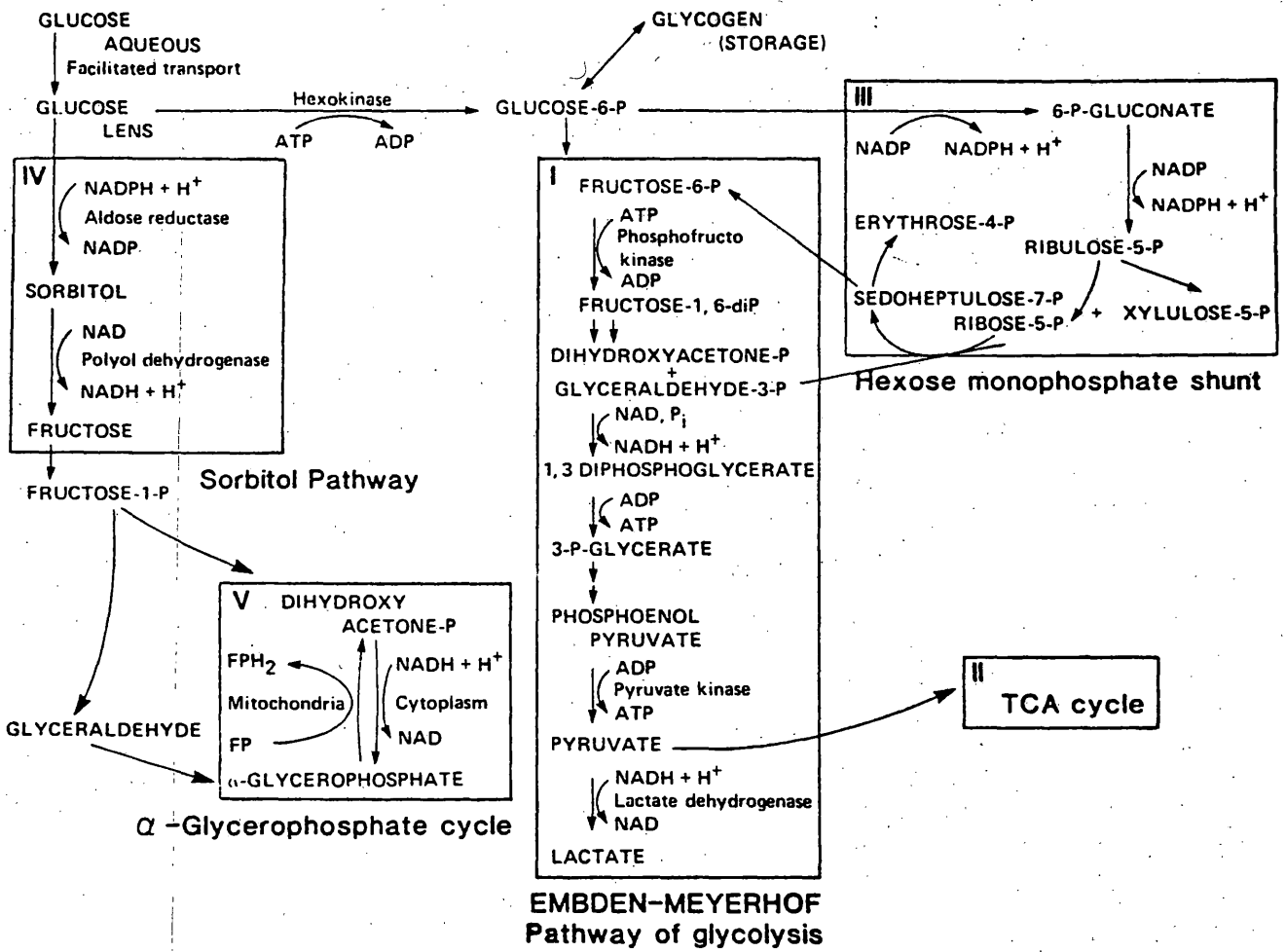
GLUCOSE
AQUEOUS
Facilitated transport
GLUCOSE
LENS
Hexokinase
ATP
ADP
GLUCOSE-6-P
GLYCOGEN
(STORAGE)
IV
NADPH + H+
Aldose reductase
NADP
SORBITOL
NAD
Polyol dehydrogenase
NADH + H+
FRUCTOSE
Sorbitol Pathway
FRUCTOSE-1-P
III
6-P-GLUCONATE
NADP
NADPH + H+
NADP
NADPH + H+
ERYTHROSE-4-P
RIBULOSE-5-P
SEDOHEPTULOSE-7-P
RIBOSE-5-P
+
XYLULOSE-5-P
Hexose monophosphate shunt
I
FRUCTOSE-6-P
ATP
Phosphofructo
kinase
ADP
FRUCTOSE-1, 6-diP
DIHYDROXYACETONE-P
+
GLYCERALDEHYDE-3-P
NAD, Pi
NADH + H+
1, 3 DIPHOSPHOGLYCERATE
ADP
ATP
3-P-GLYCERATE
PHOSPHOENOL
PYRUVATE
ADP
Pyruvate kinase
ATP
PYRUVATE
NADH + H+
Lactate dehydrogenase
NAD
LACTATE
EMBDEN-MEYERHOF
Pathway of glycolysis
V
DIHYDROXY
ACETONE-P
FPH2
Mitochondria
FP
NADH + H+
Cytoplasm
NAD
α-GLYCEROPHOSPHATE
GLYCERALDEHYDE
α -Glycerophosphate cycle
II
TCA cycle

the low oxygen tension in the lens, only about 3% of the lens glucose paces through the TCA cycle to produce ATP (45). However, even this low activity of aerobic metabolism still produces about 25% of the lens ATP (46). Given its relative isolation from any blood supply, it seems likely that the lens depends primarily on anaerobic metabolism to supply the energy needs.

A less active pathway for utilization of Glc-6-P in the lens is the pentose phosphate pathway (hexose monophoshate (HMP) shunt). In the rat lens, about 5% of lens glucose is metabolized by this route (47), although the pathway is stimulated in the presence of elevated levels of glucose. The activity of the HMP shunt is higher in the lens than in most tissues, presumably to provide NADPH necessary for glutathione reductase and aldose reductase activities in the lens.

Lens Proteins

The mammalian lens has a protein concentration of about 35% of its wet weight, twice that of most other tissues (the most notable exception is the erythrocyte which contains 30-35% hemoglobin) (41). The majority of these are structural proteins of the lens fibers, which make up the bulk of the lens. These fiber proteins exist in two major groups, those that are water-soluble and those that are water-insoluble. The former are mostly crystallins. The latter have been referred to as the "albuminoid" fraction. "Albuminoid" is no longer considered a meaningful term and is now perferable to refer to this as the "water-insoluble fraction."

Most of the water-soluble proteins fall into one of three major groups, α-, β-, and γ-crystallins, that were originally defined on the basis of their chromatographic properties. Gel filtration which separates on the basis of size yields four fractions. They have been labeled

α, β_{high}, β_{low}, and γ crystallin in the mammalian lens (Table I). Almost 100 years after the crystallins were first described in the lens, the three-dimensional structures and interrelationships between these proteins have only begun to be unraveled (48-50).

The largest crystallin, with a molecular weight of about 810,000 dalton, is α-crystallin. Representing approximately 30% of the lens proteins the α-crystallin fraction is not one discrete protein, but is composed of different sized macromolecular aggregates of four distinct but closely related protein subunits. Studies on the primary structure of α-crystallin have demonstrated a marked conservation of the sequence of the polypeptide chains during evolution (Figure 7) (51). Each of these subunits has a molecular weight of about 20,000 daltons and the chains are held together by hydrogen bonds and hydrophobic interactions. These subunits are designated alpha A1, alpha A2, alpha B1, and alpha B2. A2 and B2 are direct products of gene translation whereas A1 and B1 are post-translational modification products, arising from deamidation of A2 and B2, respectively (52). A1 and B1 are not present in the epithelium. The relative proportions of A2 and B2 change during differentiation such that their ratios are 2:1 in the epithelium and 3:1 in the cortex (53). In addition, many different chains are formed over time by limited proteolysis of the carboxy terminus. Siezen et al. (54) provided evidence that these shortened chains are involved in polymerization of the α-crystallin aggregate.

The most abundant (slightly less than 50%) water-soluble proteins in the lens are the β-crystallins. They are the most heterogeneous of the crystallins (55), and may be further separated by gel filtration chromatography into two major fractions having molecular weights of

TABLE I. Summary of generalized characteristics of major lens proteins from adult mammals

TABLE I

Protein	Average molecular weight (daltons)	Fraction of lens proteins	Thiol content	Subunits
α-Crystallin	80×10^4	30%	Low	4 with a m.w. of about 20,000 daltons (α-A_1, α-A_2, α-B_1, α-B_2)
β-Crystallin		55%	High	Multiple subunits with m.w. of 25,000-28,000 daltons
β_{High}	$10\text{-}55 \times 10^4$			
β_{Low}	$5\text{-}8 \times 10^4$			
γ-Crystallin	20×10^4	15%	High	exists as a monomer

FIGURE 7. Amino acid sequences of the αA and αB subunits

Homologous residues are enclosed in rectangles. Modified from Van Der Ouderaa, F., De Jong, W., Hilderink, A., and Bloemendal, H. (1974) The amino acid sequence of the αB_2 chain of bovine α-crystallin. Eur. J. Biochem. 49: 157.

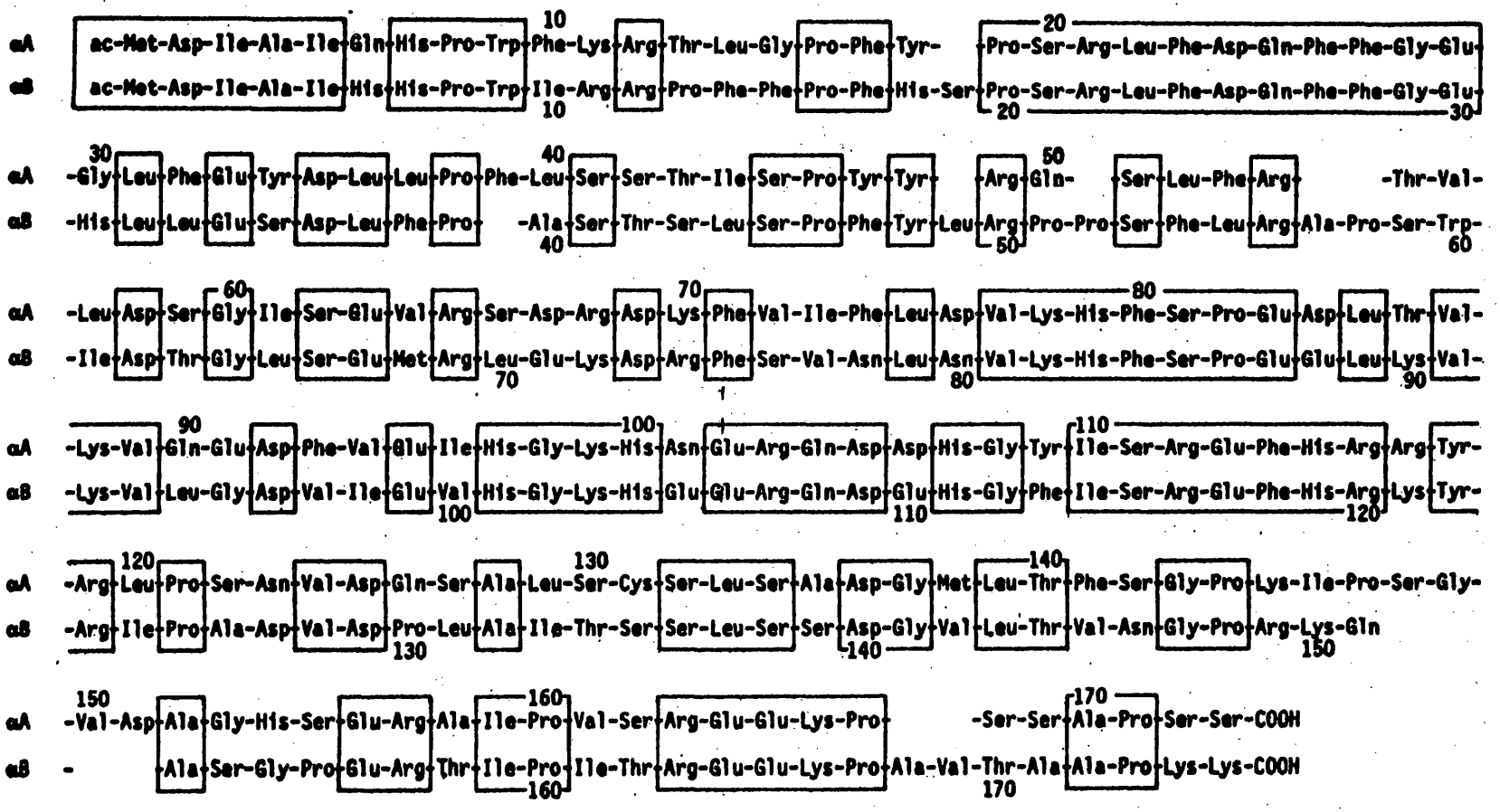
αA ac-Met-Asp-Ile-Ala-Ile-Gln-His-Pro-Trp-Phe-Lys-Arg-Thr-Leu-Gly-Pro-Phe-Tyr- Pro-Ser-Arg-Leu-Phe-Asp-Gln-Phe-Phe-Gly-Glu-
αB ac-Met-Asp-Ile-Ala-Ile-His-His-Pro-Trp-Ile-Arg-Arg-Pro-Phe-Phe-Pro-Phe-His-Ser- Pro-Ser-Arg-Leu-Phe-Asp-Gln-Phe-Phe-Gly-Glu-
αA -Gly-Leu-Phe-Glu-Tyr-Asp-Leu-Leu-Pro-Phe-Leu-Ser-Ser-Thr-Ile-Ser-Pro-Tyr-Tyr- Arg-Gln- Ser-Leu-Phe-Arg- -Thr-Val-
αB -His-Leu-Leu-Glu-Ser-Asp-Leu-Phe-Pro- -Ala-Ser-Thr-Ser-Leu-Ser-Pro-Phe-Tyr-Leu-Arg-Pro-Pro-Ser-Phe-Leu-Arg-Ala-Pro-Ser-Trp-
αA -Leu-Asp-Ser-Gly-Ile-Ser-Glu-Val-Arg-Ser-Asp-Arg-Asp-Lys-Phe-Val-Ile-Phe-Leu-Asp-Val-Lys-His-Phe-Ser-Pro-Glu-Asp-Leu-Thr-Val-
αB -Ile-Asp-Thr-Gly-Leu-Ser-Glu-Met-Arg-Leu-Glu-Lys-Asp-Arg-Phe-Ser-Val-Asn-Leu-Asn-Val-Lys-His-Phe-Ser-Pro-Glu-Glu-Leu-Lys-Val-
αA -Lys-Val-Gln-Glu-Asp-Phe-Val-Glu-Ile-His-Gly-Lys-His-Asn-Glu-Arg-Gln-Asp-Asp-His-Gly-Tyr-Ile-Ser-Arg-Glu-Phe-His-Arg-Arg-Tyr-
αB -Lys-Val-Leu-Gly-Asp-Val-Ile-Glu-Val-His-Gly-Lys-His-Glu-Glu-Arg-Gln-Asp-Glu-His-Gly-Phe-Ile-Ser-Arg-Glu-Phe-His-Arg-Lys-Tyr-
αA -Arg-Leu-Pro-Ser-Asn-Val-Asp-Gln-Ser-Ala-Leu-Ser-Cys-Ser-Leu-Ser-Ala-Asp-Gly-Met-Leu-Thr-Phe-Ser-Gly-Pro-Lys-Ile-Pro-Ser-Gly-
αB -Arg-Ile-Pro-Ala-Asp-Val-Asp-Pro-Leu-Ala-Ile-Thr-Ser-Ser-Leu-Ser-Ser-Asp-Gly-Val-Leu-Thr-Val-Asn-Gly-Pro-Arg-Lys-Gln
αA -Val-Asp-Ala-Gly-His-Ser-Glu-Arg-Ala-Ile-Pro-Val-Ser-Arg-Glu-Glu-Lys-Pro- -Ser-Ser-Ala-Pro-Ser-Ser-COOH
αB - -Ala-Ser-Gly-Pro-Glu-Arg-Thr-Ile-Pro-Ile-Thr-Arg-Glu-Glu-Lys-Pro-Ala-Val-Thr-Ala-Ala-Pro-Lys-Lys-COOH

4.9×10^4 daltons and 2×10^5 daltons designated as β_L (low) and β_H (high), respectively. Dissociation of the β_L and β_H crystallins demonstrate a number of polypeptide chains in common (56). Among the shared chains is the major β-crystallin constituent βBp (B=basic; p=principal) (57). Zigler and Sidbury (58) were able to show that the occurrence of βBp in the β-crystallin fraction of both β_H and β_L was a general feature of vertebrate species. Its primary structure has been determined and shows considerable sequence homology with repeating sequences at the N- and C-terminal regions of the protein (Figure 8) (59). There is also considerable sequence homology between this chain and the γ-crystallin (Figure 8). β-Crystallin has no α-helical coils, being structured instead as β-pleated sheet and random coils (60).

The γ-crystallins are the smallest of the crystallins, having a molecular weight in the range of 20,000 daltons (61). Absence of α-helical structure is a feature that the γ-crystallins share with other crystallins, and like the β-crystallins, γ-crystallin has a significant amount of β-pleated structured (about 22%) (62). The γ-crystallins exist as monomers rather than as aggregates. Unlike both the α- and β-crystallins, several different γ-crystallins have been isolated; however, only one type is found in a given species. Their nature and concentration are variable depending on the species examined, the age of the animal, and lens locus (63). The γ-crystallins are all very similar and possess significant sequence homology with each other. At the present time the γ-crystallins are considered a heterogenous mixture which have in common the fact that they are water-soluble, having relatively low molecular weight and are present as monomers. The γ-crystallins make up about 15% of the lens proteins of the adult mammal, but constitute as much as 60% of the soluble protein in weanling animals (64).

FIGURE 8. Optimal alignment of N-terminal and C-terminal halves of bovine βBp and γ-crystallin sequences

Interchain identical residues in homologous positions of βBp and γ-crystallin half chains are enclosed in boxes. Intrachain sequence homology between the N-terminal and C-terminal parts of βBp and γ-crystallin is emphasized by dots. Modified from Driessen, H.P.C., Herbink, P., Bloemendal, H., and De Jong, W. W. (1981) Structure of bovine β-crystallin Bp chain. Eur. J. Biochem. 121: 83.

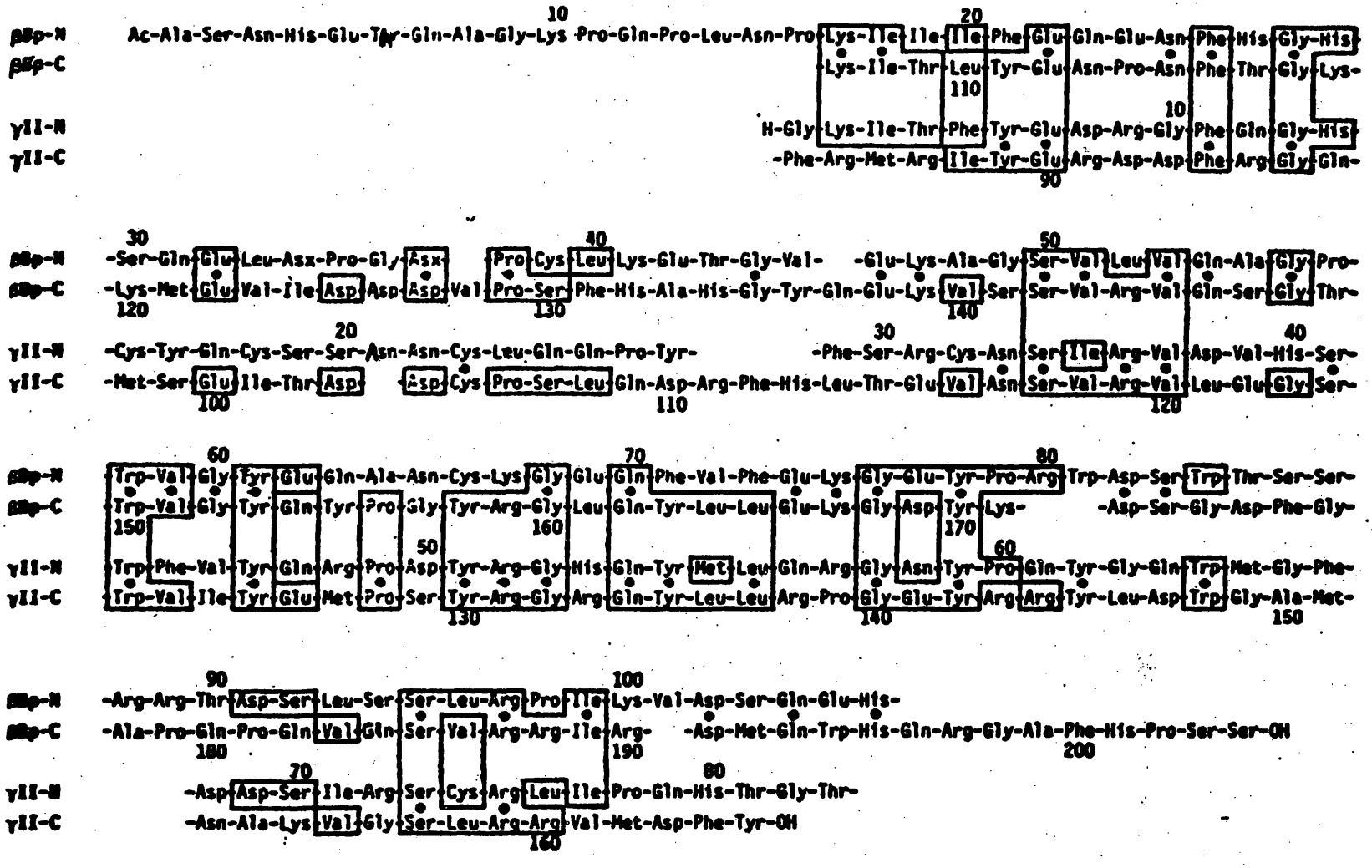
βBp-N
Ac-Ala-Ser-Asn-His-Glu-Tyr-Gln-Ala-Gly-Lys-Pro-Gln-Pro-Leu-Asn-Pro-Lys-Ile-Ile-Ile-Phe-Glu-Gln-Glu-Asn-Phe-His-Gly-His-
βBp-C
-Lys-Ile-Thr-Leu-Tyr-Glu-Asn-Pro-Asn-Phe-Thr-Gly-Lys-
γII-N
H-Gly-Lys-Ile-Thr-Phe-Tyr-Glu-Asp-Arg-Gly-Phe-Gln-Gly-His-
γII-C
-Phe-Arg-Met-Arg-Ile-Tyr-Glu-Arg-Asp-Asp-Phe-Arg-Gly-Gln-
βBp-N
-Ser-Gln-Glu-Leu-Asx-Pro-Gly-Asx-Pro-Cys-Leu-Lys-Glu-Thr-Gly-Val-Glu-Lys-Ala-Gly-Ser-Val-Leu-Val-Gln-Ala-Gly-Pro-
βBp-C
-Lys-Met-Glu-Val-Ile-Asp-Asp-Asp-Val-Pro-Ser-Phe-His-Ala-His-Gly-Tyr-Gln-Glu-Lys-Val-Ser-Ser-Val-Arg-Val-Gln-Ser-Gly-Thr-
γII-N
-Cys-Tyr-Gln-Cys-Ser-Ser-Asn-Asn-Cys-Leu-Gln-Gln-Pro-Tyr-Phe-Ser-Arg-Cys-Asn-Ser-Ile-Arg-Val-Asp-Val-His-Ser-
γII-C
-Met-Ser-Glu-Ile-Thr-Asp-Asp-Cys-Pro-Ser-Leu-Gln-Asp-Arg-Phe-His-Leu-Thr-Glu-Val-Asn-Ser-Val-Arg-Val-Leu-Glu-Gly-Ser-
βBp-N
-Trp-Val-Gly-Tyr-Glu-Gln-Ala-Asn-Cys-Lys-Gly-Glu-Gln-Phe-Val-Phe-Glu-Lys-Gly-Glu-Tyr-Pro-Arg-Trp-Asp-Ser-Trp-Thr-Ser-Ser-
βBp-C
-Trp-Val-Gly-Tyr-Gln-Tyr-Pro-Gly-Tyr-Arg-Gly-Leu-Gln-Tyr-Leu-Leu-Glu-Lys-Gly-Asp-Tyr-Lys-Asp-Ser-Gly-Asp-Phe-Gly-
γII-N
-Trp-Phe-Val-Tyr-Gln-Arg-Pro-Asp-Tyr-Arg-Gly-His-Gln-Tyr-Met-Leu-Gln-Arg-Gly-Asn-Tyr-Pro-Gln-Tyr-Gly-Gln-Trp-Met-Gly-Phe-
γII-C
-Trp-Val-Ile-Tyr-Glu-Met-Pro-Ser-Tyr-Arg-Gly-Arg-Gln-Tyr-Leu-Leu-Arg-Pro-Gly-Glu-Tyr-Arg-Arg-Tyr-Leu-Asp-Trp-Gly-Ala-Met-
βBp-N
-Arg-Arg-Thr-Asp-Ser-Leu-Ser-Ser-Leu-Arg-Pro-Ile-Lys-Val-Asp-Ser-Gln-Glu-His-
βBp-C
-Ala-Pro-Gln-Pro-Gln-Val-Gln-Ser-Val-Arg-Arg-Ile-Arg-Asp-Met-Gln-Trp-His-Gln-Arg-Gly-Ala-Phe-His-Pro-Ser-Ser-OH
γII-N
-Asp-Asp-Ser-Ile-Arg-Ser-Cys-Arg-Leu-Ile-Pro-Gln-His-Thr-Gly-Thr-
γII-C
-Asn-Ala-Lys-Val-Gly-Ser-Leu-Arg-Arg-Val-Met-Asp-Phe-Tyr-OH

Also present in the soluble fraction is a high molecular weight aggregate (HM-crystallin) with a molecular weight in excess of 1×10^6 daltons. In the bovine lens this HM-crystallin is composed of α-crystallin aggregates and may also contain some β-crystallin components (65). However, in the human and other vertebrates its composition has not been defined and varies depending on species, age of animal, and pathologic conditions (66). These HM-crystallins are believed to be precursors to even higher molecular weight aggregates present in the water-insoluble fraction which are theorized to aggregate so extensively as to cause light scattering and lens opacities (67).

Crystallins can all undergo post-translational modifications among which are C-terminal degradation, deamination, oxidation, aspartic acid racemization, and non-enzymatic glycation (4-8). It is not yet known which of these are normal modifications and which may be associated with lens opacification. Most authors have concluded that the crystallins are not integral membrane proteins although the precise role of the various crystallins is unknown (68). It is clear, however, that from their high concentration they definitely contribute to the cytoarchitecture.

Insoluble Fraction

The water-insoluble fraction of the lens did not receive much attention at the time of its discovery by Moerner in 1894 (69). The original term albumoid referred to the conjecture that it was composed primarily of insoluble α-crystallin. Only in recent years has this fraction been examined and found to be far more complex and hence the term albumoid replaced with water-insoluble fraction. The water-insoluble fraction may be further separated into two fractions, one soluble and one insoluble in 7 M urea. The urea-insoluble fraction contains the fiber plasma membrane and its associated membrane bound proteins (70).

As the lens ages there is an increase in the water-insoluble fraction. Within the fraction there is also an increase in the urea-insoluble fraction as the lens ages. In young lens most of the insoluble fraction is solubilized by 6 M urea; however, in older lenses and cataracts the lens proteins become increasingly insoluble (71). It has been hypothesized that lens proteins become water-insoluble and aggregate to form very large particles that scatter light, producing lens opacities (72). Many researchers have attempted to correlate increases in the percent of water-insoluble proteins with increases in lens opacification, but controversy continues over this hypothesis. It should be noted that the water-insoluble fraction increases with age even if the lens remains clear (71). For example, if radiolabeled methionine is injected into rats, one day later radioactivity is found only in the water-soluble fraction; but in animals killed seven weeks after isotope injection, 40% of the radioactivity is detected in the water-insoluble fraction (73). Those proteins that are initially in the water-soluble fraction eventually become incorporated into the water-insoluble fraction. It seems then that conversion of the soluble proteins into water-insoluble proteins is a natural process in lens fiber maturation. The process may, however, be accelerated or occur to excess in certain cataractous lenses.

The exact composition of the insoluble fraction remains in dispute. It is believed to contain crystallin components which have been made insoluble. Also present are small amounts of the structural proteins actin and vimiten but these proteins comprise only about 1% of the lens proteins (74). With the development of cataracts there is a decrease in titratable sulfhydryl groups (75). Also, as cataracts develop there is

an increase in a large (mw 2×10^6 daltons) disulfide linked high molecular weight (HMW) aggregate (76). It is this component of the insoluble fraction which is believed to be responsible for the light scattering found in cataracts. This HMW aggregate is believed to be composed of crystallin components, their degradation products and possibly other structural proteins held together by disulfide bridges (77). However, as with the insoluble fraction, the components of this HMW aggregate as well as the factors which contribute to its formation are in dispute.

Cataract Formation

One of the foremost directions of lens research, either directly or indirectly, is the elucidation of the mechanism or mechanisms which result in loss of normal lens transparency, i.e. cataracts. A prerequisite for this, however, is an understanding of the basis of the quite remarkable transparency of the normal lens. Surprisingly, little work has been done in this area. Current evidence by Raman spectroscopic studies suggests that lens crystallins are packed in a structural array (78). All the crystallins contain extensive amounts of β-pleated sheet regions, these regions are oriented orthogonal to the lens axis. This ordered array coupled with the absence of particulate cellular elements, aside from the epithelium, such as nuclei, mitochondria or endoplasmic reticulum is believed to be responsible for lens transparency.

The possible mechanisms of opacification are many, including any change capable of increasing the scattering or absorption of light. One of the oldest concepts is that precipitation, denaturation, coagulation or agglutination of soluble lens proteins is responsible for lens opacification. These various terms have been used for this intuitive notion

which is widely stated, but have no basis in fact other than a frequently drawn analogy to a hard-boiled egg. Such an ill-defined change may indeed occur in lenses cooked by exposure to infrared, microwave or ultrasound radiation, but the casual characterization of all cataracts as resulting from denaturation of protein has contributed nothing to the understanding of cataracts.

As implied above, there is no specific underlying cause of lens opacification. It should be recognized that any given cataractous lens has experienced many potentially destructive insults that either additively or synergistically produced the cataract. The latter possibility has been verified in the laboratory, where it has been shown that some subliminal insults to the lens that do not result in opacification when they occur separately, do cause cataracts, if they occur together (79). Table II contains a list of possible causes of cataracts in the lens.

Cataractogenic agents may be thought of in terms of how they would affect the structure and function of the major lens components. In looking simplistically at the structure of the lens, there are three main structural features: the capsule, the epithelium, and the lens fibers. Few, if any, cataracts are strictly associated with alterations in the capsule. Since the capsule is secreted by the epithelium and the cortex, it is apparent that, with the exception of trauma and post-translational protein changes, abnormalities in the capsule must arise from the underlying cells. This leaves only two major sites of cataractogenic action in the lens.

The first of these is the epithelium. These cells are the major site of internal osmolarity regulation. They have a higher concentration of ATPase activity than the fibers. Thus any agents that interfere

TABLE II. Sites of action and mechanisms possibly resulting in cataract formation

TABLE II

I. Capsular Effects

A. Trauma
B. Post-translational modification of proteins

II. Epithelial Effects

A. Depressed pump activity
B. Altered rates or nature of proteins synthesized
C. Altered enzyme activity
D. Mutational events

III. Cortical Effects

A. Anomalous differentiation from epithelial cells
B. Erroneous or altered translation or transcription
C. Post-translational modification of proteins

C-terminal degradation
oxidation, especially photo-oxidation
deamidation
racemization
crosslinking
non-enzymatic glycation

D. Alteration in membrane structure

oxidation
protein crosslinking
osmotic swelling

either with the generation of energy or with the activity of the pumps can lead to the loss of transparency. Those enzymes that can be found in the lens are generally most concentrated in the epithelium. Ohrloff et al. showed that the activity of many of these enzymes decrease with age, which they attributed to post-translational modification (80). Whatever the basis, such changes could dramatically alter the ability of the lens to function.

Secondly, modifications in the metabolic activity of the epithelium could result from alterations in the genetic makeup of the epithelial cells. The lens, like other body cells, is subject to agents such as chemicals or near UV radiation that could cause mutations in these cells. The progeny would then have a reduced capacity to function as normal lens and might not adequately contribute to the metabolic needs of the lens. Furthermore, mutated epithelial cells might not have the genetic controls necessary for proper differentiation into lens fibers. The lenses of animals having UV- and X-ray induced cataracts show histological evidence of such failure of differentiation (81). Mutated epithelial cells may attempt to differentiate, but contain information that would cause them to produce anomalous proteins. These anomalous proteins might disrupt the normal cytoarchitecture of the cortical fibers, resulting in light scattering.

The architecture can also be disrupted by direct effects on existing lens proteins. Long wave UV radiation (320 nm-400 nm) has been associated with formation of nuclear cataracts, and tryptophan has been suggested to be the major absorbing chromophore. Tryptophan is not destroyed by the radiation, but rather passes the absorbed energy on to other cell components including water, with generation of H_2O_2 or superoxide

radicals. These highly reactive species in turn are hypothesized to react with lens proteins producing the high molecular weight macromolecular species present in cataract (82). As the lens ages the proteins also demonstrate such changes as C-terminal degradation, crosslinking, deamidation, racemization, glycation, and insolubilization. If the cytoarchitecture were sufficiently disrupted by these and other post-translational modifications of the structural proteins, the resulting anomalous fibers could act as scattering points for light.

With the development of cataracts there is also a decrease in titratable sulfhydryl groups (75). Sulfhydryl oxidation has been clearly associated with increases in the insoluble fraction as well as with the disulfide linked high molecular weight aggregate. These changes are believed to result from post-translational modifications which confer on the lens proteins an increased susceptibility of crystallin sulfhydryl groups to oxidation. The sulfhydryl content of the lens crystallins varies with γ-crystallin containing the highest amount with 6 cysteine residues per polypeptide chain. The β-crystallin has somewhat less with 2 cysteines per chain and α-crystallin the least with one per αA subunit. The lens proteins are long lived, experiencing multiple potentially cataractogenic insults. It is likely that the cataract is a record of the sum of these factors.

Several theories have been put forth for cataract formation in diabetes. One theory involves the enzyme aldose reductase and the sorbitol pathway (36) which may be summed up as follows:

$$\text{glucose} + \text{NADPH} + \text{H}^+ \xleftrightarrow{\text{aldose reductase}} \text{sorbitol} + \text{NADP}^+$$

$$\text{sorbitol} + \text{NAD}^+ \xleftrightarrow{\text{polyol dehydrogenase}} \text{fructose} + \text{NADH} + \text{H}^+$$

$$\text{glucose} + \text{NADPH} + \text{NAD}^+ \longleftrightarrow \text{fructose} + \text{NADP}^+ + \text{NADH}$$

The Km for this enzyme is about 700 times that of hexokinase (700×10^{-4} M vs 1×10^{-4} M), consequently less than 5% of lens glucose is normally converted to sorbitol. However, since hexokinase is the rate limiting step of glycolysis, as glucose increases in the lens, the sorbitol pathway is activated relatively more than glycolysis and sorbitol accumulates. Sorbitol is then metabolized to fructose by the enzyme polyol dehydrogenase. Unfortunately, this enzyme has a relatively high Km (1×10^{-2} M) which means that considerable sorbitol will accumulate before it is further metabolized. This, combined with poor permeability of the lens to sorbitol results in retention of sorbitol in the lens (38). This increase in sorbitol increases the osmotic pressure within the lens, drawing in water. At first the energy dependent pumps of the lens are able to compensate but ultimately they are overwhelmed. As a result there is swelling of the fibers, disruption of the normal architecture, and ultimately lens opacification (38).

A second theory involves aldose reductase based on the cofactor NADPH. This theory postulates that as aldose reductase activity is increased the NADPH pool will be depleted. This depletion results in a decrease in the regeneration of glutathione via glutathione reductase. With reduced glutathione depleted, the lens is subject to free-radical and oxidative damage resulting in disulfide bridge formation between proteins. These disulfide linked proteins would become larger and insoluble. The resulting aggregates may act as scatterpoints for light that produce lens opacities (40).

Non-enzymatic Glycation and Cataract Formation

Non-enzymatic glycation has also been implicated as a potential cause of diabetic cataracts. There are several factors which make the

lens susceptible to non-enzymatic glycation: first, like the red cell, the lens does not require insulin for glucose uptake. Thus, the lens is exposed to high concentrations of glucose during the hyperglycemia of diabetes. Second, lens crystallins have little or no turnover and are therefore particularly susceptible to post-translational modifications. As discussed earlier, non-enzymatic glycation is dependent on glucose concentration and protein half-life.

Many researchers have examined the role of non-enzymatic glycation in the formation of diabetic and senile cataracts. The basic tenet is that glycation of lysine residues results in a conformational change which leads to aggregation and disulfide bond formation. To study this hypothesis researchers have used various methods to examine the sulfhydryl oxidation state, high molecular weight protein formation, and the extent of non-enzymatic glycation in lenses. As this research has continued several methods for examining non-enzymatic glycation have been developed (Fig. 9). One of the first techniques used with the lens proteins was reduction with tritiated sodium borohydride. This procedure both stabilizes the ketoamine linkage and results in one non-exchangeable tritium label at the glycated amino acid. The extent of glycation of the protein may then be examined and coupled with amino acid analysis and an appropriate standard, the glycated amino acids may be identified and quantified.

Flückiger and Winterhalter (83) have used mild acid hydrolysis with oxalic acid to release 5-hydroxymethyl furfuraldehyde, which may be measured colormetrically with thiobarbituric acid (TBA). This method gives an overall estimation of ketoamine linkage. However, this method is cumbersome and provides only a relative index of the extent of

FIGURE 9. Various methods for the detection and quantification of Amadori products

From Monnier, V. M. and Cerami, A.: Non-enzymatic glycosylation and browning in diabetes and aging. Diabetes 31: 57-63, 1982.

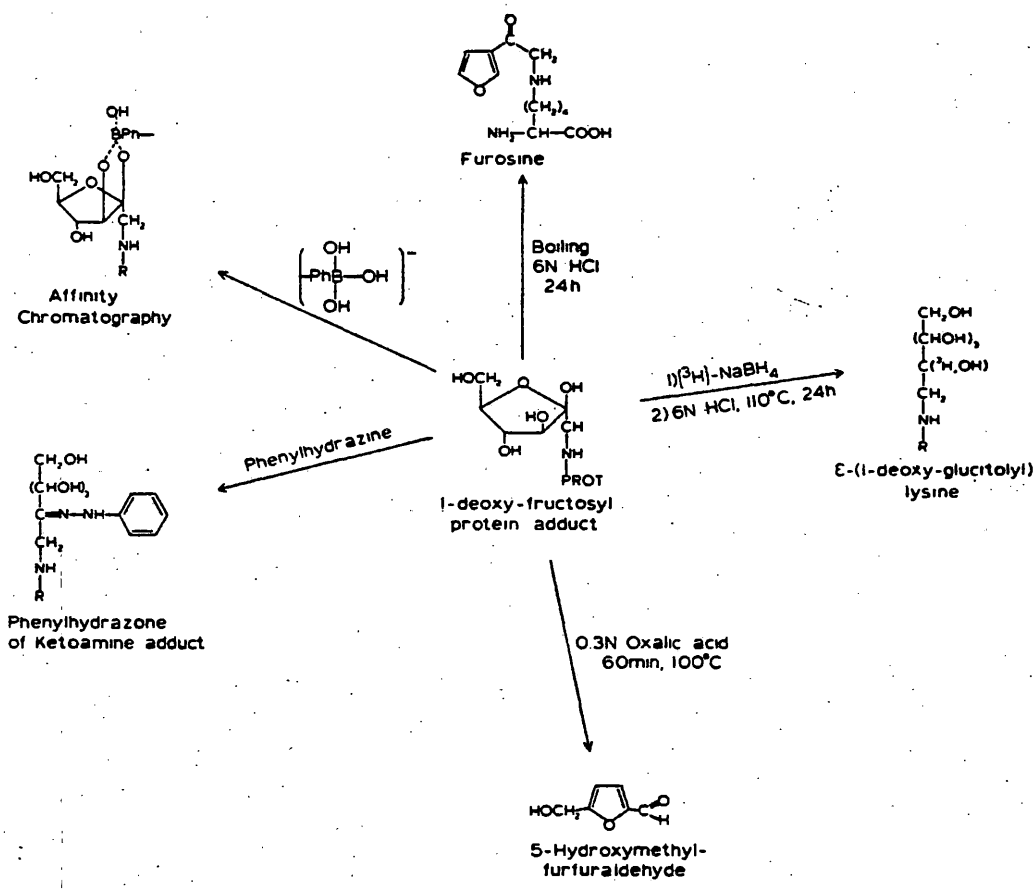
Furosine
Boiling
6N HCl
24h
Affinity
Chromatography
1)[3H]-NaBH4
2) 6N HCl, 110°C, 24h
ε-(1-deoxy-glucitolyl)
lysine
Phenylhydrazine
Phenylhydrazone
of Ketoamine adduct
1-deoxy-fructosyl
protein adduct
0.3N Oxalic acid
60min, 100°C
5-Hydroxymethyl-
furfuraldehyde

glycation. Secondly, this test requires samples free of contaminants such as reducing sugars or lipid oxidation products, which also produce color with TBA. More recently an affinity chromatographic procedure has been developed using a phenyl boronic acid resin (16). Native or borohydride reduced glycated residues contain a 1,2-vicinol group which will be retained on the phenyl boronate group.

The potential role of non-enzymatic glycation of lens crystallins in the formation of "sugar" cataracts was first investigated by Stevens et al. (84). The incubation of ^{14}C-labeled glucose or glycose-6-phosphate with lens crystallins from bovine lenses led with time to an incorporation of radioactivity into acid-precipitable proteins. Concomitantly, an opacification of the solution occurred in the presence of oxygen that mimicked the sugar cataracts of experimental diabetes and galactosemia. The opacity was found to be due to the presence of a disulfide-linked high molecular weight (HMW) aggregate. Observations by Spector and Zorn (85), showed an increase in titratable sulfhydryl groups of α-crystallin as the pH was increased from 8.8 to 10.4. They proposed that the deionization of the ε-amino groups of lysine residues altered the conformation of the protein, resulting in an unmasking of the sulfhydryl groups. Therefore, Stevens et al. hypothesized that non-enzymatic glycation of lysine residues would lead to the exposure of sulfhydryl groups, thus making the protein more susceptible to oxidation and aggregation (84).

These studies were extended to cataracts formed in diabetic and galactosemic rats. A 10- and 5-fold increase in glucose and galactose lysine adducts were detected in diabetic and galactosemic cataractous lenses, respectively. As in earlier work a disulfide linked HMW protein

aggregate was also detected (86). Overall these experiments suggest that non-enzymatic glycation could participate in the cataractous process by rendering the protein more vulnerable to oxidation.

The effects of non-enzymatic glycation have also been studied as a function of age. Bunn and coworkers showed an age dependent increase in glycation of bovine lens crystallins (87). Since the non-enzymatic glycation reaction is dependent on the protein half-life as well as glucose concentration they proposed that glycation may contribute to senile cataract formation. Using the incorporation of tritium from sodium borohydride reduction as the criterion for the extent of glycation, they showed a 2.4-fold increase in glycation of α-crystallin between 2- and 4-year-old lenses. Increases in glycation were also observed for other crystallin components.

Several authors have studied the proposed correlation between non-enzymatic glycation and disulfide formation. Awasthi et al. (88) incubated bovine lens crystallin proteins with glucose. Turbidity of the solutions followed by precipitation developed rapidly, particularly with proteins that were already in the oxidized form. However, no precipitation was observed with crystallins that had free sulfhydryl groups prior to incubation. Therefore, the authors concluded that glucose induces aggregation of crystallins by some mechanism other than exposure of sulfhydryl groups.

These observations were extended by Ansari et al. with the examination of human lenses. Human normal, diabetic cataractous, and senile cataractous lenses were separated into water-soluble, urea soluble, and insoluble protein fractions. Protein disulfide, mixed disulfide bonds and glycation (determined by tritiated borohydride reduction) were

measured in these fractions. Overall no linear correlation could be observed between sulfhydryl oxidation and glycation. However, marked increases in both borohydride-reducible bonds (glycation) and disulfide bonds were observed in the urea-soluble and insoluble fractions from diabetic cataractous lenses (89). Although these results point to a correlation between glycation and sulfhydryl oxidation in diabetic cataract formation, they can be also attributed to the consequences of polyol accumulation, osmotic stress on the lens, and loss of glutathione.

Liang and Chakrabarti (90), later studied the effect of glycation with glucose-6-phosphate on the conformation of purified bovine lens proteins. Using circular dichroism (CD) they demonstrated changes in the near ultraviolet (UV) CD characteristic of aromatic amino acid residues. However, no change in the far-UV CD was observed. Their results were interpreted to indicate that glycation causes a change in tertiary structure of the molecule but that the secondary structure (peptide background) was unaffected. Additionally, no evidence of a connection between glycation and extent of disulfide linkage was observed.

Shortly after Stevens and his associates published their results, Pande et al. (91) examined the glycation of human lenses in more detail. Their experiments involved tritiated sodium borohydride reduction of human normal, diabetic cataract, and senile cataract lenses. The results showed no significant increase in non-enzymatic glycation in any crystallin fraction or of high molecular weight aggregate. However, the insoluble HMW proteins that are believed to be involved in the cataractous process had three times the specific activity of the other protein fractions. Further analysis of the tritium incorporation in the acid

hydrolyzed protein by cation exchange chromatography demonstrated several radioactive peaks other than the expected 1-deoxyglucitolyl lysine. They concluded that there is no increase in glycation of lens proteins in diabetes, and glycation is not involved in cataract formation. They further questioned the use of tritiated borohydride reduction as a measure of non-enzymatic glycation due to other non-specific side reactions. However, further studies by other researchers has firmly established this as a reliable index for non-enzymatic glycation (92,96).

A different approach to study non-enzymatic glycation of lens proteins was used by Gopalakrishna et al. (93). They used a modified phenol-sulfuric acid reaction to quantitate the extent of glycation in diabetic cataracts, senile immature nuclear cataracts, senile immature cortical cataracts, and senile mature cortical cataracts. The soluble and urea soluble fractions were hydrolyzed under mild conditions. This results in the bound hexoses forming furfural derivatives which then react with the phenol-sulphuric acid to form a colored product which is read with a spectrophotometer. A second aliquot of the lens fraction is reacted with sodium borohydride which will prevent the formation of a furfural product with mild hydrolysis. The difference in the concentration of phenol-sulphuric acid positive material before and after reduction was used as an index of non-enzymatically bound hexoses. Their results showed a significant increase in the glycation of the diabetic cataract compared to all the other groups. However, there was an overlap between the diabetic cataracts and the senile mature cortical cataracts (SMCC). This was attributed to the decrease protein levels found in the SMCCs.

Several authors have used similar chemical methods to determine the extent of non-enzymatic glycation in diabetic cataract lens proteins. Kasai and coworkers (94) have studied the non-enzymatic glycation of diabetic cataract and senile cataract lenses and *in vitro* glycations of lens proteins with various concentrations of glucose using the thiobarbituric acid assay (TBA). Their results demonstrated that the human lens proteins can be glycated both *in vivo* and *in vitro*, and that the glycation is concentration dependent. In addition, non-enzymatic glycation was increased in both senile and diabetic cataracts and significantly higher in the diabetic than in the senile cataract group. The mean age of the diabetic patients (67 years) was significantly younger than that of the senile patients (75 years). It was concluded that the non-enzymatic glycation of lens proteins is accelerated by the hyperglycemia of diabetes.

A similar study was done by Lee and colleagues (95) using the TBA assay to measure non-enzymatic glycation of nuclear and cortical lens proteins from diabetic and senile cataracts. Their study concluded that glycation of lens cortical proteins, but not nuclear proteins, was significantly higher in diabetic patients compared to senile cataracts. Furthermore, the glycation of the lens cortex was significantly greater than that of the lens nucleus in the diabetic cataract; while it was somewhat decreased in the non-diabetic counterparts. This implied that the lens nucleus may not be exposed to as much metabolic variation of glucose in adulthood as the cortex.

The most recent work on non-enzymatic glycation of human lens crystallins was done by Garlick *et al*. (96). The glucitol-lysine (Glc-Lys) contact of soluble and insoluble crystallin fractions were

measured after reduction with ^{3}H-borohydride followed by acid hydrolysis, boronic acid affinity chromatography, and high pressure cation exchange chromatography. The study group consisted of human diabetic cataract lenses and normal lenses of various ages (0.2-99 years). The results showed that the soluble and insoluble fractions had equivalent levels of glycation. The content of Glc-Lys in normal lens crystallins increased with age in a linear fashion. Thus, the non-enzymatic glycation of non-diabetic lens crystallin reflected a biological clock. The diabetic lens crystallin samples showed about twice as much Glc-Lys residues compared to that of the control samples. Also, the Glc-Lys content of the diabetic lens crystallin samples did not increase with lens age and instead was postulated to correlate to the degree of lifetime glycemic control.

This study was designed to determine the relationship between non-enzymatic glycation and the formation of the HMW aggregates believed to be responsible for cataract formation. Streptozotocin induced diabetic rats were periodically sacrificed and the lenses were examined for glycated protein, and glycated amino acids levels were removed. The use of affinity chromatography. In addition, sensitive HPLC techniques were developed to monitor the progressive changes in lens crystallin composition and the formation of the HMW aggregates believed to be responsible for cataract formation. The sulfhydryl content was also determined to show the degree of disulfide formation as catarcts developed. Furthermore, the non-enzymatic glycation of both the water-soluble and urea-soluble fractions was characterized in control and diabetic cataract lenses. This characterization include the identification of the protein components of the urea-soluble fraction as well as

their level of glycation. Lastly, the components of the HMW aggregate were identified and the extent of glycation of each component was determined. The characterization of the glycation of the HMW components was extended to locating the specific sites of glycation within the crystallin polypeptide sequence.

MATERIALS AND METHODS

I. Materials

Animals: 90 Sprague-Dawley (Harland Co., Madison, Wisc.) rats (100-150 g) were divided into two groups consisting of 45 control and 45 experimental. The experimental group was made diabetic by injection of 65 mg/Kg streptozotocin intravenously according to the procedure of Rasch (117). Diabetes resulted within 48 hrs after injection. Every three weeks 5 experimental and 5 control animals were sacrificed and both lenses from each animal were removed. At the time of sacrifice, 5 cc of heparinized blood was drawn by cardiac puncture. Plasma glucose levels and glycated hemoglobin levels were then used to determine the level of hyperglycemia and the severity of diabetes.

II. Methods

A) Crystallin Preparation

The soluble and insoluble crystallin fractions were prepared by a modification of the procedure of Herbink et al. (57).

Lenses from individual animals were rinsed with 50 mM sodium phosphate buffer (pH 7.0) and suspended in 3 ml of the same phosphate buffer. The lenses were then homogenized under nitrogen using a Dounce ground glass tissue homogenizer. The resulting suspension was centrifuged for 1 hr at 6,000 x g at 4°. The supernatant, which comprised the water soluble fraction, was then dialized for 24 hrs against 500 volumes of 50 mM sodium phosphate (pH 7.0) at 4°. The pellet was washed with 10 volumes of the phosphate buffer and centrifuged for 10 minutes at 10,000 x g three times. The pellet was then resuspended in 2 ml 7 M urea, 100 mM HEPES, 25 mM NaCl, 1 mM EDTA (pH 8.5) and stirred by magnetic

stirrer for 2 hr at 4° under nitrogen. This suspension was centrifuged for 30 min at 10,000 x g at 4°. The resulting supernatant was the urea soluble fraction.

B) Affinity Gel Chromatography

The affinity gels used in this study contain a phenylboronate functional group covalently bound to either agarose or arylamide beads. The phenylboronate group will reversibly bind the vicinol diol groups of hexoses (Figure 10) (118). This binding occurs when the phenylboronate group is in the unprotonated form (pk 8.0). The bound glycosylated residue may be eluted by the addition of a competing compound, i.e. 100 mM sorbitol, or by lowering the pH.

1) Quantification of glycated crystallins from soluble fraction

The glycated crystallins were quantified using Isolab Glyc-Affin microaffinity columns from Isolab Inc., Akron, Ohio. These columns came prepacked with phenylboronate agarose in a column size of 0.5 cm x 4 cm. Developers needed for the chromatography were supplied by the same company. The column was equilibrated with 2 ml of the column preparation solution which consisted of 100 mM asparagine and 10 mM MgCl, pH >9.0. The sample, 5 mg, was made basic (roughly pH 9) by the addition of 15 µl of 0.1 M NaOH and applied to the top of the microcolumn. Once the sample had flowed into the gel 2 ml of the First Fraction elutant (100 mM glycine, 10 mM MgCl, pH >9.0) was applied and the elutant collected. This fraction contains the non-glycated proteins. The glycated proteins were eluted by the addition of 1 ml of the Second Fraction eluting buffer which consisted of 100 mM sorbitol. This fraction contained the glycated proteins. The percentage of glycated protein was determined by taking 100 µl from each fraction and reacting with 5 ml of

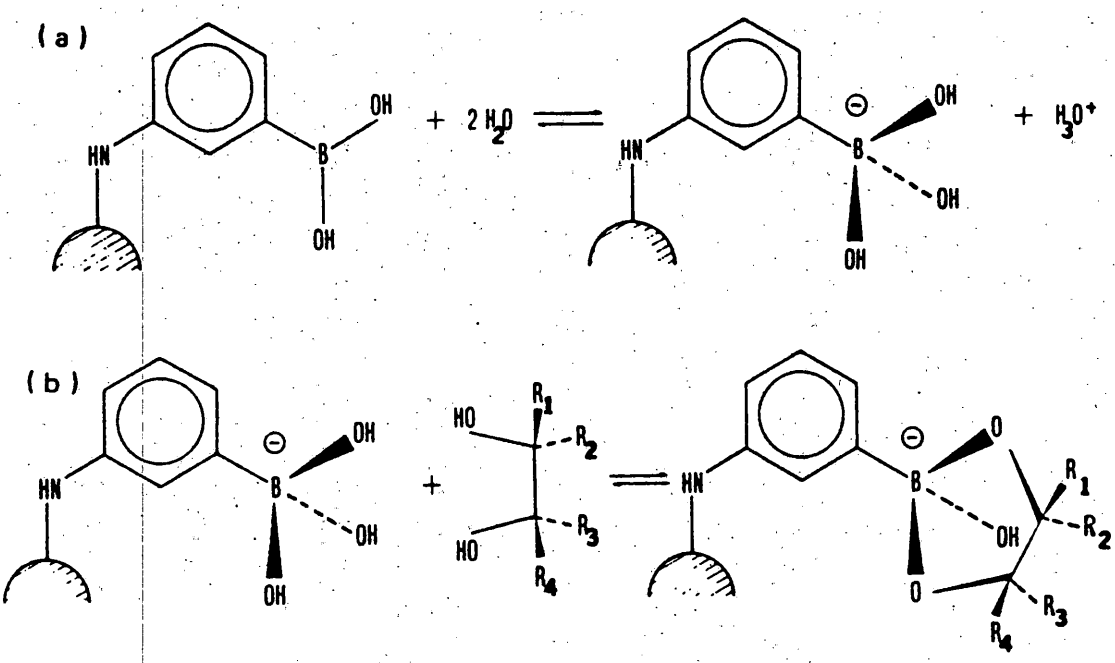
(a)
HN
B
OH
OH
+ 2 H2O
HN
B
OH
OH
OH
+ H3O+
(b)
HN
B
OH
OH
OH
HO
R1
R2
R3
R4
HO
HN
B
O
OH
O
R1
R2
R3
R4

the Bio Rad protein determination reagent. After a 5 min incubation at room temperature, each sample plus one blank was read on a spectrophotometer at 595 nm. The calculations are as follows:

$$\frac{\text{fraction 2 - blank}}{2 \times (\text{fraction 1 - blank}) + (\text{fraction 2 - blank})} \times 100 = \% \text{ glycoprotein}$$

2) Quantitation of glycated proteins from insoluble fraction

The glycated proteins from the urea soluble fraction were quantified in a procedure similar to the one used for the soluble fraction. A 7 M urea solution was made using each of the First Fraction and Second Fraction eluting buffers. The sample size was 5 mg in the urea, HEPES, EDTA buffer as described earlier. All other procedures were the same as described.

3) Quantification of glycated hemoglobin levels

Glycated hemoglobin levels has been recognized as an excellent measure of overall diabetic control. The glycated hemoglobin level was determined using the Isolab Glyc-Affin GHb microcolumns and buffers as described by the manufacturer (97). Briefly, the procedure was as follows. Fifty µl of the freshly drawn blood was mixed with 400 µl of the sample preparation reagent and incubated at room temperature for 10 min. This lysed the cells and insured the basic pH necessary for ligand binding. The column was prepared by addition of the column preparation reagent and 50 µl of the hemolysate applied to the column. The non-glycated hemoglobin was eluted with the First Fraction eluting reagent and diluted 10-fold. The glycated hemoglobin was eluted with the Second Fraction eluting reagent. Both fractions were read on a spectrophotometer at 415 nm. Calculations were as follows:

$$\frac{\text{fraction 2}}{10 \times (\text{fraction 1}) + (\text{fraction 2})} \times 100 = \% \text{ glycohemoglobin}$$

4) Quantification of glycated amino acids

The glycated amino acids were quantified using Bio Rad Affigel 601 by a modification of the procedure of Brownlee et al. (119). The Affigel 601 consists of the phenylboronate group covalently bound to acrylamide beads. The concentration of functional groups is such as that small glycated molecules, i.e. amino acids and small polypeptides, are reversibly bound. Five mg of each soluble and insoluble (urea-soluble) fraction was reacted with 50 µl of 1 M $NaBH_4$ in .1 M phosphate buffer, pH 6.0, for 1 hr. Each sample was then dialyzed for 24 hr against 500 volumes of distilled water at 4° with several changes of water. The samples were then hydrolyzed for 24 hr at 110° with 6 N HCl under vacuum. The borohydride reduction prevented any of the carbohydrate residues from being removed by the acid hydrolysis. The samples are then dried under a stream of air at 56°. The hydrolysates were redissolved with 25 mM sodium phosphate, 5 mM MgCl, pH 9.0 and the pH was adjusted to 9.0 with 0.1 M NaOH. Next, the hydrolysate was applied to a 1 cm x 10 cm column packed with the Affigel 601 equilibrated with the same phosphate buffer used to redissolve the hydrolysate. The non-glycated amino acids were eluted with 35 ml of the phosphate, MgCl buffer. To elute the glycated amino acids 15 ml of 25 mM HCl was applied to the column. Both fractions were lyophilized to dryness using a dry ice/acetone bath and a Labconco freeze drier lyophilizer. The samples were then redissolved with one ml distilled H_2O. 100 µl of the non-glycated fraction and 200 µl of the glycated fraction was then reacted with ninhydrin and read at 570 nm with a spectrophotometer as described elsewhere in Methods.

5) Isolation of glycated polypeptides

Affigel 601 affinity gel was also used to isolate glycated polypeptides obtained by enzymatic cleavage (118). Sixty mg of the insoluble fraction labeled by tritiated borohydride reduction solubilized in the urea buffer was applied to the molecular sieve HPLC system. One ml fractions were collected and peaks were pooled based on absorbance monitored at 280 nm. Pooled fractions of $[^3H]NaBH_4$ labeled high molecular weight protein in 7.2 M urea buffer obtained by molecular sieve HPLC was concentrated by Amicon ultra filtration (filter size YM10, 10,000 mw cut-off) to a concentration of 10 mg/ml. β-Mercaptoethanol was added to a final concentration of .55% and the sample incubated at 40° for 30 min. The sample was then diluted to a urea concentration of 2 molar.

Two aliquots of the diluted sample containing 10 mg each were then digested by trypsin or chymotrypsin (120). The enzyme (trypsin or chymotrypsin, 1 mg/ml in 1 mM HCl) was added to give an enzyme concentration of 1% and stirred by magnetic stirrer at room temperature for 1 hr. At the end of 1 hr half of the original enzyme amount was added and the sample was stirred for an additional hour. The resultant peptides were then lyophilized.

The total enzymatic digest was redissolved in 3 ml of 25 mM sodium phosphate, 5 mM $CaCl_2$, pH 9.0. The redissolved peptides were added to 5 ml of the Affigel 601 equilibrated in the same buffer in a 10 ml siliconized stoppered test tube. The tube was rocked gently for 5 min at room temperature. The slurry was poured into a 1 cm x 5 cm glass column and the non-glycated peptides were eluted with 50 ml of the equilibrating buffer. The glycated peptides were next eluted with 20 ml of 25 mM HCl and both fractions lyophilized and stored at -40°C for further separations by C-18 reverse phase HPLC (section C.4).

C) High Performance Liquid Chromatographic (HPLC) Techniques

1) Equipment

The HPLC equipment consisted of a Beckman dual 110 A pump gradient system with a 421 controller. Detection was accomplished with a Beckman Model 160 fixed wavelength spectrophotometer with a 10 µl flow cell. Peaks were recorded and integrated using a Hewlett Packard 3390 A recording integrator.

2) Molecular sieve HPLC

High performance liquid chromatographic size exclusion separations of proteins have only recently become available with development of rigid silica based packing material. The columns used in the separation of lens crystallins were Altex TSK size exclusion columns. These columns have a microparticulate rigid silica support with a bounded polyvinyl matrix. This provides a neutral, hydrophilic, matrix of varying pore sizes for the separation of molecules based on size and molecular shape (121).

The lens crystallins from the soluble fraction were separated using an Altex TSK 3000 SW, 7.5 mm x 600 mm column coupled with an Altex TSK 4000 SW, 7.5 mm x 300 mm column (Figure 11A). This combination resulted in a molecular weight range of approximately 1.5×10^6 to 2×10^3 daltons. The mobile phase consisted of 50 mM sodium phosphate, 50 mM NaCl, pH 6.8 with a flow rate of 1 ml/min and an isocratic gradient.

The crystallin components from the insoluble fraction were separated using similar size exclusion columns and a denaturing buffer system. The columns used consisted of an Altex TSK 2000 SW, 7.5 mm x 600 mm coupled in series with an Altex TSK 3000 SW, 7.5 mm x 300 mm

FIGURE 11. Molecular sieve HPLC separations of the soluble fraction and insoluble fraction

A) Separation of soluble lens crystallins from the soluble fraction using TSK 4000 SW column in series with TSK 3000 SW column. B) Separation of the insoluble proteins in the insoluble fraction using TSK 2000 SW column coupled with TSK 3000 SW column in the presence of 7 M urea buffer. Conditions of chromatogram are described in Methods.

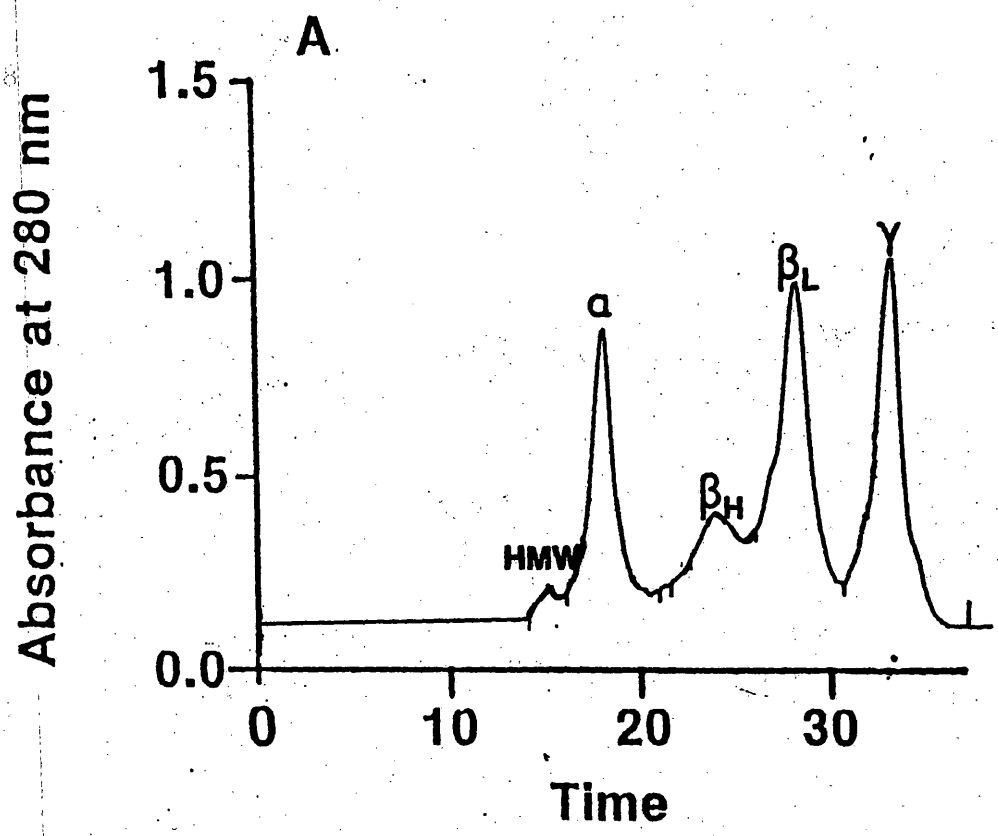
A
Absorbance at 280 nm
1.5
1.0
0.5
0.0
HMW
α
β_H
β_L
γ
0
10
20
30
Time

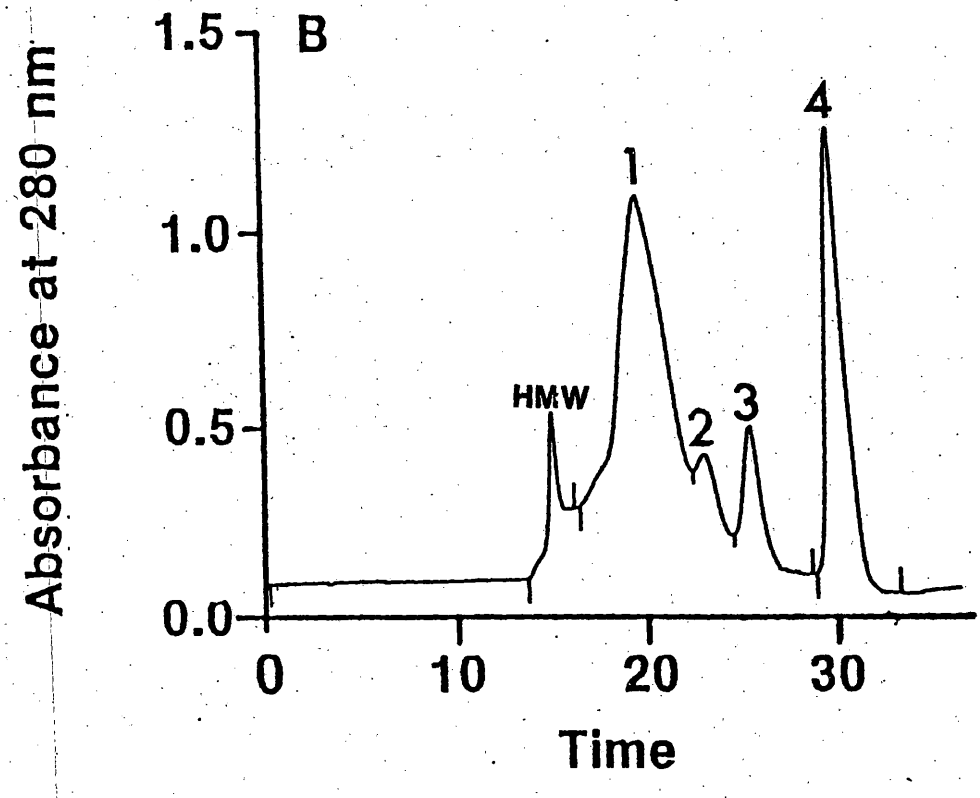
B
Absorbance at 280 nm
1.5
1.0
0.5
0.0
HMW
1
2
3
4
0
10
20
30
Time

(Figure 11B). The molecular weight range was approximately 5 x 10^5 to 1 x 10^4 daltons. The mobile phase consisted of 7 M urea, 100 mM sodium phosphate, 100 mM NaCl, 5 mM EDTA, pH 6.5 with an isocratic flow rate of 1 ml/min.

All chromatograms were run at ambient temperature and absorbance was monitored at 280 nm. Sample size for analytical runs for both soluble and insoluble fractions was 200 µg in 20 µl of the mobile phase. For semi-preparative applications, up to 20 mg in 200 µl could be applied and fractions collected every 30 sec with a LKB fraction collector.

The molecular sieve HPLC systems for both soluble and insoluble protein separations were calibrated using a mixture of proteins of known molecular weights. A mixture of thyroglobulin (m.w. 670,000), gamma globulin (m.w. 157,000), ovalbumin (m.w. 44,000), myoglobin (m.w. 17,000), and cyanocobalamine (m.w. 1,250) was injected onto each of the molecular sieve HPLC system described above. The results were plotted as the log molecular weight as Kav (Kav = (Ve-Vo/(Vi-Vo) where Ve = elution volume of peak, Vi = column volume, and Vo = void volume) (Figure 12).

3) Reverse phase HPLC separation of crystallin subunits

Reverse phase chromatography (RPC) separates proteins, peptides or other molecules based on a molecule's hydrophobic-hydrophilic properties. The column packing consists of a silica based support with a bound matrix of long chain alkyl groups. These side chain carbon units provide a hydrophobic environment which will bind molecules when the column is equilibrated with hydrophilic buffer. The molecules are eluted with a gradient of organic hydrophobic solvents in order of their

FIGURE 12. Calibration curves of molecular sieve HPLC systems

A) Curve obtained by TSK 3000 SW-TSK 4000 SW columns in series. B) TSK 2000 SW-TSK 3000 SW columns in series: 1) Thyroglobulin (m.w. 670,000), 2) Gamma Globulin (m.w. 157,000, 3) Ovalbumin (m.w. 44,000), 4) Myoglobin (m.w. 17,000), 5) Cyanocobalamine (m.w. 1,250).

50

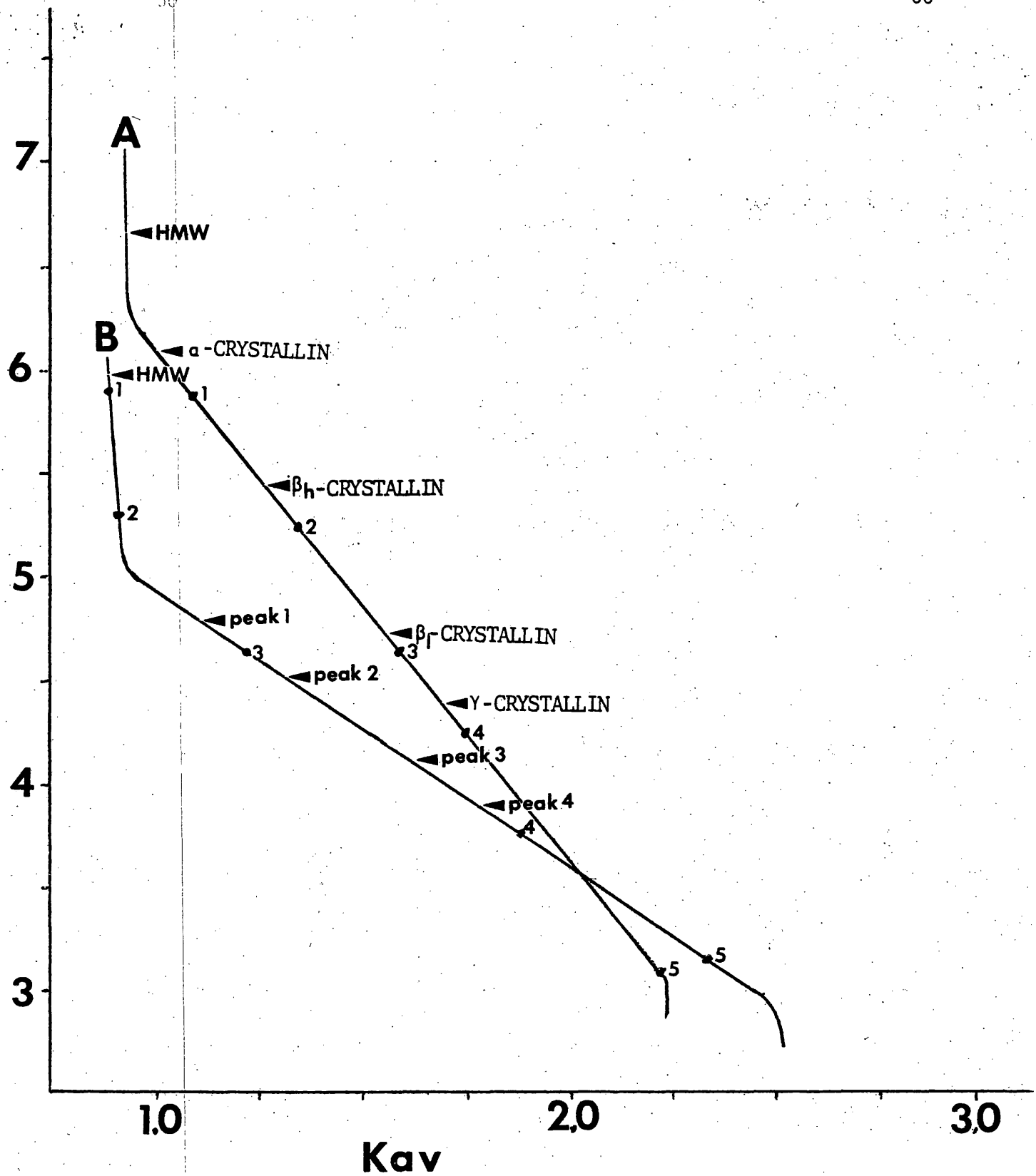
A
B
HMW
HMW
α-CRYSTALLIN
β_h-CRYSTALLIN
β_l-CRYSTALLIN
Y-CRYSTALLIN
peak 1
peak 2
peak 3
peak 4
1
2
3
4
5
7
6
5
4
3
1.0
2.0
3.0
Kav

hydrophobic properties. The column used for the RPC separation of lens crystallin subunits was a Vydac C-4 column. The matrix is composed of a mild hydrophobic four carbon side chain bounded to a macroporous silica support. The large pore (300 Å) support combined with the short alkyl side chain allows for larger molecules to be separated such as proteins without the irreversible binding which occurs on smaller pore long chain octyldecyl (C-18) columns. The lens crystallin subunits were separated by RPC by a modification of the procedure of Shelton et al. (109) using a 1% trifluoroacetic acid:acetonitrile gradient. This system will dissociate the crystallins into their individual subunits without the use of urea, SDS, or guanidine HCl. The developer A consisted of 1% trifluoroacetic acid in water and developer B was 100% acetonitrile with a gradient system as follows: After 20 min equilibration with 20% B the sample is injected and developed first with a linear gradient from 20% B to 50% B in 50 min. This was followed by an isocratic gradient of 50% B for 10 min then a steep gradient from 50% B to 70% B in one min and then an isocratic gradient of 70% B for 10 min. The column is then purged for 10 min at 100% B. The flow rate is maintained at 1.5 ml/min and the system is run at room temperature. The sample size was between 100 and 500 µg in 20 µl. Absorbance was monitored at 280 nm. All developers were filtered and degassed under vacuum prior to use.

4) Reverse phase separation of tryptic and chymotryptic polypeptides

The glycated tryptic and glycated chymotryptic peptides isolated by affinity chromatography were separated through the use of reverse phase C-18 HPLC (122). The column used was an Altex C-18 4.5 x 250 mm which utilizes a silica support with an octyldecyl (C-18)

alkyl side chain. This matrix provides a strong hydrophobic environment which optimizes the separation of small peptides and amino acids. Developer A consisted of 0.1% trifluoroacetic acid in water and developer B consisted of 100% acetonitrile. Elution of the polypeptides was accomplished after a 20 min equilibration with 100% A followed by a linear gradient from 0% B to 100% B in 90 min. Flow rate was maintained at 1 ml/min and 30 sec fractions were collected. Absorbance was monitored at 214 nm.

5) Amino acid analysis with C-8 reverse phase HPLC

The amino acid analysis of the lens proteins and their subunits were performed using a Beckman 121M amino acid analyzer. This procedure utilizes a cation exchange column followed by post-column derivatization with ninhydrin. Subsequently, techniques for amino acid analysis were developed using C-8 reverse phase HPLC and pre-column derivatization with phenylisothiocyanate (PITC) by a modification of the procedure of Heindrick et al. (98). This method was used to determine the amino acid composition of the glycated peptides isolated by affinity chromatography.

PITC reacts with the unprotonated free amino group of amino acids to yield a derivative which absorbs at 254 nm. Proteins and polypeptides were hydrolyzed to individual amino acids by hydrolysis in 6 N HCl at 110° under vacuum for 24 hr. The hydrolysate was then dried under a stream of air at 50° and then redissolved with 1 ml of a derivatization buffer composed of pyridine, methanol, and triethanolamine (10:3:2). The amino acids were then derivatized with 10 µl PITC and incubated for 5 min at room temperature. The samples were next dried in a vacuum dessicator at 50° (approximately 20 min). The drying of the

samples under vacuum was essential to remove the excess PITC and miscellaneous byproducts. The dried samples were redissolved in 100 µl of the HPLC developer A. Reverse phase HPLC was used to separate the derivatized amino acids using an Altex C-8 column (4.5 x 250 mm) and an ammonium acetate:acetonitrile gradient. Developer A consisted of 50 mM ammonium acetate, pH 4.5, and developer B was composed of a 50:50 mixture of 200 mM ammonium acetate, pH 4.5:acetonitrile. The column was equilibrated with 100% developer A for 20 min. After sample injection, a gradient from 0% B to 50% B in 30 min was initiated to elute the amino acids followed by purging at 100% B for 10 min. Absorbance was monitored at 254 nm and flow rate was maintained at 1 ml/min.

The amino acid composition was determined by comparison to a standard mixture containing 20 nmol/µl of amino acids (Figure 13). In addition to the standard mixture, a ε-amino glycated lysine standard was prepared by incubating poly-lysine with 1 M glucose followed by sodium borohydride reduction and acid hydrolysis. The glycated lysine was isolated by affinity chromatography as described. This glycated lysine was added to the commerical standard mixture prior to derivatization.

D) Sodium Borohydride Reduction

Borohydride has been used for over 50 years in carbohydrate chemistry as a reducing agent which will reduce an aldehyde or ketone group of a carbohydrate to its corresponding alcohol. In the case of non-enzymatic glycation, borohydride reduction results in a structure which is stable to acid hydrolysis. This was essential prior to glycated amino acid quantification and analysis. Secondly, the use of tritiated borohydride ($H^3[NaBH_4$) to reduce the bound carbohydrate resulted in the

FIGURE 13. Standard amino acid separation after pre-column derivatization by PITC followed by C-8 reverse phase HPLC

The amino acid standard mixture consisted of the following: D=Asp, E=Glu, S=Ser, G=Gly, H=His, T=Thr, A=Ala, R=Arg, P=Pro, Y=Tyr, V=Val, M=Met, W=Trp, I=Ile, L=Leu, GK=glyco-Lysine, F=Phe, K=Lys.

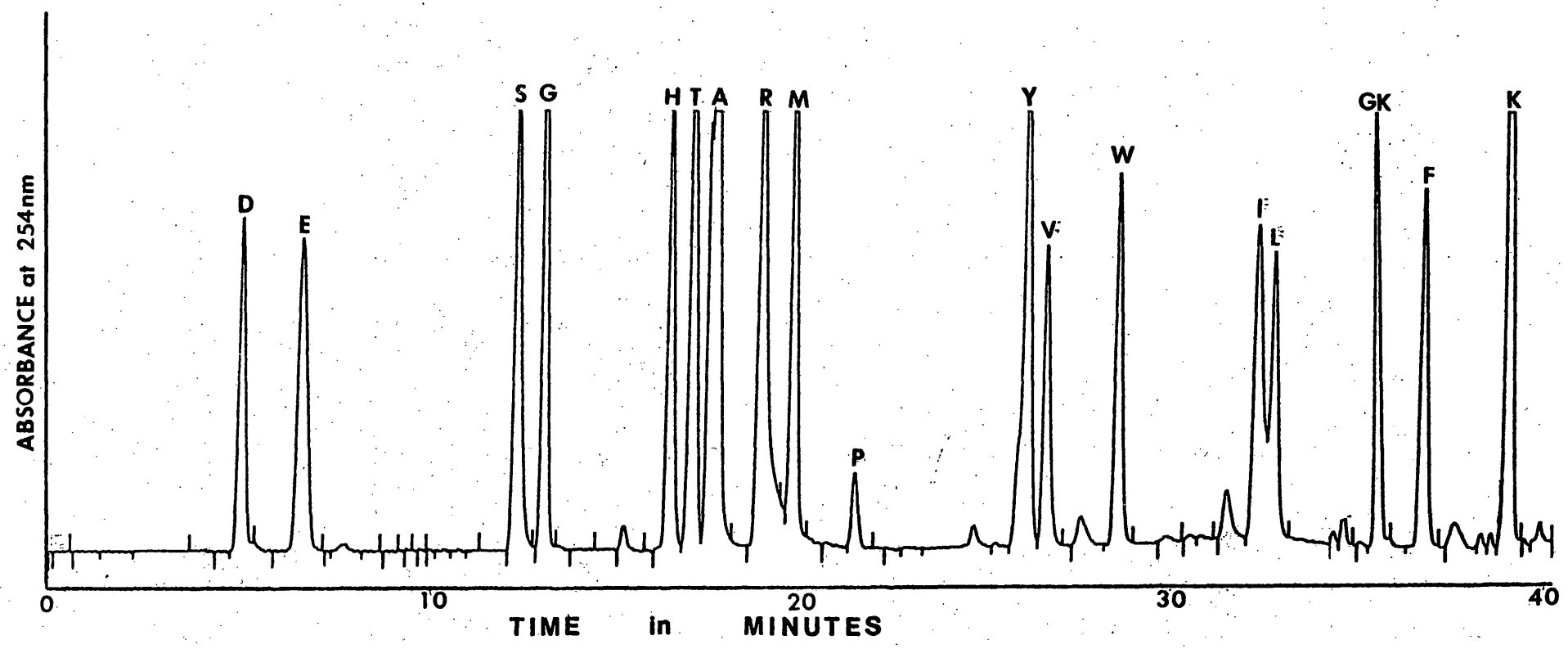
ABSORBANCE at 254nm
D
E
S
G
H
T
A
R
M
P
Y
V
W
I
L
GK
F
K
0
10
20
30
40
TIME in MINUTES

incorporation of one non-exchangeable tritium label for each non-enzymatically glycated residue.

The borohydride reduction using unlabeled sodium borohydride was carried out by a modification of the method of Chiou et al. (87). A 1 M solution of $NaBH_4$ is prepared in 100 mM potassium phosphate, pH 6.0. A 100 molar excess of the borohydride was added to the lens protein sample and allowed to react at room temperature for 10 min. The sample is then allowed to react for an additional 50 min at 4°. The unreacted borohydride was removed by extensive dialysis against 100 volumes of distilled water at 4° for 48 hrs with distilled water changes every 8 to 12 hr.

The tritium labeled borohydride reaction was carried out as follows: 1.8 mg of $[H^3]NaBH_4$ (specific activity 550 mCi/mmole), 25 mCi, was dissolved in 1 ml of 0.1 M KH_2PO_4, pH 6.0. The protein solutions were reacted with 100 μCi/mg protein which was approximately a 25-fold molar excess of the sodium borohydride. The samples were allowed to react as described above and then dialyzed.

E) Ninhydrin Reaction

Ninhydrin reacts with primary amino groups, particularly the α-NH_2 groups of amino acids, to generate a blue color, Ruheman's purple. The glycated amino acids isolated by affinity chromatography were quantified by reaction with ninhydrin by a modification of the procedure of Moore and Stein (99). The ninhydrin solution was prepared by dissolving 2 g ninhydrin in 50 ml of peroxide free methyl cellosolve (2-methoxyethanol). This was added to 50 ml of citrate buffer, pH 5 (80 mg $SnCl_2 \cdot 2\ H_2O$, 2.1 g citric acid monohydrate, and 20 ml of 1 M NaOH, diluted to 50 ml with water). The ninhydrin solution was then filtered

through glass fiber, saturated with N_2 and stored at 4° in a dark bottle. The dried amino acid samples were redissolved in 400 µl of H_2O and 0.50 ml ninhydrin reagent, and the tubes vortexed to mix the solutions. The tubes were covered and heated for 20 min in a boiling water bath. The tubes were then cooled, and 2.5 ml 50% (v/v) propan-2-ol was added to each tube. The contents of each tube were mixed thoroughly by vortexing and the absorbance at 570 nm measured within 1 hr. The approximate molar extinction coefficient, E_{570}, is 2×10^4. Blank tubes should give little absorbance (≤ 0.05).

F) Plasma Glucose Determinations

Plasma glucose levels were performed on each animal immediately at the time of sacrifice to confirm the level of diabetic control. Five ml of blood was obtained by cardiac puncture using a syringe containing 10 mg EDTA (ethylenediamine tetraacetate). The blood was then centrifuged at 2000 x g for 10 min and the plasma obtained. The plasma glucose levels were determined by the glucose oxidase-peroxidase assay of Raabo and Terkildsen (100) provided in kit form from Sigma chemical company. The procedure is based on the simultaneous use of glucose oxidase and peroxidase coupled with a chromogenic oxygen acceptor such as O-dianisidine. Glucose is oxidized to gluconic acid and H_2O_2 by glucose oxidase. The peroxidase catalyzes the oxidation of O-dianisidine (colorless) by H_2O_2 to the oxidized form (brown color). The intensity of the brown color measured at 450 nm was proportional to the glucose concentration. A standard of 100 mg/dl glucose was used to determine the actual glucose level. Briefly, 25 µl of plasma (also standard and H_2O blank) is added to 0.5 ml water and 5.0 ml of combined enzyme-color

reagent solution (Reagent A). Incubate tubes for 45 min at room temperature and read absorbance at 450 nm. Calculations are as follows:

$$\text{Serum Glucose (mg/dl)} = \frac{\text{Abs sample - blank}}{\text{Abs standard - blank}} \times 100$$

G) Protein Concentration Determination

Protein concentrations were determined using the Bio-Rad protein assay. The assay is based on the dye-binding assay developed by Bradford (101) and involves a color change of a dye in response to various concentrations of protein. Bovine serum albumin was used as a standard and the initial results were compared to those obtained by the method of Lowry (102).

H) Sulfhydryl Titrations

The concentration of free and total sulfhydryls were determined by titration with para-chloromercuricbenzoic acid (pCMB) by a modification of the method of Boyer et al. (103). This method involves an increased absorbance at 252 nm when pCMB reacts with sulfhydryl groups. Two sets of measurements are taken, one in the absence and one in the presence of 0.01% SDS. The addition of SDS was used to determine the total reactive sulfhydryl groups. A 2 mM solution of pCMB was prepared by dissolving pCMB in a small amount of 0.1 N NaOH and then diluting to 2 mM with 0.05 M sodium phosphate buffer (pH 8.0). Two matched quartz cuvettes were filled with 3 ml of the protein solution (0.5 mg/ml) and placed in a double beam spectrophotometer set at 252 nm. One cuvette serves as a blank while 0.01 ml increments of pCMB were added to the second cuvette and absorbance was measured at 252 nm. A second set of cuvettes containing only the phosphate buffer was used to determine the absorbance of pCMB in the absence of protein as 0.01 ml increments were added. The changes in optical densities were plotted against mmoles of pCMB added.

FIGURE 14. Sulfhydryl titration with pCMB

The equivalence point (arrow) is determined by the pCMB concentration where the two lines cross. Shown are titrations obtained from control lens and 168 day diabetic cataract lens.

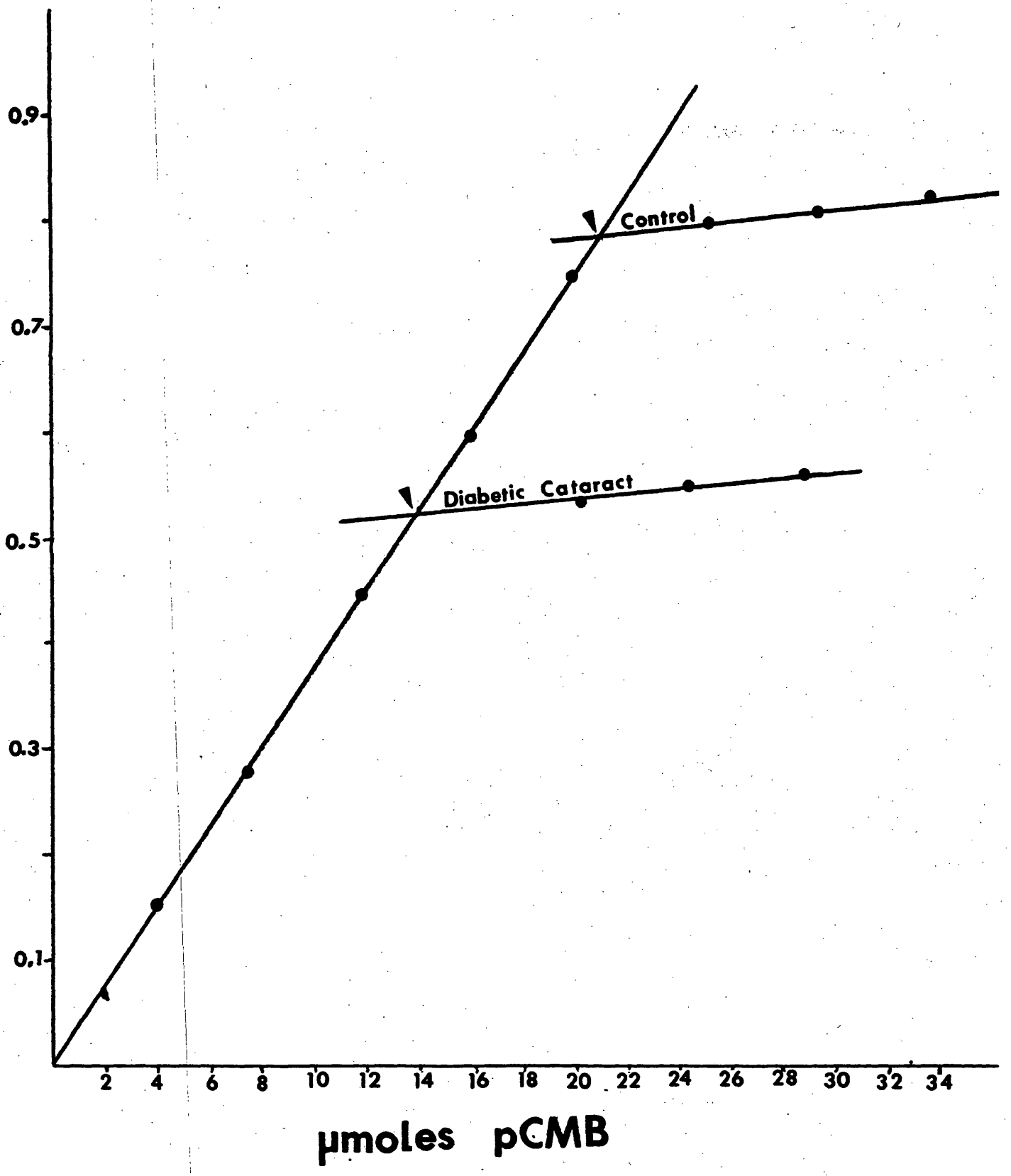
0.9
0.7
0.5
0.3
0.1
Control
Diabetic Cataract
2
4
6
8
10
12
14
16
18
20
22
24
26
28
30
32
34
µmoles pCMB

The classical method for determining the number of reactive sulfhydryls involves plotting the absorbance against the mmoles of pCMB added with the equivalence points occurring at the break of the curve where two lines through the titration points on the curve intersect (Fig. 14). However, a more accurate measure of the equivalence point was developed by determining the second derivative of the mmoles of pCMB added.

The number of reactive sulfhydryl groups was calculated based on the moles of pCMB corresponding to the equivalence point and the concentration of the protein solution. The concentration of the pCMB solution was measured using the molar extinction coefficient at 252 nm, $\Sigma_m \times 10^{-3} = 3.12$.

RESULTS

I. Progressive Changes Within the Lenses of Diabetic Rats

A) Plasma Glucose and Glycated Hemoglobin Levels

The plasma glucose levels and percentage of glycated hemoglobin were determined on each animal at the time of sacrifice to determine the degree of hyperglycemia. As shown in Figure 15 the control plasma glucose levels maintained a consistent value between 110 and 133 mg/dl. This is reflected by the glycated hemoglobin values which ranged from 4.2% to 5.7%. By comparison to the human system, the normal plasma glucose values range from 80 to 120 mg/dl and the glycated hemoglobin values fall between 4% and 6%. The plasma glucose levels in the diabetic group rose immediately to a hyperglycemic state which ranged from 483 mg/dl to 779 mg/dl. The glycated hemoglobin values showed a more gradual increase that plateaued at approximately 42 days with values between 13.1% to 16.9%. Similar changes are seen in human diabetics where glycated hemoglobin values may exceed 20% with the maximum value reached after approximately 60 days (25). The somewhat lower values and shorter time prior to the plateau reflect the decreased hemoglobin life span in the rat (90 days) vs human (120 days).

B) Glycated Lens Protein Levels in the Soluble and Insoluble Fractions

The glycated lens protein content was determined in the water-soluble and urea-soluble fractions at the time of sacrifice. Five milligrams of protein from each fraction of individual animals was applied to a microcolumn containing a phenylboronate affinity gel as described in the methods section. The results shown in Figure 16 demonstrate that the level of glycated protein in the control group remained constant

FIGURE 15. Glycated hemoglobin index of diabetic control

Glycated hemoglobin values were obtained by affinity chromatography to indicate the level of diabetic hyperglycemia of each animal at time of sacrifice. Plasma glucose levels were also determined to confirm diabetic condition. Each group consisted of 5 control and 5 diabetic animals. Values are mean ± S.E.M.

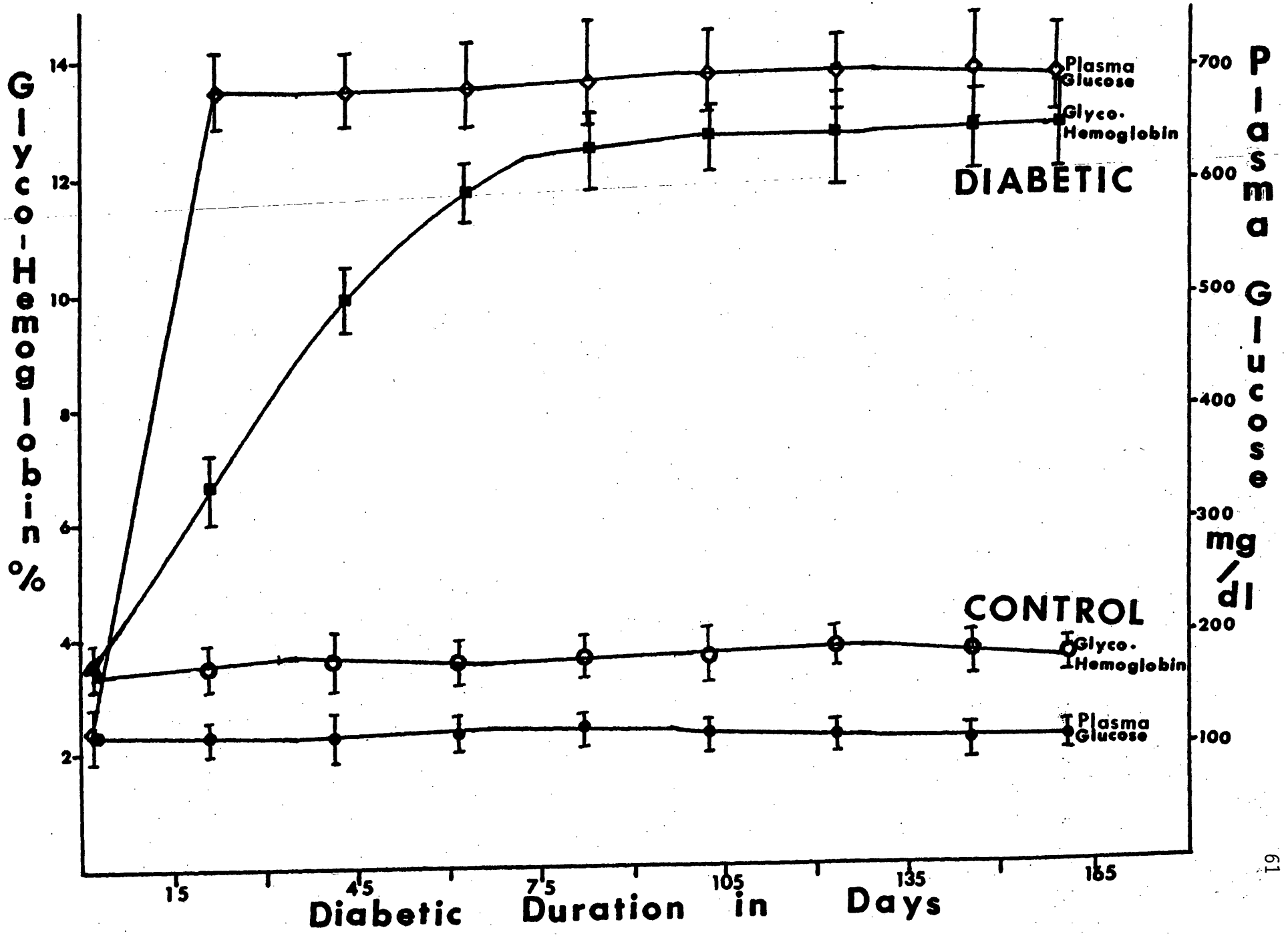
Glyco-Hemoglobin %
Plasma Glucose mg/dl
Plasma Glucose
Glyco. Hemoglobin
DIABETIC
CONTROL
Glyco. Hemoglobin
Plasma Glucose
Diabetic Duration in Days
1'5
4'5
7'5
10'5
13'5
16'5
2
4
6
8
10
12
14
100
200
300
400
500
600
700

FIGURE 16. Diabetic hyperglycemia dependent changes in glycated lens proteins

The progressive increases in glycated protein from the soluble fraction and the insoluble fraction were monitored by affinity chromatography. Closed square = control soluble fraction; closed triangle = control insoluble fraction; open diamond = diabetic soluble fraction; open triangle = diabetic insoluble fraction. Five animals were sacrificed in each group, experimental and control. Values are mean ± S.E.M.

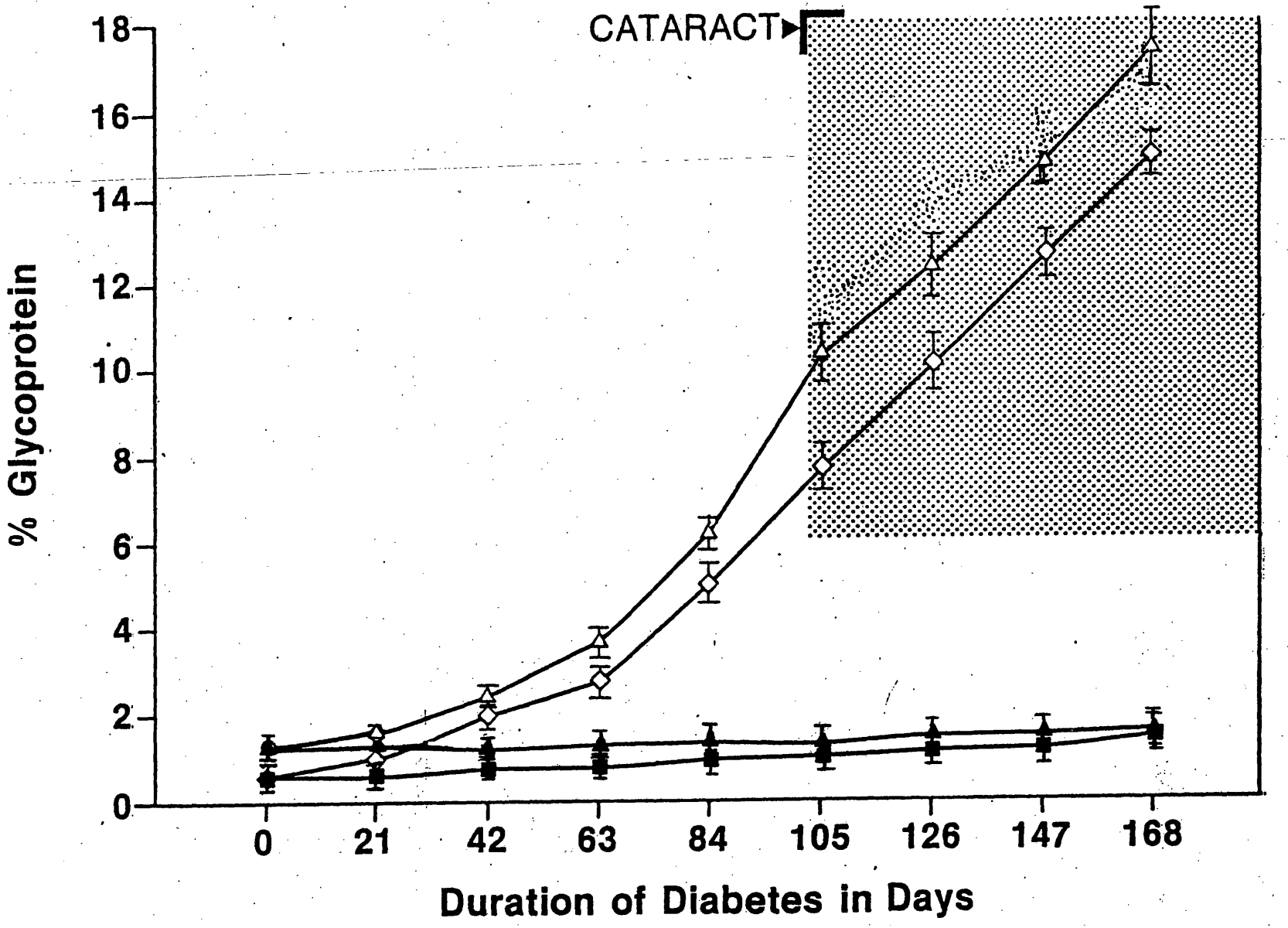
CATARACT
% Glycoprotein
18
16
14
12
10
8
6
4
2
0
0
21
42
63
84
105
126
147
168
Duration of Diabetes in Days

through at the experiment. The insoluble (urea-soluble) fraction demonstrated a slightly higher level of glycation than the water-soluble fraction. This is contrasted by the diabetic group which showed a continual increase in glycation of the water-soluble fraction from 0.5% (±0.1) at the beginning of the experiment to 7.7% (±1.1) at the onset of cataracts and continuing upward to 14.5% (±1.0) by 168 days. A more dramatic increase was demonstrated by the urea-soluble fraction which rose from 1.5% (±0.2) at day 0 to 10.2% (±1.5) at the onset of cataracts and increasing further to 17.4% (±2.6) at 168 days. The level of glycated protein from the urea-soluble fraction remained consistently higher than the water-soluble fraction. In contrast with the glycated hemoglobin values the glycated lens proteins did not show any plateau phase and continued to increase in a linear fashion throughout the 168 day experiment.

C) Levels of Glycated Amino Acids

In addition to determining the glycated lens protein concentration, the glycated amino acids were also quantified and used in conjunction with the glycated protein levels as an index of progressive hyperglycemic changes. The glycated amino acids from borohydride reduced protein hydrolysates were quantified by phenylboronate affinity chromatography followed by reaction with ninhydrin as described in methods. It is assumed that the glycated lysine residues will react with ninhydrin as would a monoamine amino acid due to the borohydride reduced ketoamine group blocking the second site of ninhydrin reaction. The data directly reflect the results obtained with the glycated protein value. As shown in Figure 17, the glycated amino acids in the control group increased only marginally with the urea-soluble fraction consistently higher than

FIGURE 17. Glycated amino acids quantified by affinity chromatography

The glycated amino acids from acid hydrolyzed borohydride reduced soluble fraction were quantifed by Affigel 601 affinity chromatography. Each group consisted of 5 control and 5 diabetic rats. Values are mean ± S.E.M.

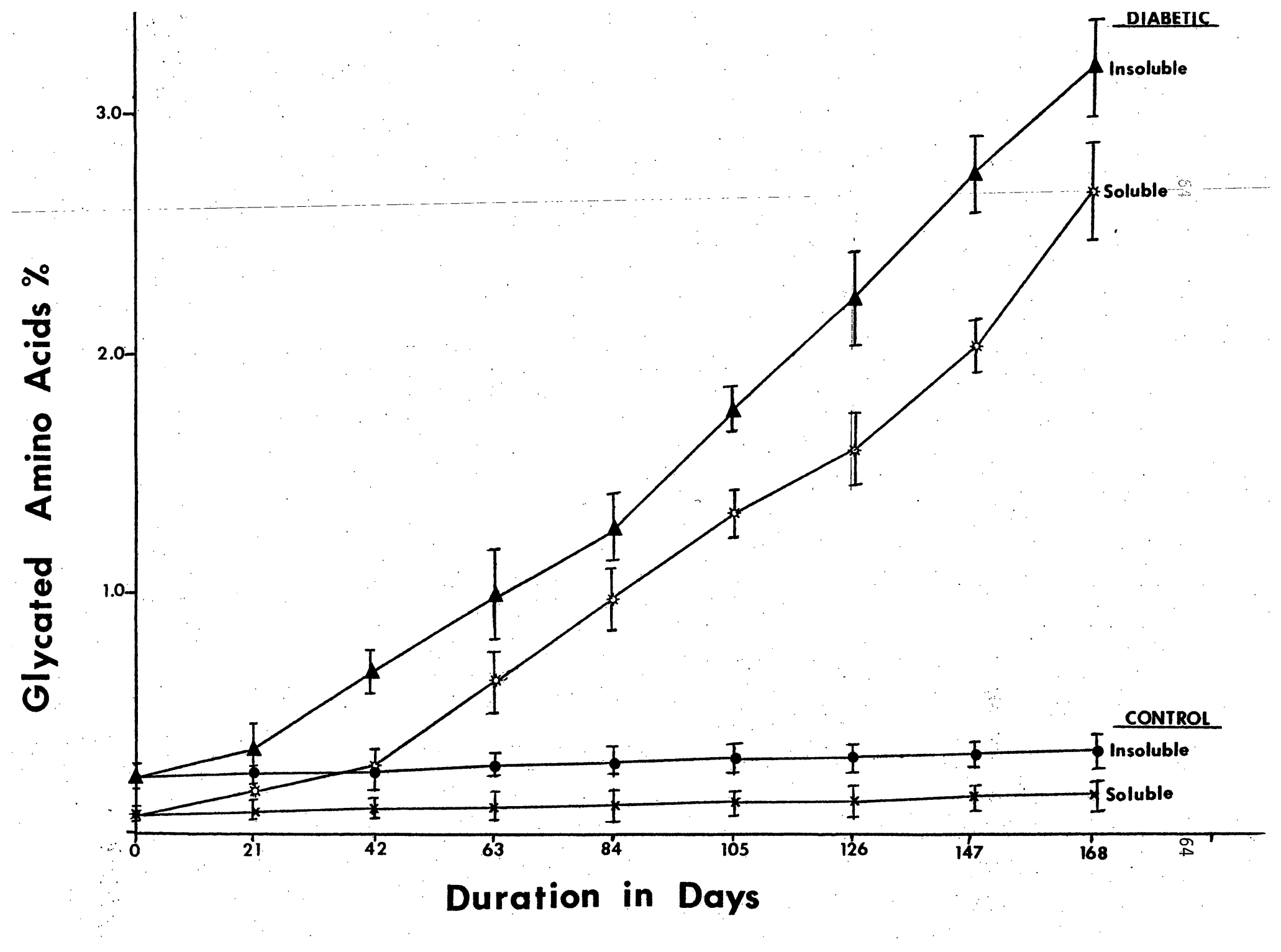
DIABETIC
Insoluble
Soluble
CONTROL
Insoluble
Soluble
Glycated Amino Acids %
3.0
2.0
1.0
0
21
42
63
84
105
126
147
168
Duration in Days

the water-soluble fraction. The control group water-soluble fraction showed an increase from 0.07% ± 0.002 to 0.15% ± 0.01 while the urea-soluble fraction increased from 0.23% ± 0.002 to 0.33% ± 0.02. A significant increase of glycated amino acids in both fractions was observed in the diabetic group. A 30-fold increase in glycated amino acids in the water-soluble fraction with the 0 day value of 0.08% (±0.002) increasing to 2.73% (±0.3) by day 168. The urea-soluble fraction showed a similar increase with the initial value of 0.23% (±0.02) increasing linearly to 3.15 at day 168.

D) Free Sulfhydryl Groups as Determined by pCMB Titrations

Free reactive sulfhydryl groups were determined by titration with pCMB in the presence and absence of SDS. The values obtained with SDS will give a measure of the sulfhydryls after lens crystallin denaturation, i.e. the total sulfhydryls. Decreasing sulfhydryls also indicate disulfide bond formation, an antecedent to cataract formation. The levels of free reactive sulfhydryls in the control animals remained consistent throughout the 168 day as did the total sulfhydryl levels (Figure 18). There was only a slight decrease in the free sulfhydryls from 36.7 ± 0.5 to 35.9 ± 0.6 µmol -SH/mg protein and the total reactive sulfhydryls decreased from 42.1 ± 0.7 to 40.3 ± 0.5 µmol -SH/mg protein. Also, the ratio between the free sulfhydryls and total sulfhydryls remained at a constant level. In the diabetic lens there was a steady decrease in the free sulfhydryls from 36.1 ± 0.8 to 21.0 ± 0.8 µmol -SH/mg protein. Also, there was a greater decrease in the total sulfhydryls with a decrease from 41.3 ± 0.5 to 24.3 ± 0.6 µmol -SH/mg protein. There was also a significant decrease in the ratio of total to free sulfhydryl from 1.15 to 1.09 indicating increased protein denaturation or structural unfolding revealing hidden sulfhydryls.

FIGURE 18. Reactive sulfhydryls determined by titration with pCMB

The reactive free and total sulfhydryls from the soluble fraction were determined by titration with pCMB. The free sulfhydryls were determined by titration in the absence of SDS. Titrations with the addition of SDS was used to determine the total sulfhydryls. Each group consisted of 5 control and 5 diabetic rats. Values are mean ± standard error.

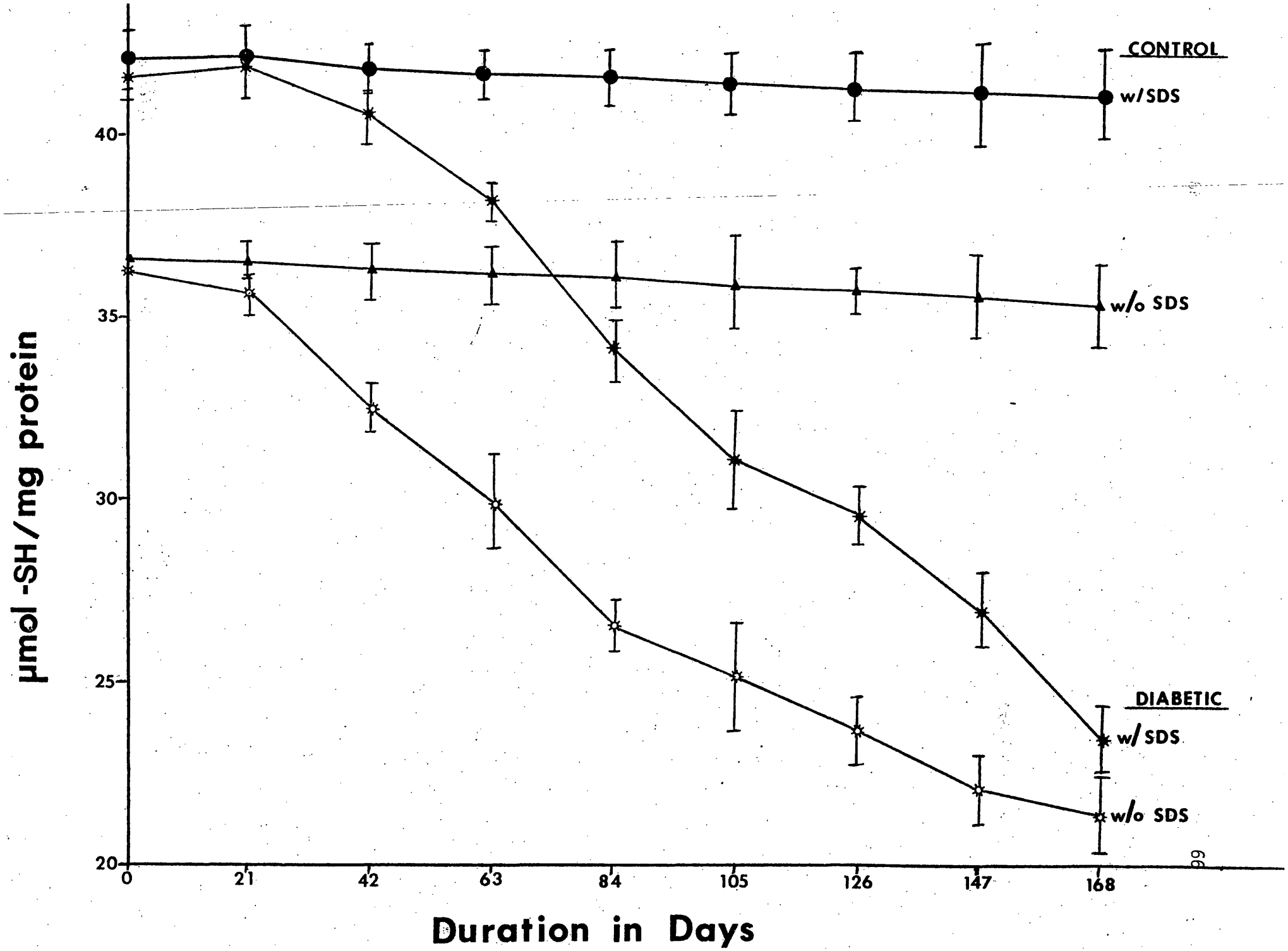
CONTROL
w/SDS
w/o SDS
DIABETIC
w/ SDS
w/o SDS
µmol -SH/mg protein
40
35
30
25
20
0
21
42
63
84
105
126
147
168
Duration in Days

E) Progressive Changes in the High Molecular Weight Aggregate and the Individual Crystallin Components

Sensitive molecular sieve HPLC techniques were developed to quantitate the high molecular weight (HMW) aggregates and crystallin component in both the soluble and insoluble fractions (Figs. 19 and 20). Development of these HPLC methodologies was essential to the study of progressive changes occurring in the lens of individual animals because it enabled us to study lenses from single animals.

1) Soluble and insoluble HMW proteins:

Examples of HPLC separations of proteins in the soluble and the insoluble fractions are given in Figures 19 and 20, and the results of such analysis as done on five control and five diabetic rats over a period of 168 days are summarized in Figures 21 and 22.

The soluble HMW protein is believed to be a precursor to the insoluble HMW protein, the increasing presence of which is indicative of cataract formation. The soluble HMW protein was present in only small amounts in the control group comprising a total of 0.8% (±0.08) at the onset of the experiment (Figs. 19 and 21). By day 168 the value had risen to 3.8% (±0.9). The diabetic group showed a dramatic increase in the soluble HMW protein from an initial value of 0.8% (±0.08) and increasing linearly to 27.1% (±1.3) after 168 days of diabetes. The insoluble HMW protein was present in slightly higher amounts in the control animals and showed similar increases from 3.3% (±0.5) to 5.2% (±0.8) during the 168 days (Figs. 20 and 22). This is contrasted by the diabetic group which showed an increase in the insoluble HMW protein from 3.3% (±0.5) to 27.2% (±1.9) at the onset of cataracts and increasing further to 42.7% (±3.6) after 168 days of hyperglycemia.

FIGURE 19. Molecular sieve HPLC separation of soluble crystallins

One hundred micrograms of soluble fractions were applied to the HPLC system using the TSK 3000 SW column in series with the TSK 4000 SW gel permeation columns. Mobile phase and conditions are as described in methods section. A) Control lens soluble fraction. B) Diabetic cataract lens soluble fraction at 168 days hyperglycemic duration.

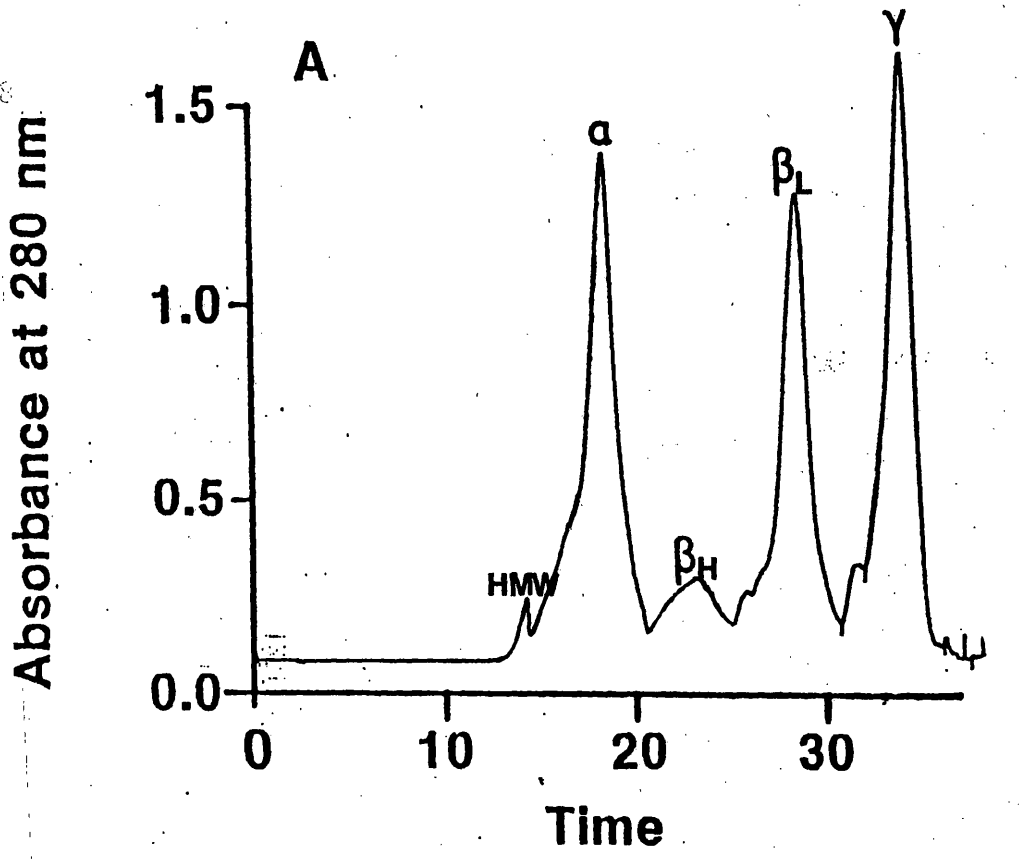
A
Absorbance at 280 nm
1.5
1.0
0.5
0.0
HMW
α
β_H
β_L
γ
0
10
20
30
Time

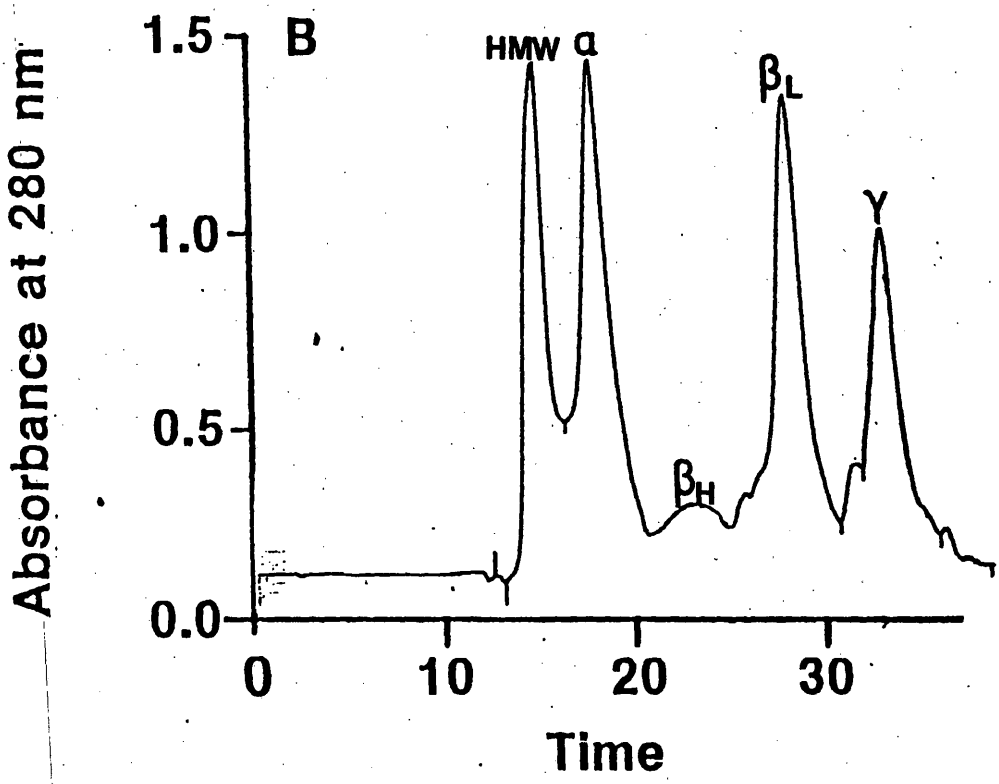
B
Absorbance at 280 nm
1.5
1.0
0.5
0.0
HMW
α
β_H
β_L
γ
0
10
20
30
Time

FIGURE 20. Molecular sieve HPLC separations of insoluble crystallins

One hundred micrograms of urea-soluble fraction was applied to the HPLC system using the TSK 2000 SW and TSK 3000 SW gel permeation HPLC columns in series. Mobile phase was 7 M urea, 100 mM sodium phosphate, 100 mM sodium chloride, pH 6.0. A) Control lens insoluble fraction. B) Diabetic cataract lens insoluble fraction at 168 day hyperglycemic duration.

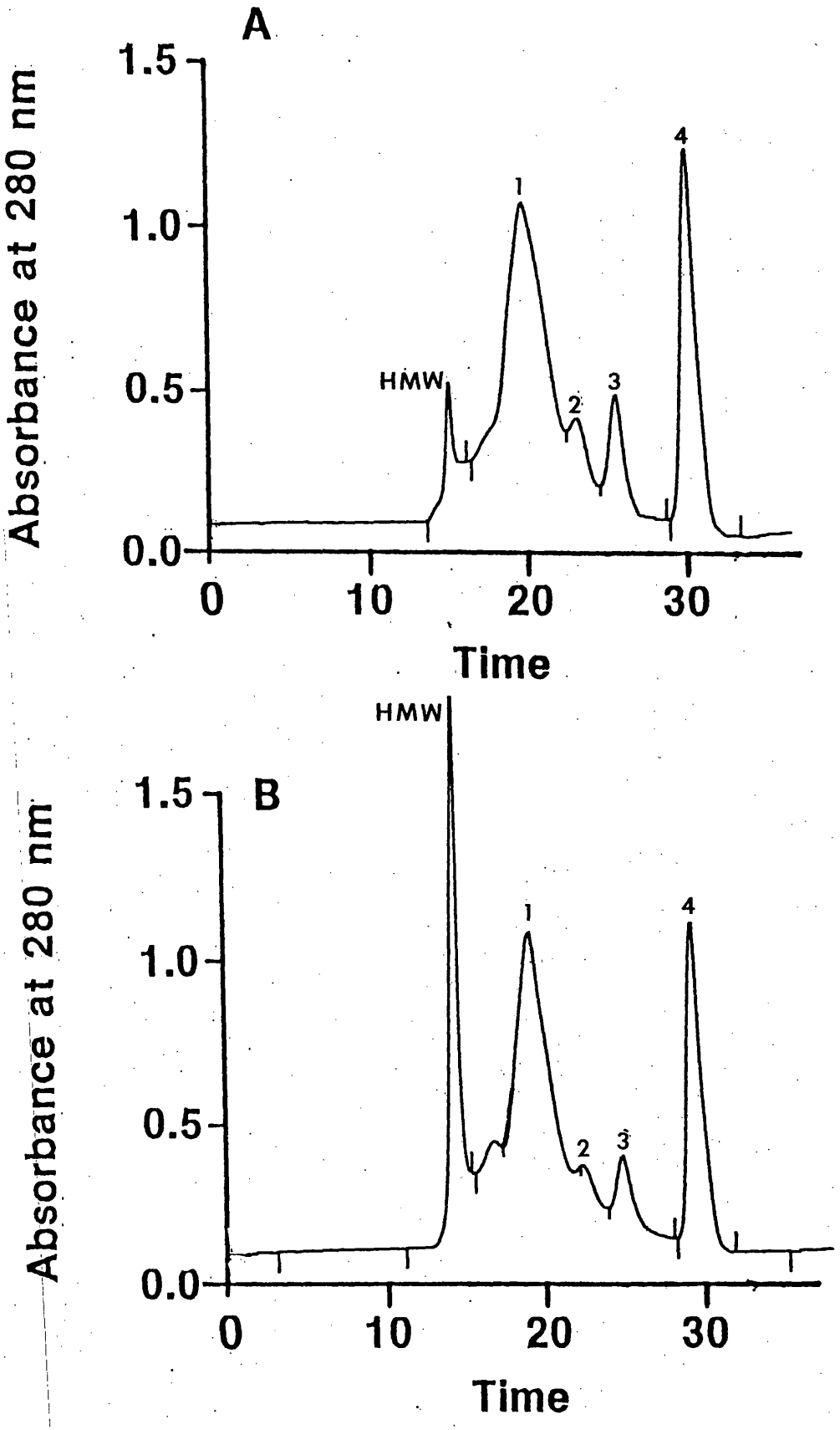
A
1.5
1.0
0.5
0.0
Absorbance at 280 nm
HMW
1
2
3
4
0
10
20
30
Time
B
HMW
1.5
1.0
0.5
0.0
Absorbance at 280 nm
1
2
3
4
0
10
20
30
Time

FIGURE 21. Progressive increases in soluble HMW aggregate

The soluble HMW aggregate was quantified by molecular sieve HPLC. Soluble fraction from each animal were injected (100 μg) onto the HPLC system as described. Shaded bar= diabetic soluble HMW aggregates; unshaded bar=control soluble HMW aggregates. Each group consists of 5 control and 5 diabetic rats. Values are mean ± std. error.

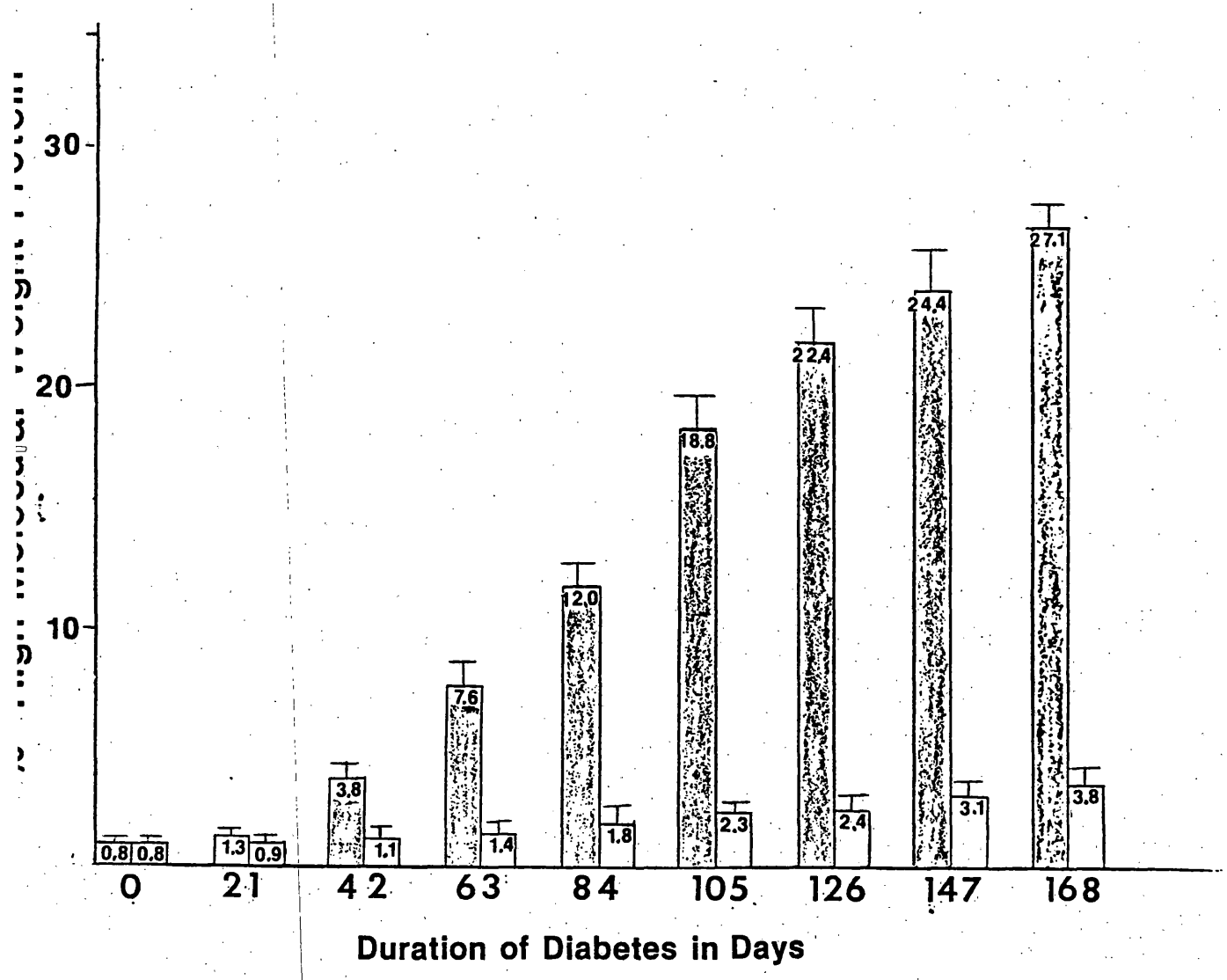
30
20
10
0.8
0.8
1.3
0.9
3.8
1.1
7.6
1.4
12.0
1.8
18.8
2.3
22.4
2.4
24.4
3.1
27.1
3.8
0
21
42
63
84
105
126
147
168
Duration of Diabetes in Days

FIGURE 22. Levels of insoluble HMW aggregate in diabetic and control rats

The insoluble HMW aggregate was quantified by injection (100 µg) of insoluble fraction onto molecular sieve HPLC as described. Shaded bar=diabetic insoluble HMW aggregates; unshaded bar=control insoluble HMW aggregates. Each group consists of the individual lenses from 5 control and 5 diabetic rats. Values are mean ± std. error.

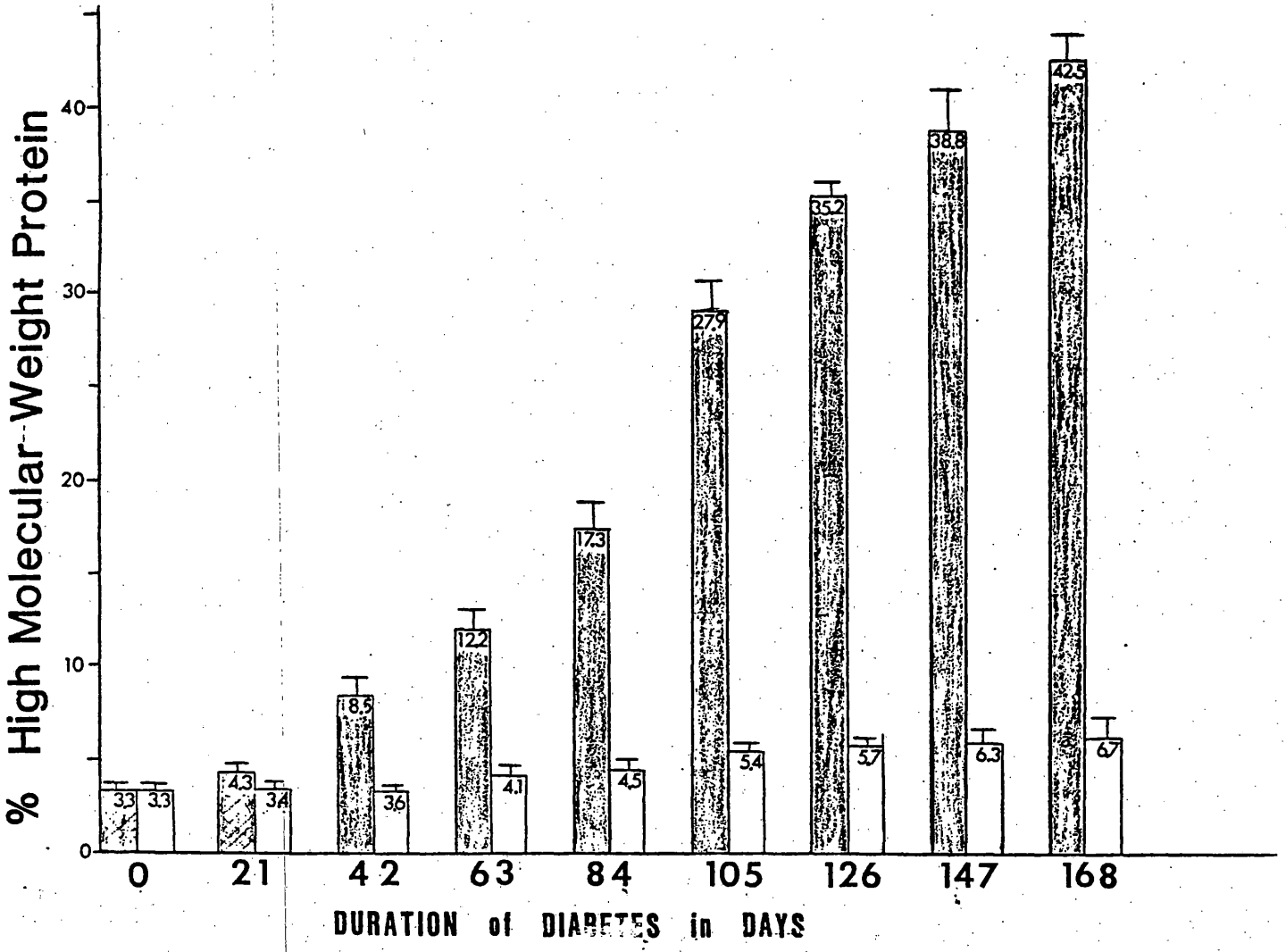
% High Molecular Weight Protein
0
10
20
30
40
3.3
3.3
4.3
3.4
8.5
3.6
12.2
4.1
17.3
4.5
27.9
5.4
35.2
5.7
38.8
6.3
42.5
6.7
0
21
42
63
84
105
126
147
168
DURATION of DIABETES in DAYS

2) Progressive changes in the soluble lens crystallin composition:

The molecular sieve HPLC methodologies developed for the quantification of the HMW proteins was also used to separate and examine the various crystallin components from the soluble fraction. The results in Table III show only a minimal change in the crystallin composition of the soluble fraction from the control animal lenses. As noted previously there was a slight increase in the HMW fraction, although the α-crystallin and β-crystallins remained constant. Neither the α-crystallin or the β-crystallins demonstrated any pattern of increasing or decreasing percentages while the γ-crystallin showed only a slight decrease from 38% to 31% (Table IV). In the diabetic group there is not only an increase in the HMW protein but a corresponding decrease in the γ-crystallin fraction. The γ-crystallin values decreases in a linear fashion from 38.5% to 16.8% at the onset of cataracts and decreasing further to 11.3% as the experiment continues to 168 days. However, there was no overall change in either the α-crystallin or β-crystallins percentages within the soluble fraction.

3) Progressive changes in the protein composition of the insoluble fraction:

As with the soluble fraction, the insoluble (urea-soluble) fraction demonstrates changes in its protein composition as diabetic hyperglycemia continues. In addition to the HMW protein there are 4 protein fractions separated by molecular sieve HPLC. These peaks are labeled peak 1 through 4 as shown in Figure 20. Table V shows the percent composition of the various components of the urea-soluble fraction as measured during the 168 day experimental duration. Similar to the

TABLE III. Hyperglycemia dependent changes in water-soluble fraction crystallin composition from diabetic lenses

TABLE III

Day	Crystallin component (%)			
	HMW	α	β	γ
0	0.8 ± 0.2	26.0 ± 0.4	34.7 ± 2.1	38.5 ± 3.0
21	1.3 ± 0.3	25.4 ± 0.5	37.4 ± 1.8	35.9 ± 2.1
42	3.8 ± 0.5	27.3 ± 1.3	38.7 ± 2.0	30.2 ± 2.7
63	7.6 ± 0.6	25.9 ± 1.8	39.9 ± 1.3	26.6 ± 3.4
84	12.0 ± 0.8	26.9 ± 1.5	40.4 ± 3.1	20.7 ± 2.7
105	18.8 ± 0.9	28.0 ± 2.1	36.4 ± 2.6	16.8 ± 1.9
126	22.4 ± 1.4	27.2 ± 1.8	36.2 ± 3.0	14.2 ± 3.4
147	24.4 ± 2.3	28.3 ± 2.0	34.6 ± 2.1	12.7 ± 4.0
168	27.1 ± 3.1	25.7 ± 2.4	35.9 ± 1.8	11.3 ± 3.5

Values are mean ± std. error

n = 5

TABLE IV. Age dependent changes in the water-soluble lens crystallins from nondiabetic control rats

TABLE IV

Day	Crystallin component (%) HMW	α	β	γ
0	0.8 ± 0.2	26.0 ± 3.4	34.7 ± 2.1	38.5 ± 1.6
21	0.9 ± 0.4	25.8 ± 0.5	35.3 ± 3.8	38.0 ± 3.1
42	1.1 ± 0.3	25.9 ± 1.2	35.8 ± 2.7	37.2 ± 3.4
63	1.4 ± 0.8	26.2 ± 2.8	35.4 ± 3.1	37.0 ± 2.8
84	1.8 ± 0.9	27.1 ± 2.4	36.0 ± 2.5	35.1 ± 3.7
105	2.3 ± 1.2	26.3 ± 3.6	37.1 ± 4.0	34.3 ± 2.4
126	2.4 ± 2.3	25.4 ± 2.3	37.8 ± 3.2	34.4 ± 1.9
147	3.1 ± 1.4	25.9 ± 3.1	38.7 ± 4.1	32.3 ± 3.2
168	3.8 ± 1.8	27.3 ± 3.4	37.1 ± 3.4	31.8 ± 2.1

Values are mean ± std. error

n = 5

TABLE V. Progressive changes in urea-soluble fraction components from diabetic lenses determined by molecular sieve HPLC

TABLE V

Day	Fraction component (%)				
	HMW	Peak 1	Peak 2	Peak 3	Peak 4
0	3.3 ± 0.5	25.3 ± 3.8	13.5 ± 2.1	20.0 ± 2.3	41.2 ± 3.2
21	4.3 ± 1.2	26.4 ± 2.1	14.2 ± 3.1	19.1 ± 2.1	36.0 ± 2.4
42	8.5 ± 2.4	28.2 ± 3.4	14.9 ± 1.9	18.3 ± 3.4	30.1 ± 3.1
63	12.2 ± 1.8	28.1 ± 2.7	18.4 ± 4.2	15.9 ± 2.0	25.4 ± 4.3
84	17.3 ± 2.0	30.9 ± 4.1	16.7 ± 2.1	12.8 ± 1.9	22.3 ± 2.7
105	27.2 ± 1.9	32.2 ± 2.3	11.2 ± 4.8	11.4 ± 1.3	18.0 ± 3.9
126	25.2 ± 2.3	34.3 ± 3.0	7.4 ± 3.1	10.2 ± 2.4	12.9 ± 4.6
147	38.8 ± 3.2	35.7 ± 3.6	9.5 ± 3.8	9.3 ± 3.2	6.7 ± 4.8
168	42.7 ± 3.6	36.6 ± 4.1	9.9 ± 4.0	8.6 ± 3.1	2.2 ± 4.0

Values are mean ± std. error

n = 5

soluble fraction, there was little change in the protein components within the control lenses (Table VI). In addition to the HMW increase there was also a small increase in peak 1 and a decrease in peak 4. The peaks 2 and 3 demonstrated no significant changes. As hyperglycemia continued in the diabetic animals, significant changes occurred in all the components. Most notably peak 4 decreases from 41% (±3.2) at day 0 to 2.2% (±4.0) after 168 days of hyperglycemia. Peaks 2 and 3 showed similar but not as dramatic decreases with peak 2 decreasing from 13.5 (±2.1) to 9.9 (±4.1) and peak 3 dropping from 20% (±2.3) to 8.6 (±3.1). The protein component represented in peak 1 showed an increase from 25.3% (±3.8) to 36.6% (±4.1), however this increase was not as dramatic as the increase noted in the HMW protein.

The nature of the bonds which held together the components of the HMW aggregates was examined by the use of molecular sieve HPLC in the presence of dissociating buffers. Figure 23 shows the effect of 7 M urea on the crystallin components from the soluble fraction. The presence of 7 M urea completely dissociated the HMW fraction as well as the other cyrstallin aggregates into their various subunit components. By using molecular weight markers the molecular weight for peak A was 43,000 daltons, peak B was 28,000 daltons, and peak C was 20,000 daltons, which correspond to the β-crystallin subunits, α-crystallin subunits, and γ-crystallin, respectively.

The insoluble HMW aggregate is not dissociated by the presence of urea as shown in Figure 24A. But is dissociated by the addition of β-mercaptoethanol which disrupts disulfide bonds (Fig. 24B). Thus, it appears that the soluble HMW aggregate is held together by non-covalent forces while the insoluble HMW aggregate is disulfide linked. As

TABLE VI. Age dependent changes in the urea-soluble proteins from non-diabetic control rats

TABLE VI

Day	Protein component (%)				
	HMW	Peak 1	Peak 2	Peak 3	Peak 4
0	3.3 ± 0.5	25.3 ± 3.8	13.5 ± 2.1	20.0 ± 2.3	41.2 ± 3.2
21	3.4 ± 1.2	25.8 ± 4.3	11.8 ± 3.1	20.3 ± 3.1	40.3 ± 3.1
42	3.6 ± 1.8	25.7 ± 3.1	10.1 ± 4.3	20.4 ± 2.9	40.2 ± 2.8
63	4.1 ± 1.5	26.7 ± 4.2	11.8 ± 3.8	20.9 ± 4.1	41.5 ± 4.3
84	4.5 ± 1.4	27.1 ± 3.2	14.1 ± 4.1	19.7 ± 3.7	38.6 ± 2.8
105	5.4 ± 2.1	27.4 ± 2.4	12.8 ± 2.8	18.3 ± 3.9	39.1 ± 3.9
126	5.7 ± 1.3	28.5 ± 4.0	12.1 ± 3.3	18.4 ± 2.2	37.3 ± 3.4
147	6.3 ± 1.4	29.4 ± 3.6	11.2 ± 1.3	20.3 ± 1.8	35.8 ± 4.1
168	6.7 ± 1.1	29.8 ± 2.2	12.4 ± 3.1	21.4 ± 3.1	35.7 ± 3.7

Values are mean ± std. error

n = 5

FIGURE 23. Molecular sieve HPLC separations of the soluble fraction in the absence and presence of 7 M urea

The soluble fraction from 168 day diabetic cataract lens was separated by molecular sieve HPLC in the absence (A) and presence of 7 M urea (B). The addition of the urea completely dissociated the soluble HMW aggregate.

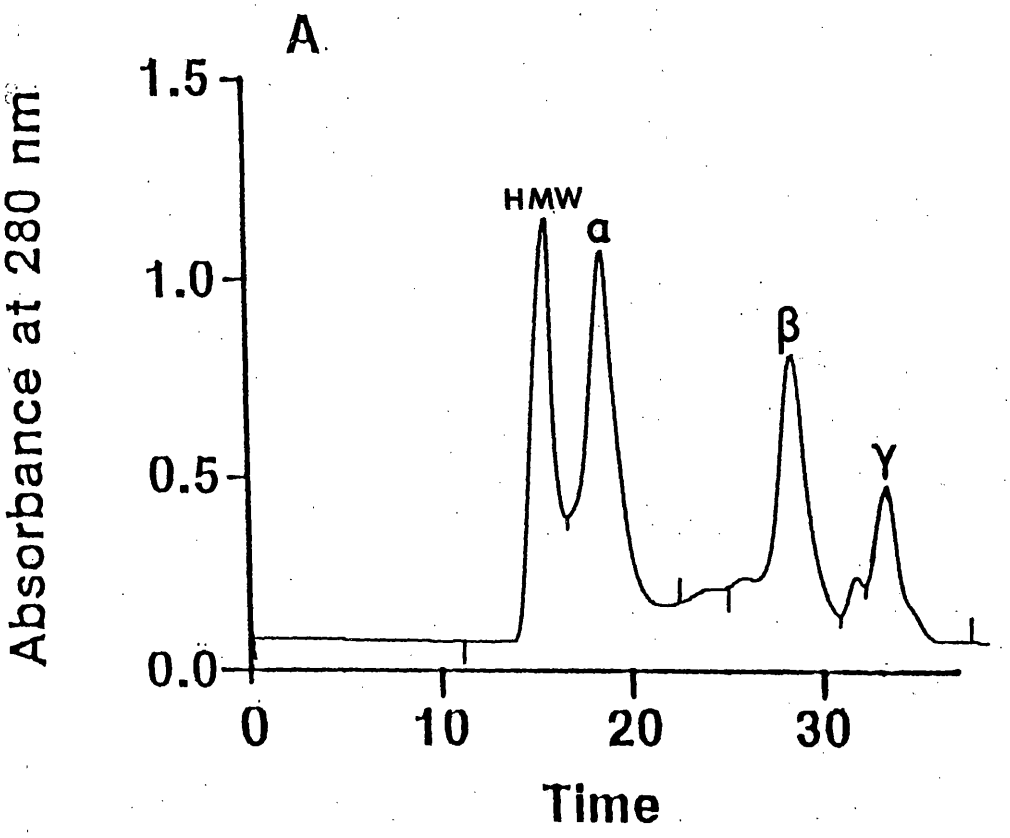
A
Absorbance at 280 nm
1.5
1.0
0.5
0.0
HMW
α
β
γ
0
10
20
30
Time

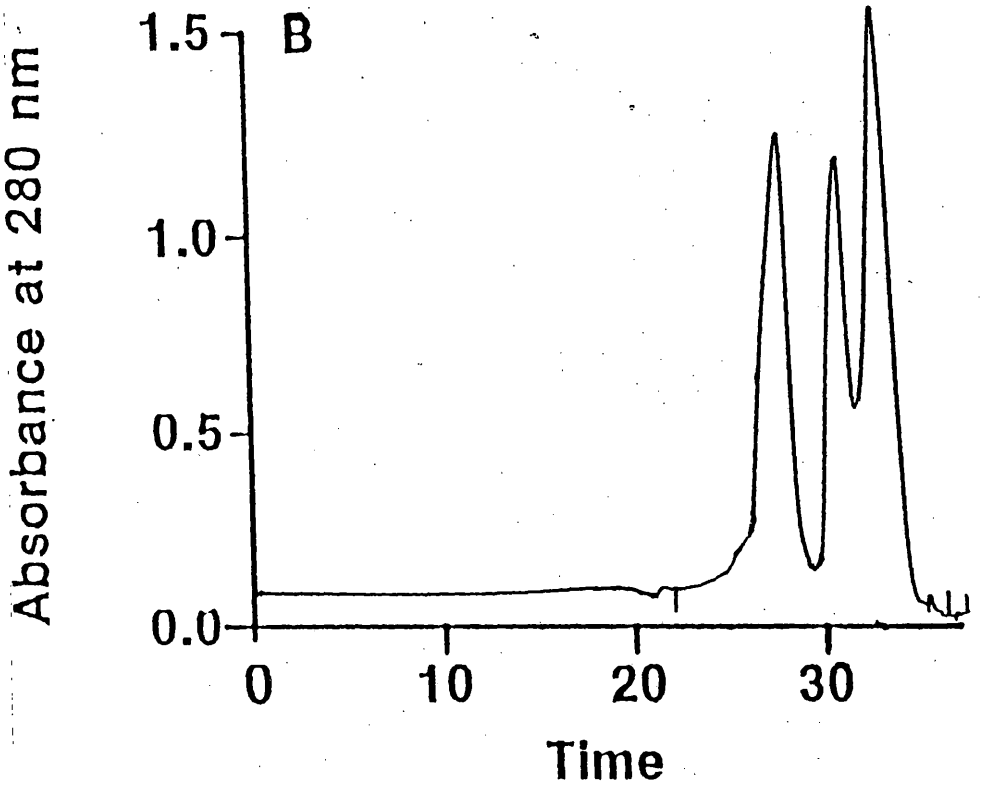
B
Absorbance at 280 nm
1.5
1.0
0.5
0.0
0
10
20
30
Time

FIGURE 24. Molecular sieve HPLC separations of the urea-soluble fraction: effect of β-mercaptoethanol

The insoluble fraction from 168 day diabetic cataract lens was separated by molecular sieve HPLC using 7 M urea buffer as described in methods. A) Insoluble fraction before addition of β-mercaptoethanol showing prominant insoluble HMW aggregate. B) Insoluble fraction after incubation with 0.5% β-mercaptoethanol demonstrating dissociation of the HMW peak.

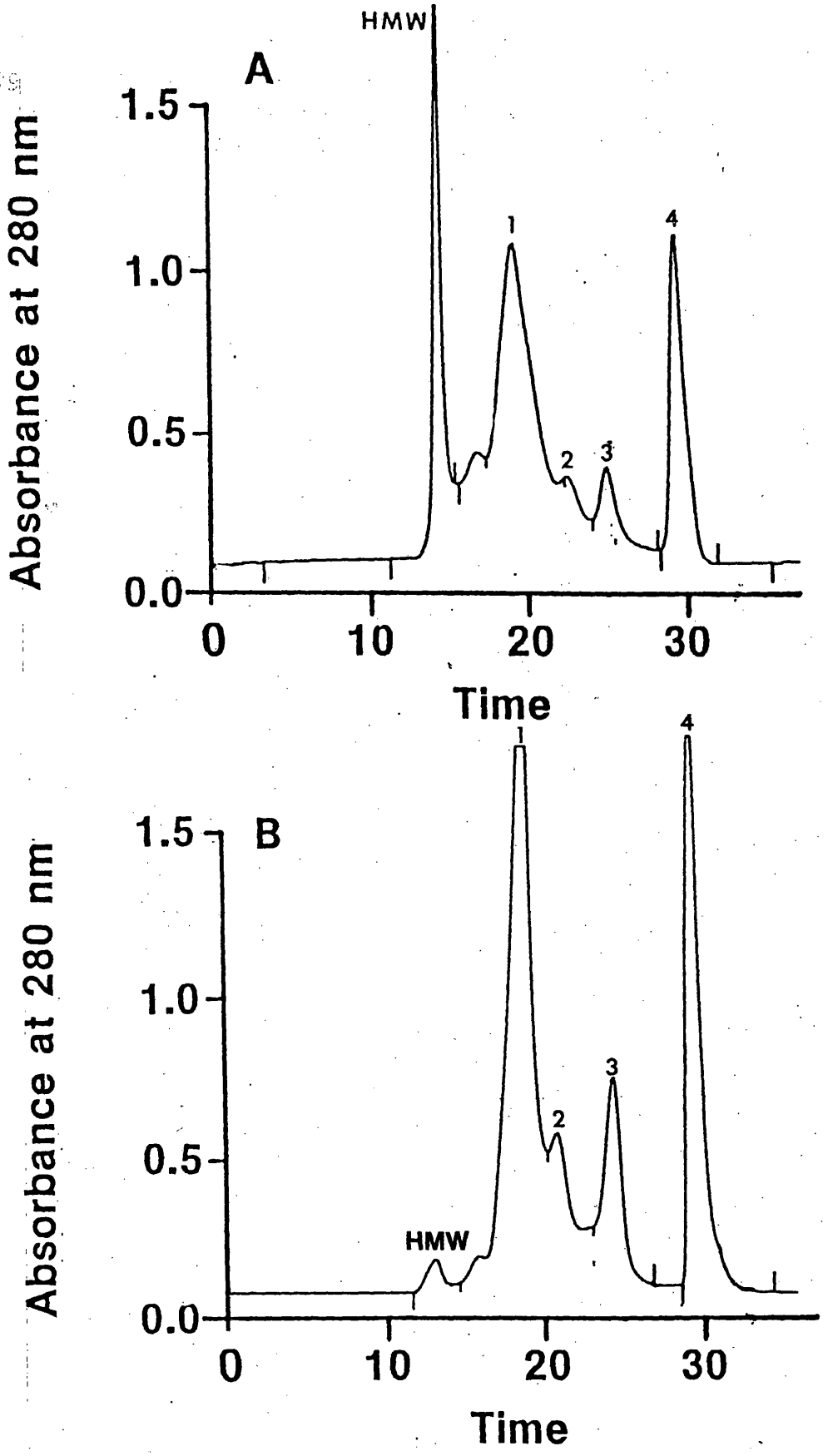
A
HMW
1
2
3
4
1.5
1.0
0.5
0.0
Absorbance at 280 nm
0
10
20
30
Time
B
HMW
1
2
3
4
1.5
1.0
0.5
0.0
Absorbance at 280 nm
0
10
20
30
Time

demonstrated in Figure 24B, reduction of the insoluble HMW aggregate with β-mercaptoethanol results in dissociation of the aggregate and an increase in peaks 1, 3, and 4.

II. Characterization of the Insoluble Fraction and High Molecular Weight Aggregates

A) Crystallin Components of the Insoluble (Urea-soluble) Fraction

The composition of the soluble crystallins has been extensively studied while the exact nature of the insoluble fraction has remained in debate. A reverse phase HPLC system was developed using a large pore C-4 column and a 1% TFA:acetonitrile gradient for the separation of the lens crystallin subunits. The TFA:acetonitrile mobile phase dissociated each crystallin into its individual subunits (Figure 25A). The identity of each peak was determined by amino acid analysis using the Beckman 121M amino acid analyzer and is shown in Table VII. This C-4 reverse phase HPLC system separates the α-crystallin into its αA and αB subunits as well as the β-crystallin into the βBp, βBs, βB1, and βB2 constituent subunits. The γ-crystallin, which is a monomer, was also separated from the other crystallin subunits as a single peak.

This C-4 reverse phase HPLC system was used to elucidate the nature of the urea-soluble fraction. The urea solubilized insoluble fraction was first reduced with β-mercaptoethanol prior to injection onto the reverse phase HPLC system. The β-mercaptoethanol reduction was essential without which the large insoluble HMW aggregate would have clogged the C-4 column. The results of the injection of the treated insoluble fraction from control lenses are shown in Figure 25B. The resulting chromatogram demonstrated that the urea-soluble fraction is comprised of the same crystallin subunits found in the soluble fraction.

FIGURE 25. C-4 reverse phase HPLC separations of lens crystallin subunits from the soluble and insoluble fractions of control lenses

The crystallin subunit components from the soluble fraction (A) and the insoluble fraction (B) of 168 day control lens were separated and quantified by C-4 reverse phase HPLC. The peak identities were confirmed by amino acid analysis as described. Mobile phase was TFA:acetonitrile gradient, 1.0 AUFS, sample size of 200 µg.

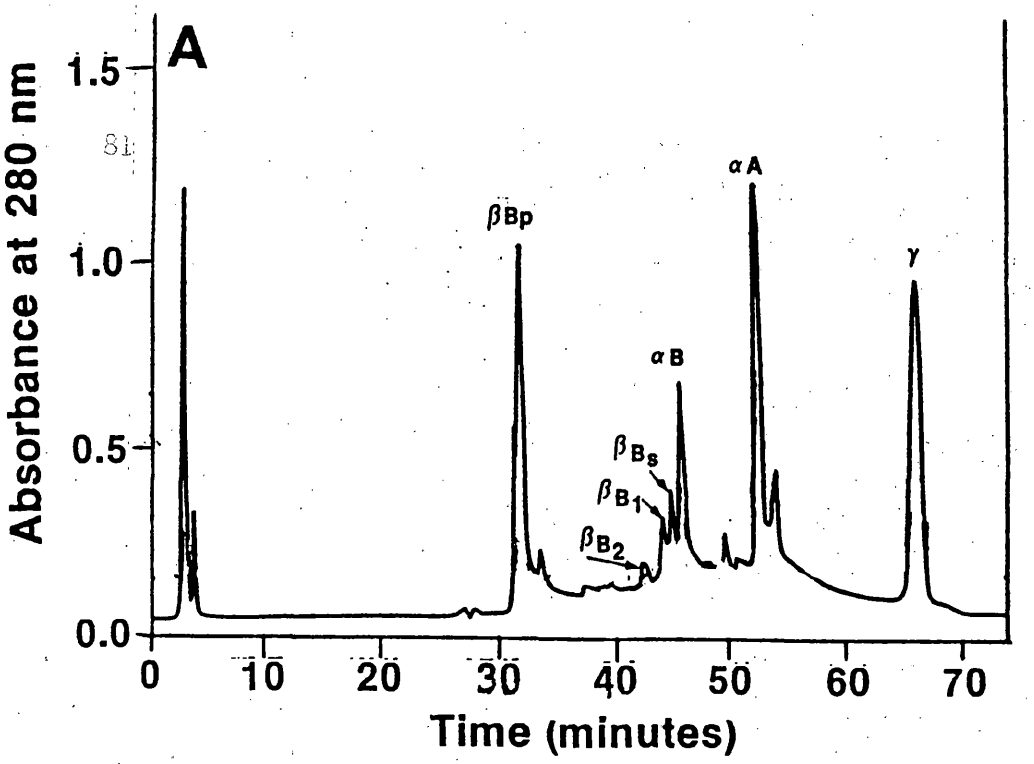
A
Absorbance at 280 nm
1.5
1.0
0.5
0.0
βBp
αA
γ
αB
βBs
βB1
βB2
0
10
20
30
40
50
60
70
Time (minutes)

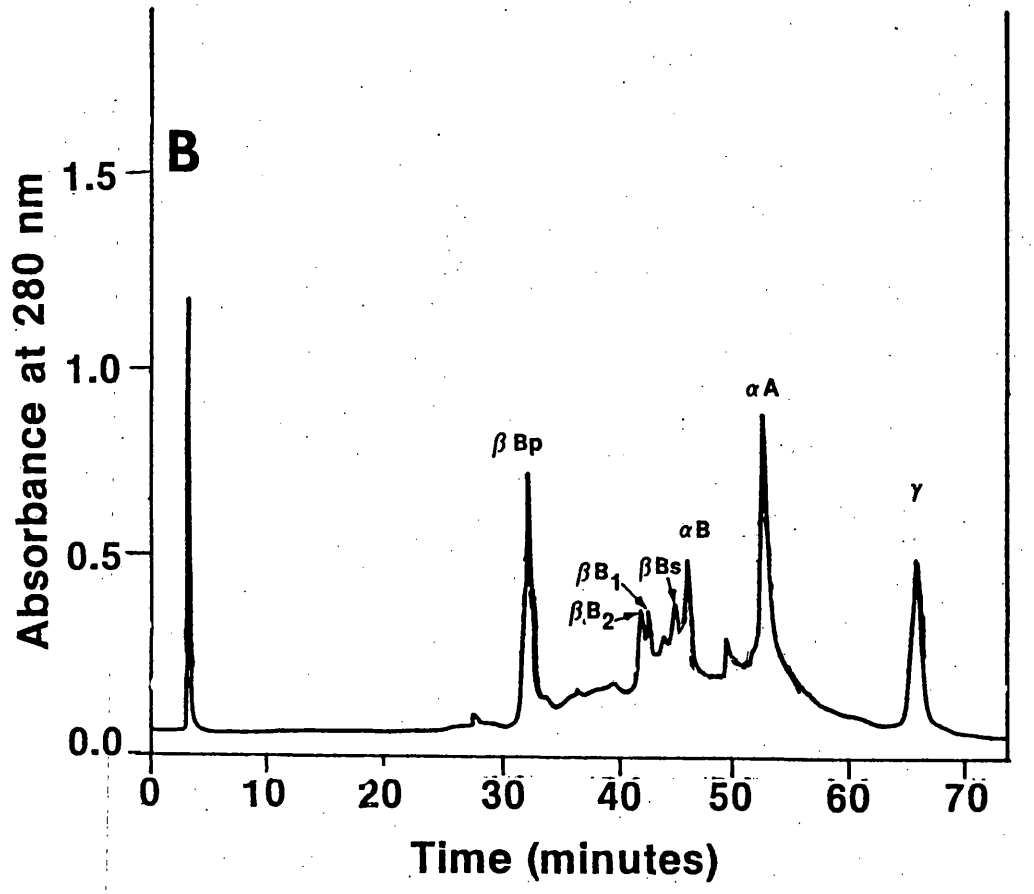
B
Absorbance at 280 nm
1.5
1.0
0.5
0.0
βBp
αA
γ
αB
βB1
βBs
βB2
0
10
20
30
40
50
60
70
Time (minutes)

TABLE VII. Relative amino acid composition of crystallin subunits of soluble fraction

Values are from control animals at 168 day experimental duration. The total values not equal to 1000 are due to rounding of the numbers.

TABLE VII

Amino Acid	Peak 1 βBp	Peak 2 βBs	Peak 3 βB2	Peak 4 βB1	Peak 5 αB	Peak 6 αA	Peak 7 γ
Asp	85(83)[a]	78(80)[b]	82(80)[c]	90(89)[d]	79(75)[e]	93(97)[f]	165(166)[g]
Thr	27(34)	30(28)	37(35)	25(28)	42(44)	30(37)	29(30)
Ser	86(84)	77(75)	88(85)	61(61)	92(96)	125(126)	77(76)
Glu	155(158)	148(148)	156(158)	125(126)	100(100)	99(95)	130(127)
Pro	68(68)	72(76)	51(49)	37(37)	92(94)	65(67)	50(48)
Gly	91(93)	78(80)	104(106)	83(87)	58(56)	63(60)	55(57)
Ala	40(42)	57(58)	53(53)	57(57)	52(53)	36(35)	30(29)
Cys	10(09)	12(?)	14(13)	30(37)	00(00)	05(06)	43(?)
Val	72(75)	58(59)	68(67)	47(49)	52(55)	54(55)	50(50)
Met	11(09)	21(18)	07(09)	27(33)	19(13)	13(12)	28(30)
Ile	30(31)	33(32)	30(26)	37(41)	38(47)	45(50)	32(36)
Leu	48(50)	45(47)	59(59)	57(57)	84(84)	82(84)	70(70)
Tyr	47(44)	45(43)	50(47)	59(65)	17(14)	29(33)	70(83)
Phe	42(40)	52(50)	60(55)	57(57)	73(70)	77(78)	60(57)
His	44(41)	39(37)	46(47)	43(41)	50(47)	38(41)	37(35)
Lys	59(60)	59(60)	50(52)	47(49)	54(58)	38(41)	24(25)
Arg	52(50)	87(90)	68(62)	74(73)	82(78)	80(73)	110(111)
TOTAL	967	991	1023	956	984	972	1060

Values in parentheses represent expected values (Ref. 66).

a-f = from bovine

g = from rat

The peak identity was confirmed by amino acid composition (Table VIII). The chromatogram demonstres that the proportion of the subunits are only slightly different in the urea-soluble fraction compared to the water-soluble fraction.

These differences in composition between the soluble and urea-soluble fraction are more dramatic in the cataract lenses. Figure 26 shows the chromatograms from the soluble and urea-soluble fraction from diabetic cataract lenses after 168 days of hyperglycemia. There is considerably more β-crystallin subunits and γ-crystallin present in the urea-soluble fraction compared to the water-soluble fraction. Conversely, there is significantly less of the α-crystallin subunits in the urea-soluble fraction than in the water-soluble fraction. The same differences were also noted when the urea-soluble fraction from the cataract lenses was compared to both fractions from the control lenses.

B) Crystallin Components of the HMW Aggregates

1) Soluble HMW aggregate:

The soluble HMW aggregate from diabetic cataract was isolated by molecular sieve HPLC from the water-soluble fraction and concentrated by ultra-filtration. This aggregate was then injected onto the C-4 reverse phase HPLC system to separate the crystallin subunits. The results shown in Figure 27A demonstrate that the soluble HMW aggregate is composed primarily of γ-crystallin (85%) with the remainder being a combination of α- and β-crystallin subunits. This finding in conjunction with C-4 reverse phase HPLC separations of the cataract soluble fraction are in agreement with the results obtained by molecular sieve HPLC separations of the cataract soluble fraction. These results all demonstrate a loss of γ-crystallin and an increase in the HMW aggregate compared to the normal lenses.

FIGURE 26. C-4 reverse phase HPLC separations of lens crystallin subunits from the soluble and insoluble fractions of diabetic cataract lenses

The crystallin subunits from the soluble fraction (A) and the insoluble fraction (B) from diabetic cataract lens were separated and quantified by C-4 reverse phase HPLC. Mobile phase consisted of TFA:acetonitrile gradient, absorbance monitored at 280 nm with sensitivity set at 1.0 AUFS and sample size of 200 µg.

84

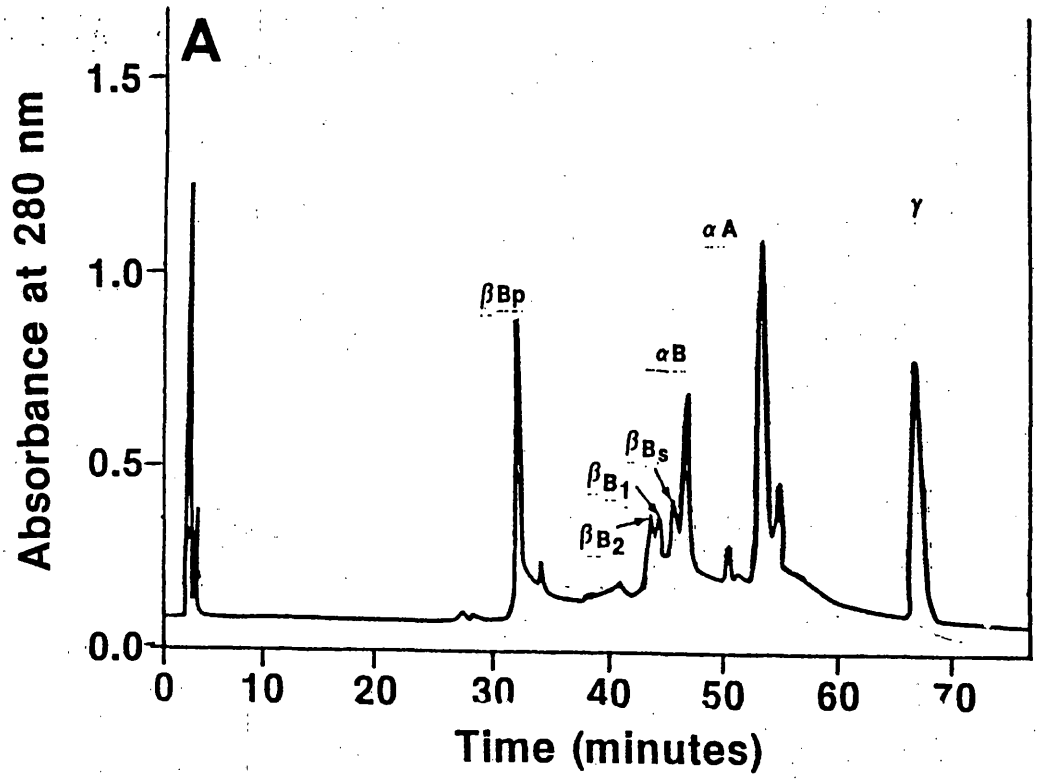
A
Absorbance at 280 nm
1.5
1.0
0.5
0.0
βBp
αA
γ
αB
βBs
βB1
βB2
0
10
20
30
40
50
60
70
Time (minutes)

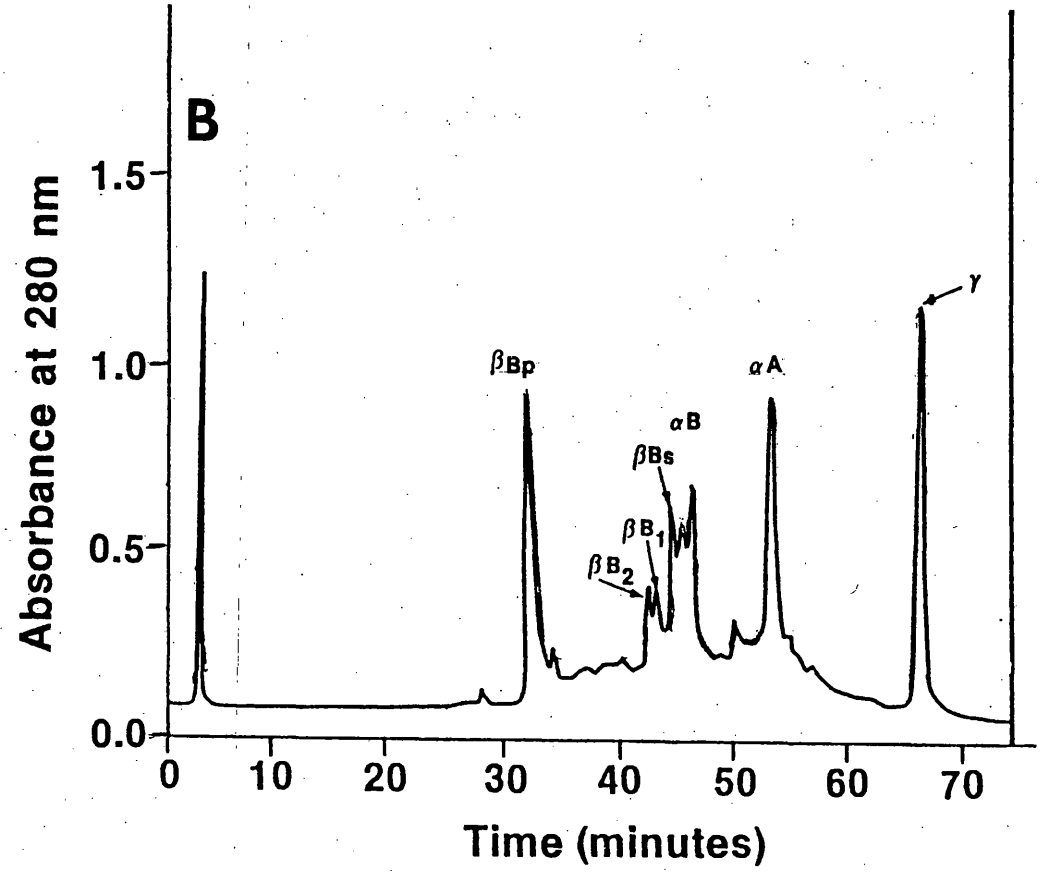
B
Absorbance at 280 nm
1.5
1.0
0.5
0.0
γ
βBp
αA
αB
βBs
βB1
βB2
0
10
20
30
40
50
60
70
Time (minutes)

TABLE VIII. Relative amino acid composition of crystallin subunits of insoluble fraction

Values are from control animals at 168 day experimental duration. Values not equal to 1000 are due to rounding of the numbers.

TABLE VIII

Amino Acid	Peak 1 βBp	Peak 2 βBs	Peak 3 βB2	Peak 4 βB1	Peak 5 αB	Peak 6 αA	Peak 7 γ
Asp	85(83)[a]	78(80)[b]	80(80)[c]	90(89)[d]	79(75)[e]	95(97)[f]	160(166)[g]
Thr	28(34)	30(28)	37(35)	26(28)	43(44)	31(37)	29(30)
Ser	86(84)	76(75)	88(85)	61(61)	94(96)	125(126)	77(76)
Glu	155(158)	148(148)	156(158)	125(126)	100(100)	99(95)	121(127)
Pro	68(68)	72(76)	51(49)	37(37)	92(94)	65(67)	45(48)
Gly	91(93)	78(80)	104(106)	82(87)	59(56)	63(60)	54(57)
Ala	40(42)	57(58)	53(53)	57(57)	52(53)	36(35)	28(29)
Cys	10(09)	12(?)	14(13)	30(37)	00(00)	05(06)	42(?)
Val	74(75)	58(59)	68(67)	49(49)	55(55)	54(55)	45(50)
Met	11(09)	21(18)	07(09)	27(33)	19(13)	13(12)	29(30)
Ile	28(31)	33(32)	29(26)	37(41)	42(47)	45(50)	35(36)
Leu	48(50)	45(47)	59(59)	57(57)	84(84)	82(84)	70(70)
Tyr	47(44)	45(43)	50(47)	59(65)	17(14)	29(33)	81(83)
Phe	42(40)	52(50)	60(55)	57(57)	73(70)	77(78)	52(57)
His	44(41)	39(37)	46(47)	43(41)	50(47)	38(41)	37(35)
Lys	59(60)	59(60)	50(52)	47(49)	54(58)	38(41)	24(25)
Arg	52(50)	87(90)	68(62)	74(73)	82(78)	80(73)	110(111)
TOTAL	968	990	1020	960	995	975	1039

Values in parentheses represent expected values (Ref. 1).

a-f = from bovine

g = from rat

FIGURE 27. Separation and identification of crystallin subunit components of the soluble HMW aggregate and the insoluble HMW aggregate by C-4 reverse phase HPLC

C-4 reverse phase HPLC was used to identify the crystallin subunit components of the soluble HMW aggregate isolated by molecular sieve HPLC (A) and the insoluble HMW aggregate also isolated by molecular sieve HPLC (B). Two hundred micrograms of each sample were injected onto the C-4 reversed phase HPLC system with absorbance monitored at 280 nm and sensitivity of 1.0 AUFS.

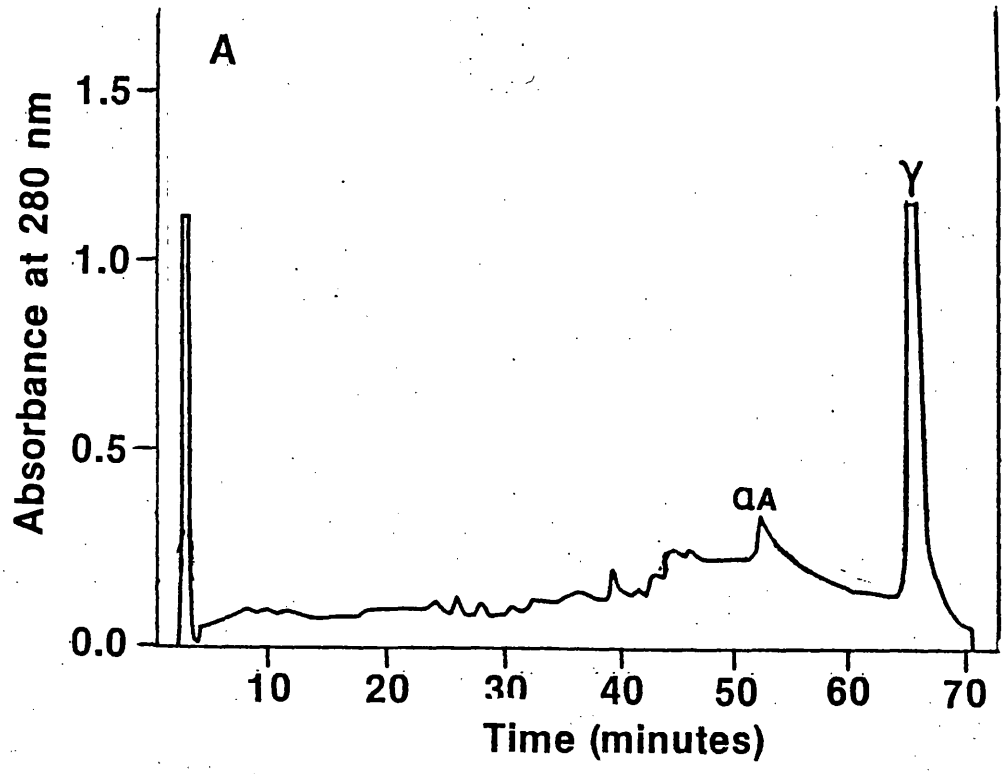
A
Absorbance at 280 nm
1.5
1.0
0.5
0.0
γ
αA
10
20
30
40
50
60
70
Time (minutes)

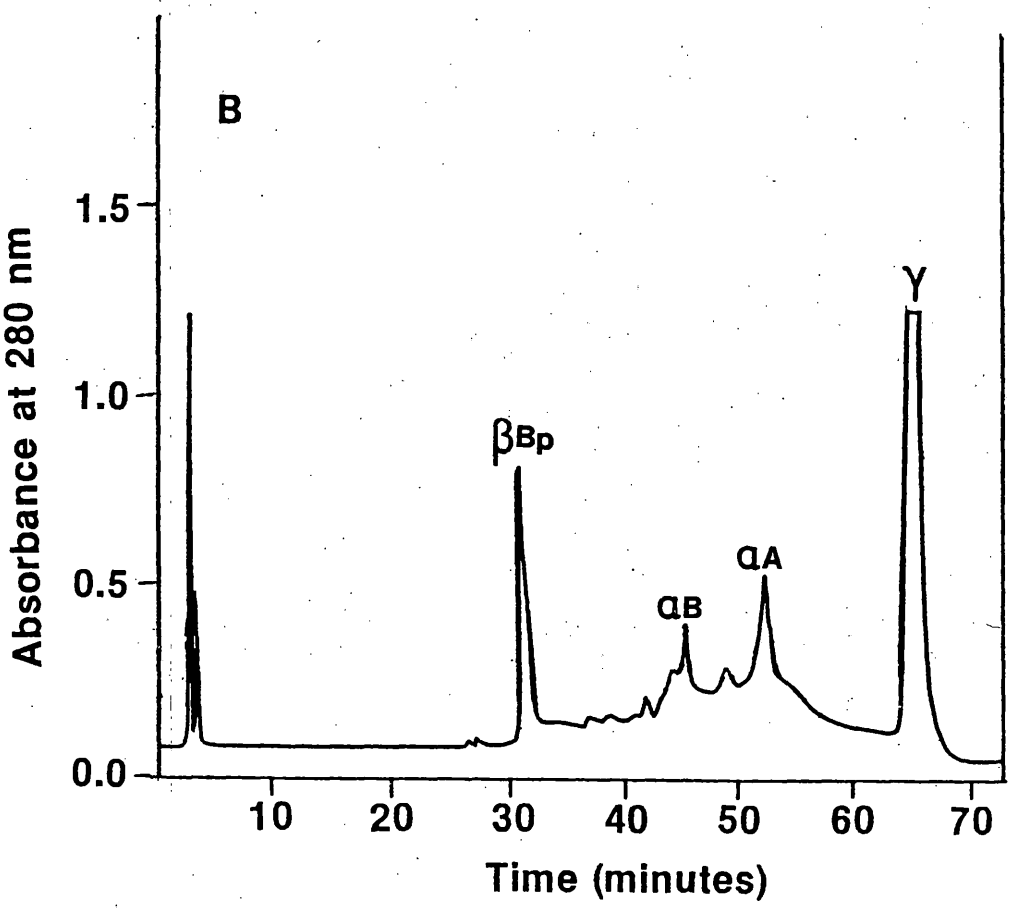
B
Absorbance at 280 nm
1.5
1.0
0.5
0.0
γ
βBp
αA
αB
10
20
30
40
50
60
70
Time (minutes)

2) Insoluble HMW aggregate:

It is believed that the water-soluble HMW aggregate is a precursor to the urea-soluble HMW aggregate. If this were true then the polypeptides which compose the insoluble HMW aggregate should be similar to those of its soluble precursor.

The identities of the crystallin components of the insoluble HMW aggregate were determined by injection of β-mercaptoethanol reduced aggregates onto the C-4 reverse phase HPLC system. The results demonstrate that the composition is quite similar to the soluble HMW aggregate (Fig. 27B). THe insoluble HMW aggregate is composed primarly of γ-crystallin (60%) as well as other crystallin components. This aggregate also contains significant amounts of the β-crystallin βBp subunit (25%) and the remainder αA crystallin subunit (15%).

These results are in agreement with the proposed disulfide involvement in the formation of the insoluble aggregate as these components all contain sulfhydryl groups for potential crosslinking. The major component, γ-crystallin, has the highest sulfhydryl content with 6 cysteine residues per polypeptide chain. The other components of this aggregate also contain sulfhydryls with βBp crystallin subunit containing two cysteines and the αA crystallin subunit with one.

III. Characterization and Structural Aspects of Non-enzymatic Glycation of the Lens Crystallin

The extent of non-enzymatic glycation of the lens crystallins and their relationship to the components of the insoluble HMW aggregate was examined through the use of HPLC technique, affinity chromatography, and tritiated borohydride reduction for separation of the glycated protein and followed by peptide and amino acid analysis.

A) Molecular Sieve HPLC Separations of Lens Crystallins After [^{3}H]$NaBH_4$ Reduction

Reduction of the non-enzymatically glycated protein with [^{3}H]sodium borohydride results in the incorporation of one non-exchangeable titrium label for each glycated residue. By separating the crystallins by molecular sieve HPLC after such reductions the extent of glycation of each crystallin component of the soluble fraction may be determined. Figure 28 demonstrates the extent of glycation of each of the soluble components. The specific activity was determined for each peak by dividing the total cpm for each peak by the mg protein for each peak (calculated by % area x total mg injected assuming 100% recovery). In the control lens the highest specific activity is found in the HMW aggregate with 7,500 cpm/mg protein. This is followed by the α-crystallin with 2940 cpm/mg protein. The β- and γ-crystallin have only minimal amounts with 875 cpm/mg protein and 727 cpm/mg protein, respectively. These values are in sharp contrast to the cataract lens. The HMW aggregate specific activity remained consistent with 7380 cpm/mg protein, while the α-crystallin increased to 9340 cpm/mg protein. The β-crystallins demonstrated a moderate increase to 3345 cpm/mg protein, while the γ-crystallin demonstrated the largest increase to 9735 cpm/mg protein.

A more detailed characterization of non-enzymatic glycation of the lens crystallin subunits was demonstrated by C-4 reverse phase HPLC separations of [^{3}H]$NaBH_4$ reduced soluble fraction. As mentioned previously, the C-4 reverse phase HPLC allows for one-step separations of the individual lens crystallin subunits. This system coupled with the tritium borohydride label allows for examination of the non-enzymatic

FIGURE 28. Molecular sieve HPLC separation of [^{3}H]$NaBH_4$ labeled soluble fractions

Tritium borohydride reduced soluble lens crystallins from control (A) and diabetic (B) lenses were separated by molecular sieve HPLC. Fractions were collected (0.5 ml) and added to 10 ml scintillation cocktail and radioactivity counted. Solid line=absorbance at 280 nm; Dashed line=radioactivity in cpm.

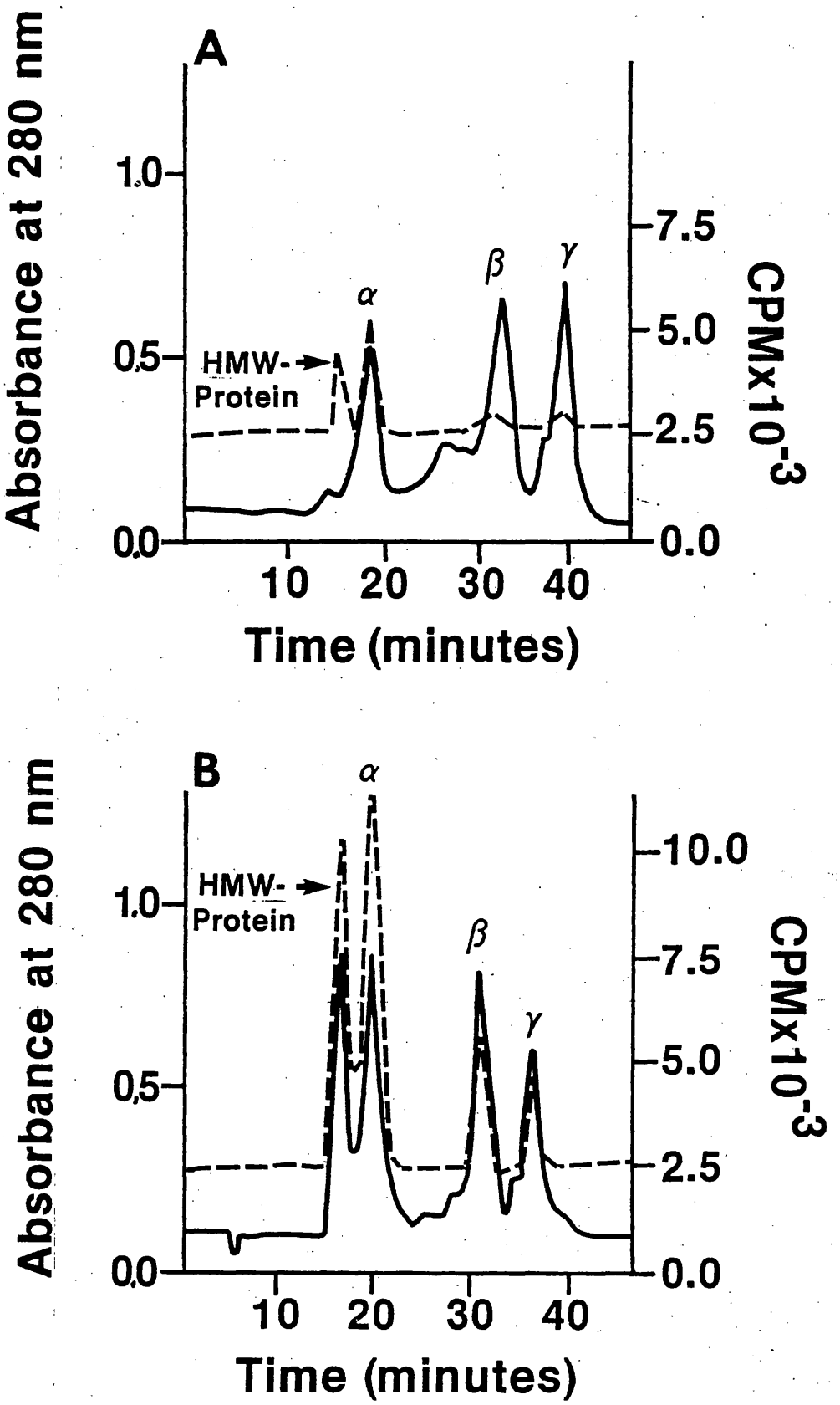
A
Absorbance at 280 nm
1.0
0.5
0.0
HMW-
Protein
α
β
γ
7.5
5.0
2.5
0.0
CPMx10-3
10
20
30
40
Time (minutes)
B
Absorbance at 280 nm
1.0
0.5
0.0
HMW-
Protein
α
β
γ
10.0
7.5
5.0
2.5
0.0
CPMx10-3
10
20
30
40
Time (minutes)

glycation at the subunit level. Figure 29 shows the subunit separations and radioactive distribution of the various crystallin subunits from control lenses and diabetic cataract lenses. These data correlate well with that obtained from molecular sieve HPLC separations. The control lenses show glycation (measured by tritium incorporation) present primarily in the α-crystallin subunits, αB and αA with only marginal incorporation in the β-crystallin Bp subunit. The γ-crystallin showed slightly more activity than the β-crystallin Bp subunit but much less than the α-crystallin subunits. The diabetic cataract lens subunits showed a significant increase in glycation, again similar to that demonstrated by molecular sieve HPLC separations of the intact lens crystallins. The γ-crystallin had the largest increase in glycation of any of the crystallin components. The α-crystallin subunits αB and αA also showed an increase in tritium incorporation. All of the β-crystallin subunits, especially Bp, demonstrated significant increases in glycation as compared to the control. These increases in glycation of the crystallin subunits can also be demonstrated by comparison of the specific activities presented in Table IX. This comparison shows that the largest increase in glycation occurred in the γ-crystallin and the β-crystallin subunits. The α-crystallin subunits demonstrated a high level of glycation in the diabetic cataract lens but the increase from the control lens values was less than the other crystallin components.

B) Tritiated Borohydride Reduction of the Insoluble Crystallin Components

The insoluble (urea-soluble) fraction was reduced with the $[^3H]NaBH_4$ in the same manner as the soluble fraction and the components separated by the molecular sieve and C-4 reverse phase HPLC systems.

FIGURE 29. C-4 reversed phase HPLC separation of [^{3}H]$NaBH_4$ labeled soluble fractions

Tritiated borohydride reduced soluble lens crystallins from control lens (A) and diabetic cataract lens (B) were separated into their constituent crystallin subunits by C-4 reverse phase HPLC. Radioactivity was monitored in 0.5 ml fractions. Solid line=absorbance at 280 nm; Dashed line=radioactivity in cpm.

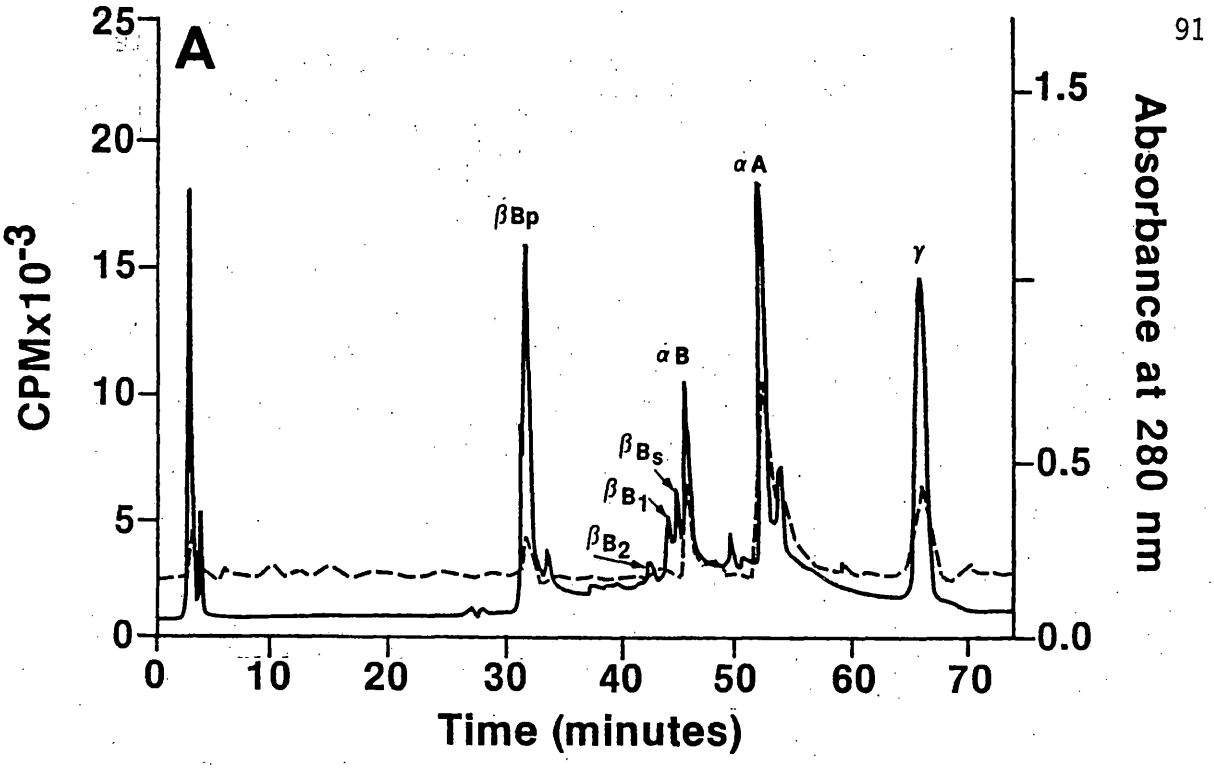
A
CPMx10-3
Absorbance at 280 nm
Time (minutes)
βBp
αA
γ
αB
βBs
βB1
βB2
25
20
15
10
5
0
1.5
0.5
0.0
0
10
20
30
40
50
60
70

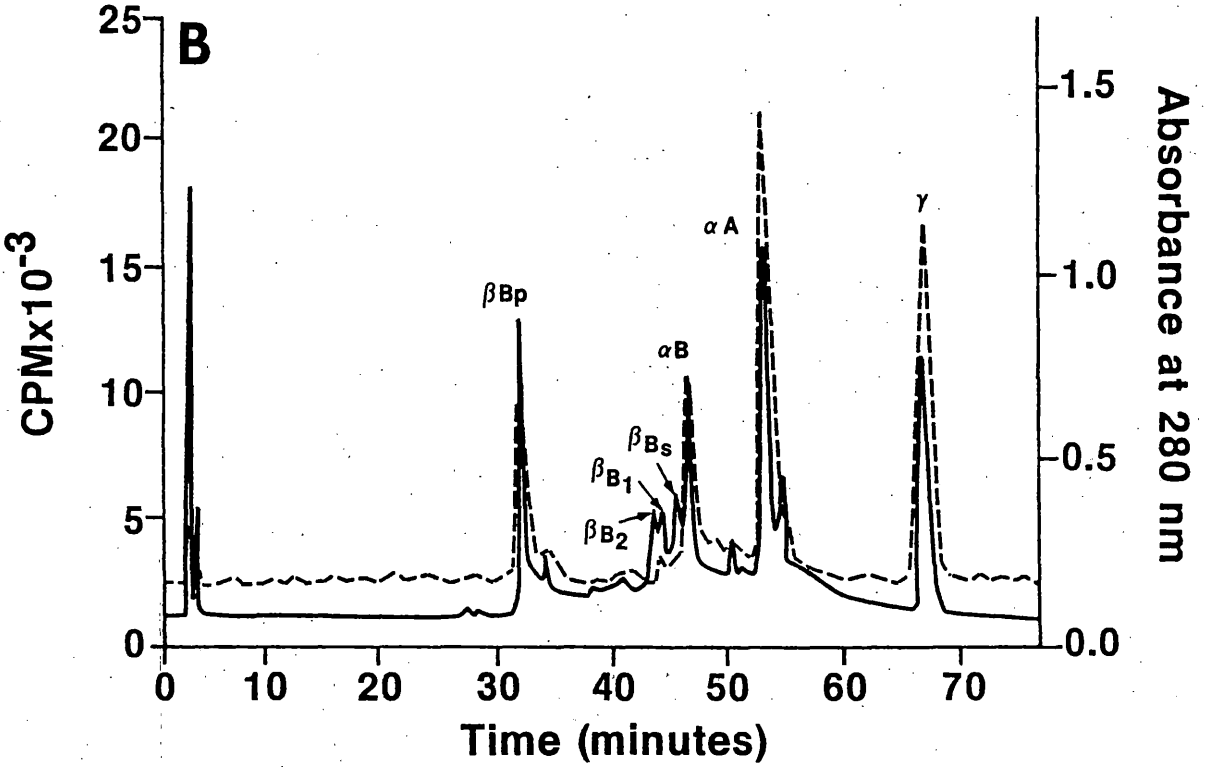
B
CPMx10-3
Absorbance at 280 nm
Time (minutes)
βBp
αA
γ
αB
βBs
βB1
βB2
25
20
15
10
5
0
1.5
1.0
0.5
0.0
0
10
20
30
40
50
60
70

TABLE IX. Specific activities of the soluble lens crystallin subunits from [^{3}H]$NaBH_4$ reduced soluble fractions

Lens crystallin subunits were separated by C-4 reverse phase HPLC from tritiated borohydride labeled soluble fractions from control and diabetic cataract lenses as shown in Figure 23. (Day 168)

TABLE IX

	Crystallin Subunit						
	βBp	βB1	βB2	βBs	αB	αA	
	Specitic Activity (cpm/mg)						
Control Soluble	355	70	75	120	1,742	1,650	859
Cataract Soluble	2,239	730	690	800	4,500	4,740	13,421

Figure 30 shows the molecular sieve HPLC separation of the insoluble fraction from control lenses and diabetic cataract lenses. The results show that the greatest amount of tritium incorporation (glycation) is found in the HMW protein in both control and cataract lenses. In the control lens there is moderate increase in the insoluble protein peaks 1, 3, and 4. The diabetic cataract lens shows a dramatic increase in the same peaks 1, 3, and 4. It was also observed that the total glycation of the insoluble fractions were greater than their respective soluble fractions.

As with the soluble HMW, the specific activity of the insoluble HMW from both the control and diabetic cataract lenses were consistent. The control insoluble HMW protein specific activity was 11,6000 cpm/mg protein, and the diabetic cataract HMW protein was 17,000 cpm/mg protein. The remainder of the protein peaks showed significant differences in specific activity between the control lenses and the diabetic cataract lenses. Insoluble peak 1 from the control lens showed a specific activity of 935 cpm/mg protein compared to 3520 cpm/mg protein for peak 1 from the diabetic cataract lens. Similarly, the control lens peak 3 had 310 cpm/mg protein compared to 950 cpm/mg protein in the diabetic cataract. A more dramatic difference existed for peak 4 which in the control exhibited a specific activity of 255 cpm/mg protein compared to the diabetic cataract with 4265 cpm/mg protein.

The non-enzymatic glycation of the urea-soluble fraction was further characterized by C-4 reverse phase HPLC separation of the crystallin subunits. Figure 31 demonstrates the crystallin subunits and tritium borohydride label distribution in the control and diabetic cataract urea-soluble fractions. The results show that there is moderate

FIGURE 30. Molecular sieve HPLC separation of [^{3}H]$NaBH_4$ labeled insoluble fractions

Tritium borohydride labeled insoluble lens proteins from control lens (A) and diabetic cataract lens (B) were separated by molecular sieve HPLC. Fractions of 0.5 ml were collected and radioactivity determined. Solid line=absorbance at 280 nm; Dashed line=radioactivity in cpm.

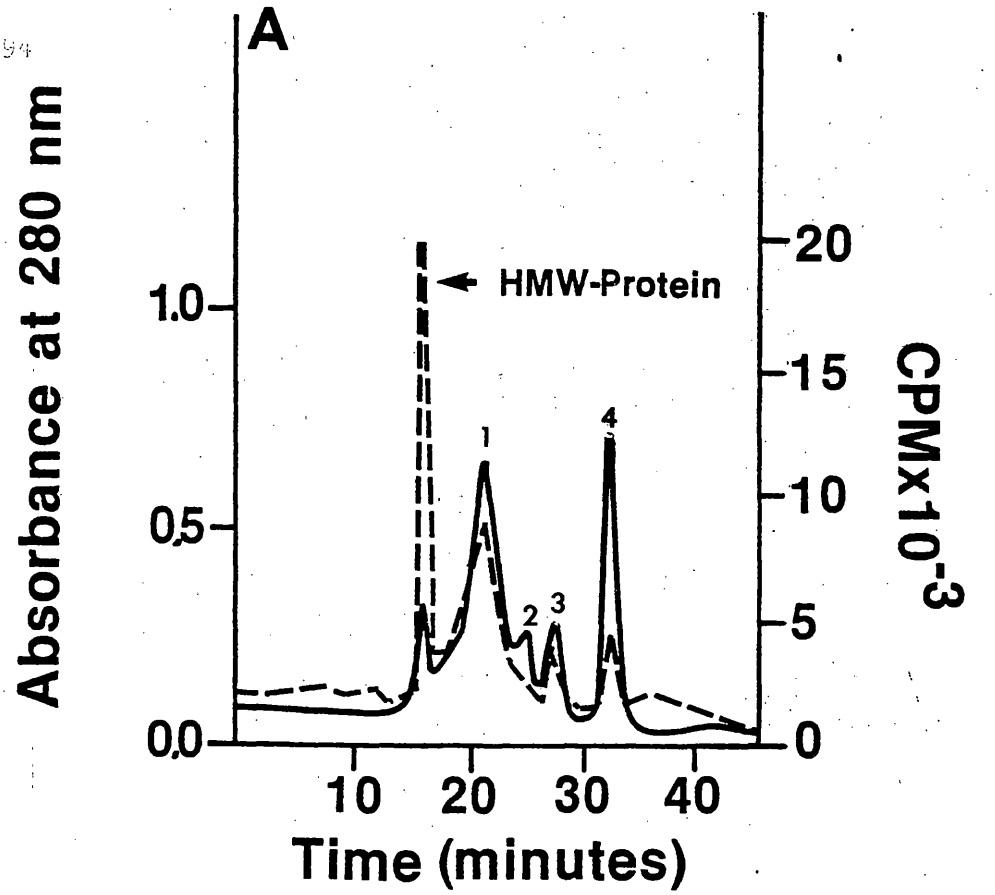
A
Absorbance at 280 nm
1.0
0.5
0.0
HMW-Protein
1
2
3
4
20
15
10
5
0
CPMx10-3
10
20
30
40
Time (minutes)

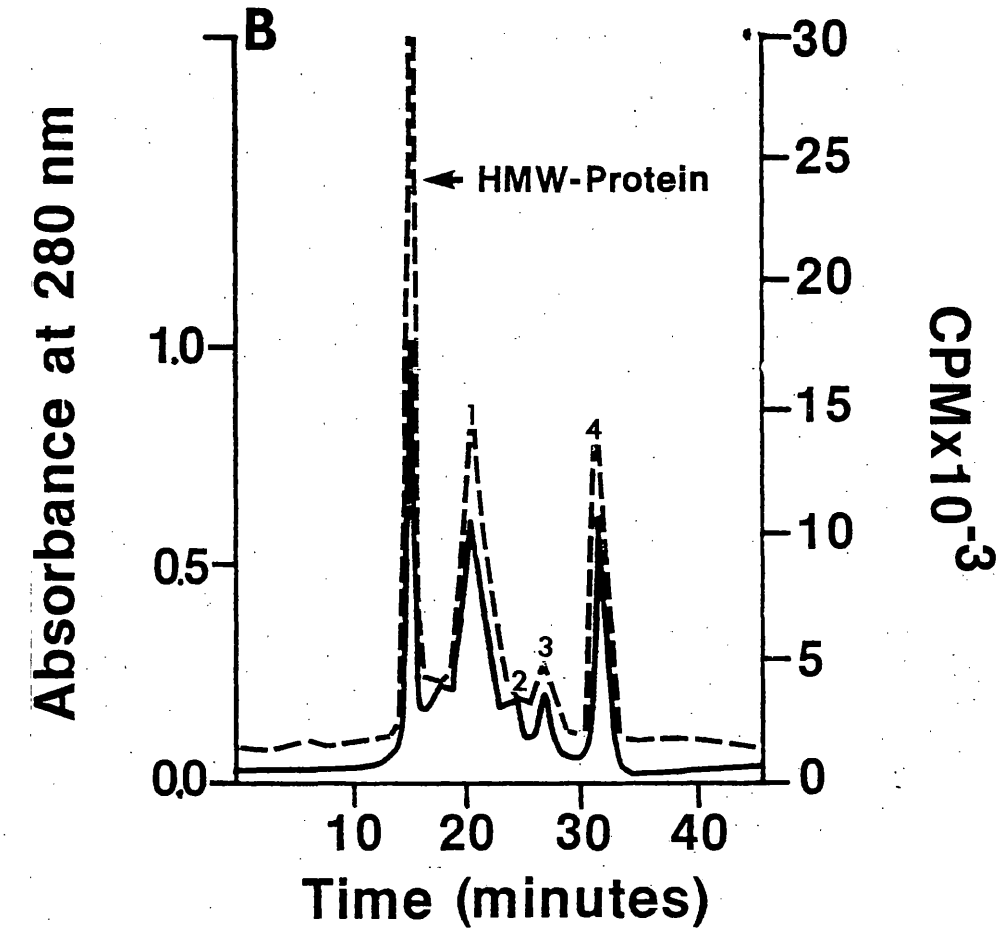
B
Absorbance at 280 nm
1.0
0.5
0.0
HMW-Protein
1
2
3
4
30
25
20
15
10
5
0
CPMx10-3
10
20
30
40
Time (minutes)

FIGURE 31. C-4 reverse phase HPLC separations of [^{3}H]$NaBH_4$ labeled insoluble fractions

Tritiated borohydride reduced insoluble lens proteins from control lens (A) and diabetic cataract lens (B) were separated into their constituent crystallin subunits by C-4 reverse phase HPLC. Radioactivity was monitored in 0.5 ml fractions. Solid line=absorbance at 280 nm; Dashed line= radioactivity in cpm.

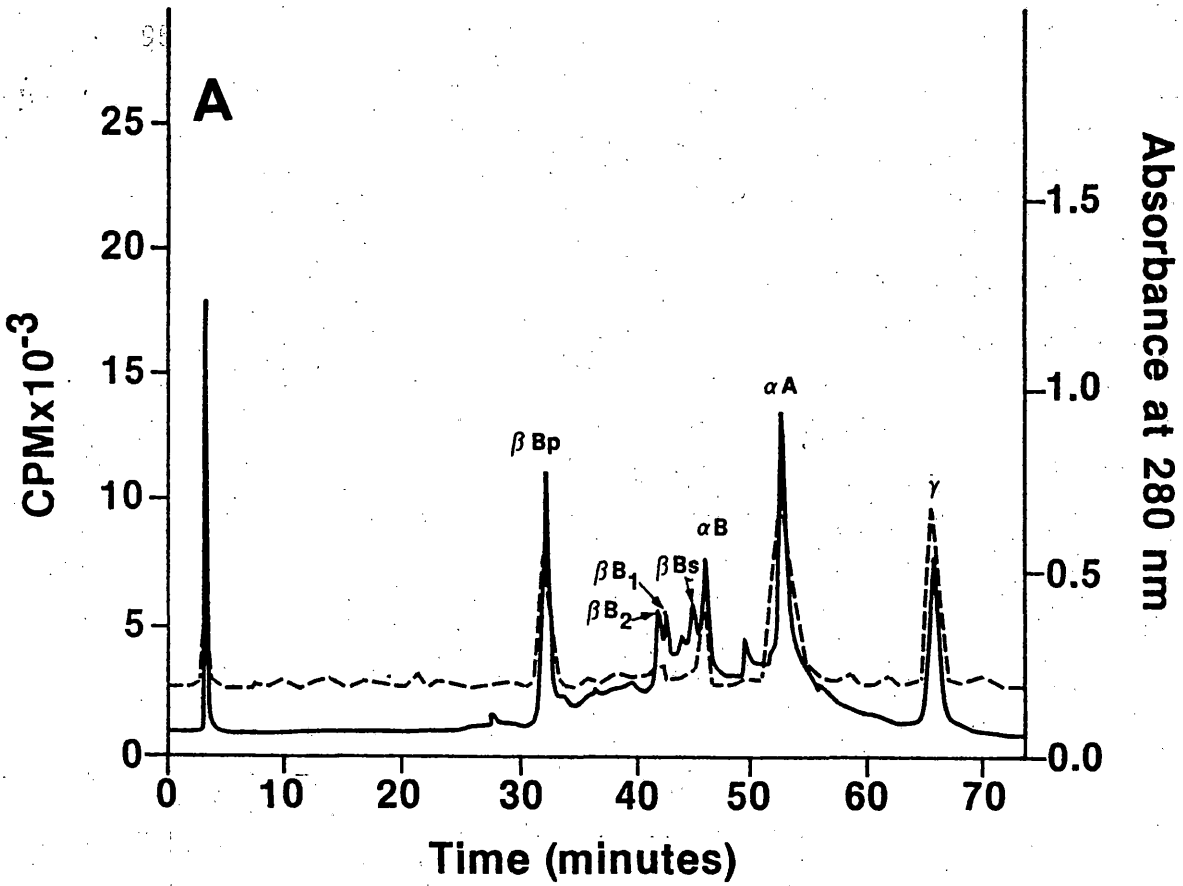
A
CPMx10-3
Absorbance at 280 nm
Time (minutes)
βBp
αA
γ
αB
βB1
βBs
βB2
0
5
10
15
20
25
0.0
0.5
1.0
1.5
0
10
20
30
40
50
60
70

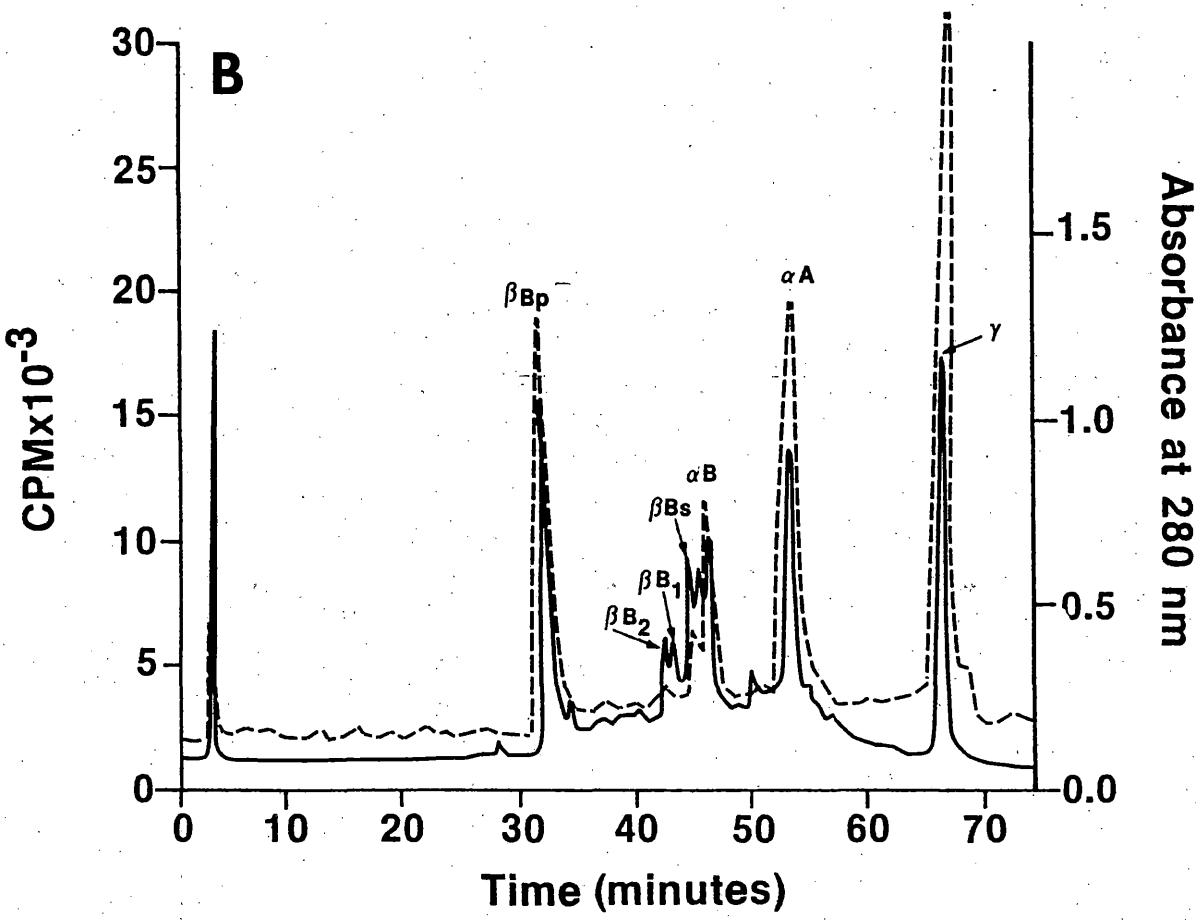
B
CPMx10-3
Absorbance at 280 nm
Time (minutes)
βBp
αA
γ
αB
βBs
βB1
βB2
0
5
10
15
20
25
30
0.0
0.5
1.0
1.5
0
10
20
30
40
50
60
70

glycation in the major crystallin subunits of the control lenses. Compared to its soluble fraction counterpart (Fig. 28), the largest increase in glycation occurs in the βBp crystallin subunit and the γ-crystallin. The diabetic cataract urea-soluble fraction demonstrated a significant increase in glycation of the major crystallin components compared to the control urea soluble fraction. The largest increase was found in the γ-crystallin followed by the β-crystallin Bp subunit and the subunits. A more accurate expression of the differing levels of glycation between the various urea-soluble components from the control and diabetic cataract lenses is provided by the calculated specific activities presented in Table X (calculated by % area x total mg injected assuming 100% recovery). The γ-crystallin present in the urea-soluble fraction had the highest specific activity both in the control and diabetic cataract lenses. The specific activity of the β-crystallin subunits demonstrate the significant increase in glycation found in the diabetic cataract as compared to the control lenses. Also shown is the significant levels of glycation in the α-crystallin subunits in both control and diabetic cataract lenses. However, the increase from control to diabetic cataract was not as great as found in the γ- and β-crystallins.

C) Glycation of the High Molecular Weight Aggregate Components

Experiments involving the water-soluble and urea-soluble fractions have shown that the HMW aggregate from both control and diabetic cataract lenses contain a significant level of glycation. The soluble HMW aggregate and insoluble HMW aggregate were isolated by molecular sieve HPLC from their respective tritiated borohydride reduced fraction and concentrated by pressure filtration. Figure 32 demonstrates the crystallin subunits and their extent of glycation of the soluble and

TABLE X. Specific activities of insoluble lens crystallin subunits from [^{3}H]$NaBH_4$ reduced insoluble fractions

The insoluble crystallin subunits were separated by C-4 reverse phase HPLC from tritiated borohydride labeled insoluble fractions from control and diabetic cataract lenses (Fig. 21).

TABLE X

	Crystallin Subunit						
	βBp	βB1	βB2	βBs	αB	αA	
	Specific Activity (cpm/mg)						
Control Insoluble	1,830	140	110	260	1,965	2,350	4,895
Cataract Insoluble	5,250	405	310	461	4,830	6,923	19,480

FIGURE 32. C-4 reverse phase HPLC separations of [^{3}H]$NaBH_4$ reduced HMW aggregates

Tritiated borohydride labeled HMW aggregates isolated by molecular sieve HPLC from the soluble (A) and insoluble (B) fractions were separated into their individual crystallin subunit components by C-4 reverse phase HPLC. Radioactivity was monitored in 0.5 ml fractions (dashed lines). Solid line=absorbance at 280 nm.

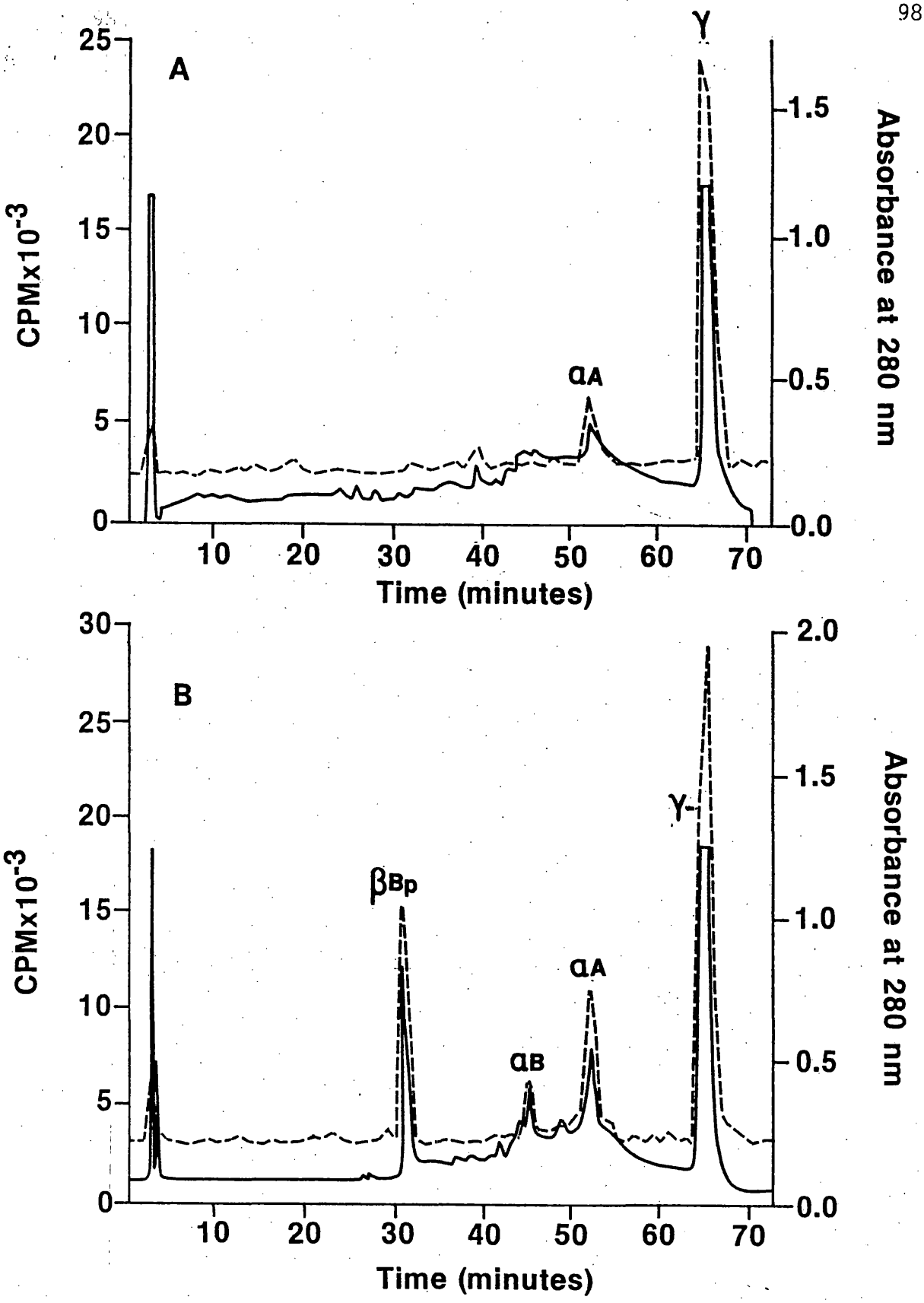
A
γ
αA
CPMx10-3
Absorbance at 280 nm
Time (minutes)
B
γ
βBp
αA
αB
CPMx10-3
Absorbance at 280 nm
Time (minutes)

insoluble HMW aggregates as determined by C-4 reverse phase HPLC. The results showed that in the soluble HMW aggregate the primary component, γ-crystallin, is also significantly glycated. The other minor components, primarily αA crystallin subunit, also contained a significant amount of glycation. Similarly, the insoluble HMW aggregate components were all significantly glycated. The γ-crystallin contained the largest amount of glycation followed by the β-crystallin Bp subunit which was found only in the insoluble HMW aggregate.

D) Identification of the Sites of Glycation

Control and diabetic cataract glycated lens proteins from the water-soluble and urea-soluble fractions were isolated by affinity chromatography. The crystallin components were then separated and quantified by molecular sieve HPLC. This approach was designed to confirm the results obtained by tritium borohydride reduction coupled with HPLC separations. Previous experiments have demonstrated that in the soluble fraction the HMW contains the highest level of glycation. Molecular sieve HPLC separations of the glycated proteins confirm these results (Fig. 33). Also demonstrated is the increase in glycated γ- and β-crystallins in the diabetic cataract. Similar results were obtained with the urea-soluble fraction with the insoluble HMW aggregate demonstrating the highest percentage of the glycated urea-soluble fraction (Fig. 34). In addition, the peaks 1, 3, and 4 also demonstrate a significant level of glycation in both control and diabetic cataract lenses. These results support those obtained using the tritium borohydride.

Confirmation that lysine was the primary glycated amino acid residue was obtained by affinity chromatography followed by amino acid analysis by precolumn derivatization with PITC and C-8 reverse phase

FIGURE 33. Glycated crystallins from the soluble fraction separated by molecular sieve HPLC

Glycated lens crystallins were isolated by affinity chromatography from control (A) and diabetic caratact (B) lenses and separated by molecular sieve HPLC.

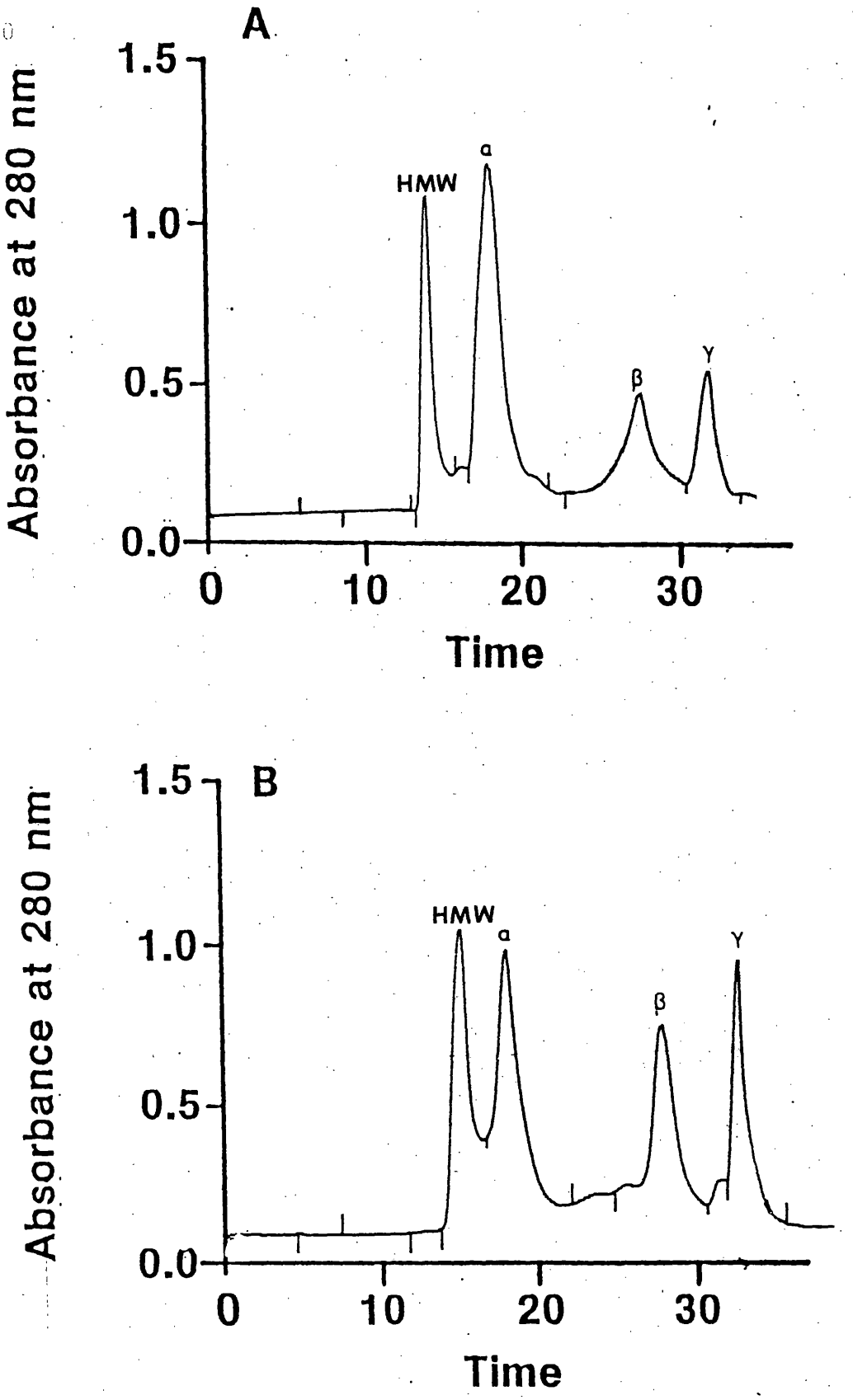
A
1.5
1.0
0.5
0.0
Absorbance at 280 nm
HMW
α
β
γ
0
10
20
30
Time
B
1.5
1.0
0.5
0.0
Absorbance at 280 nm
HMW
α
β
γ
0
10
20
30
Time

FIGURE 34. Glycated crystallins from the insoluble fraction separated by molecular sieve HPLC

Glycated lens crystallins from the insoluble fractions from control (A) and diabetic caratact (B) lenses were isolated by affinity chromatography. The glycated insoluble crystallins were subsequently separated by molecular sieve HPLC.

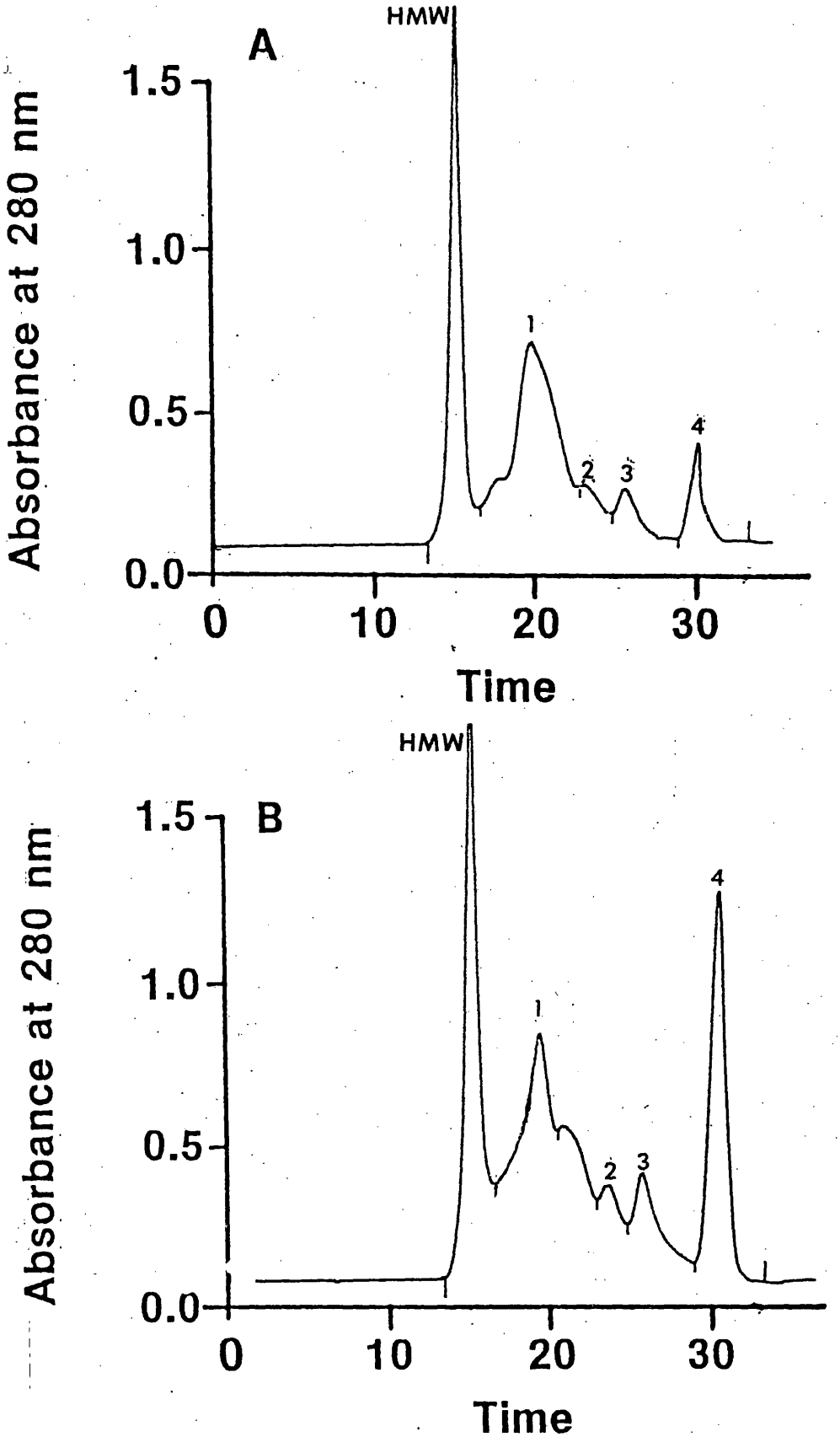
A
HMW
1.5
1.0
0.5
0.0
Absorbance at 280 nm
1
2
3
4
0
10
20
30
Time
B
HMW
1.5
1.0
0.5
0.0
Absorbance at 280 nm
1
2
3
4
0
10
20
30
Time

HPLC. Borohydride reduced lens crystallins from diabetic cataract soluble fraction were hydrolyzed by 6 N HCl under vacuum at 110° for 24 hrs and the glycated amino acids were isolated by affinity chromatography as described in the Methods. A ε-amino glycated lysine standard was prepared by incubation of poly-L-lysine (a homopolymer) with glucose followed by borohydride reduction. The glycated poly-L-lysine was hydrolized by 6 N HCl and the ε-amino glycated lysines were isolated by Affigel 601 chromatography. A standard of glyco-lysine, and lysine was reacted with PITC and separated by C-8 reverse phase HPLC as described. Figure 35 demonstrates the chromatographs obtained by the standards (Fig. 35A) and the crystallin amino acids obtained by affinity chromatography (Fig. 35B). This confirms that lysine is the primary glycated amino acid present in the lens crystallins.

The final characterization of the non-enzymatic glycation of the insoluble HMW aggregate involved quantifying the glycated residues and subsequent identification of the glycated residues within the various crystallin components' primary sequence. This was done by enzymatic digests followed by affinity chromatographic isolation of the glycated polypeptides. A sample of the ^{3}H-borohydride reduced HMW protein (10 mg) was digested with either trypsin or chymotrypsin as described in the Methods section. Affinity chromatography with AffiGel 601 was used to isolate the glycated peptides. The glycated peptides from each enzymatic digest were then separated by C-18 reverse phase HPLC and fractions collected. There was some debate as to whether or not trypsin could cleave at a glycated lysine residue or cleave at the next non-glycated cleavage site within the polypeptide sequence. Therefore, a chymotryptic digest was also used to provide overlapping polypeptides to aid in determining the sites of glycation. Separation of the glycated peptide

FIGURE 35. Identification of glycated amino acids isolated by affinity chromatography

A) Standards of lysine and glycated lysine were derivatized with PITC and separated by C-8 reverse phase HPLC.
B) Glycated amino acids from acid hydrolyzed soluble fraction of diabetic cataract lenses were isolated by affinity chromatography and similarly derivatized and separated by C-8 reverse phase HPLC.

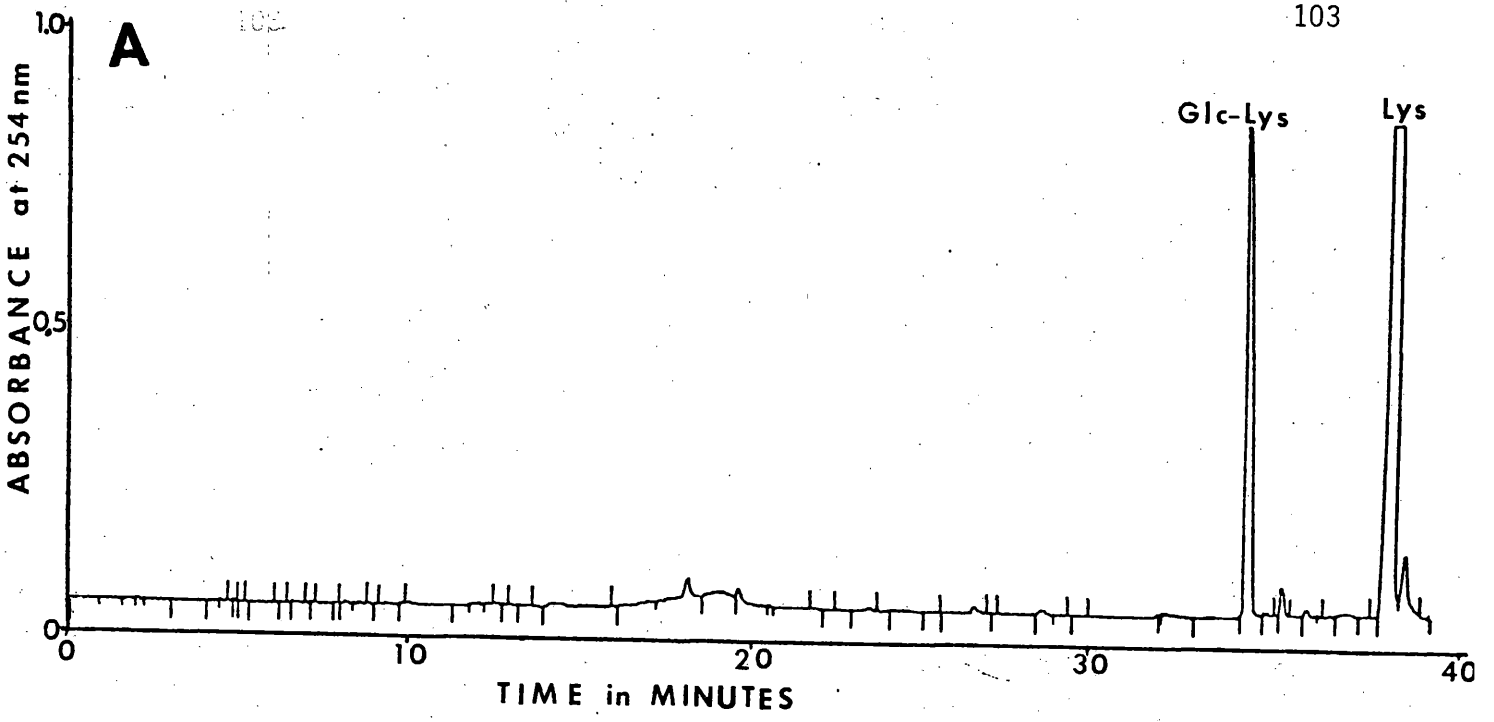
A
Glc-Lys
Lys
ABSORBANCE at 254 nm
1.0
0.5
0
0
10
20
30
40
TIME in MINUTES

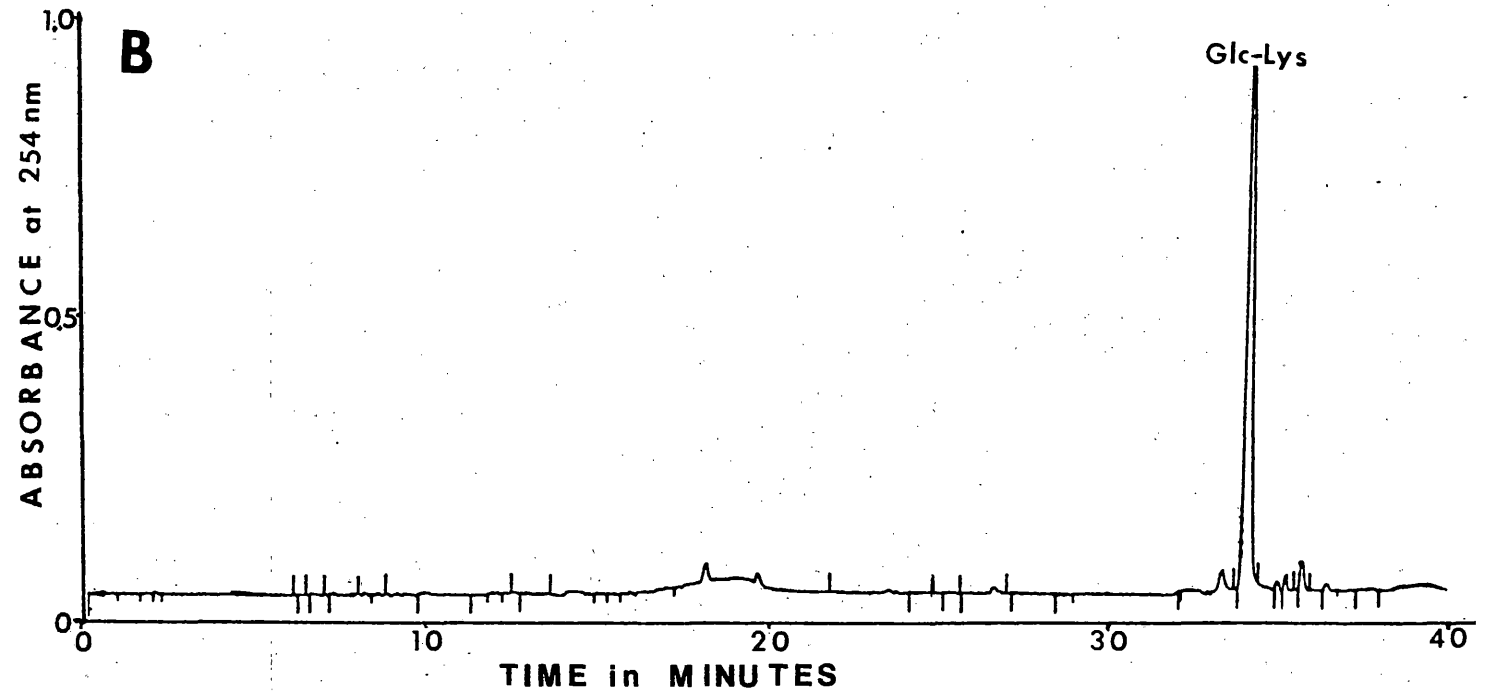
B
Glc-Lys
ABSORBANCE at 254 nm
1.0
0.5
0
0
10
20
30
40
TIME in MINUTES

by C-18 reverse phase HPLC results in a myriad of peaks shown in Figure 36. The tryptic digest separation results in 15 peaks of which 2 peaks (Chromatogram A peaks 4 and 11) are significantly larger than the other peaks in both absorbance and tritium incorporation. Similarly, the chymotryptic digest results in 13 major peaks, 2 of which are significantly increased (Chromatogram B peaks 7 and 8). Some of the smaller peaks in both digests contain no radioactivity which indicates a non-specific binding to the affinity gel. Each peak was subsequently analyzed for amino acid composition. To determine the location of the glycated residues from the amino acid composition of isolated glycated peptide several factors were taken into consideration. First, in the trypsin digest it was assumed that trypsin would not cleave at a blocked (glycated) lysine residues. Therefore, the amino acid composition must include both a glycated lysine peak (Fig. 35) as well as either a free lysine or arginine. Secondly, in the chymotryptic digest, glycated lysine residues must be present. The results of the amino acid analysis are shown in Tables XI and XII. Using this criterion in conjunction with the overlapping amino acid data and the known amino acid sequence of the lens crystallins results in the proposed location of the glycated residues presented in Figure 37.

These results confirm those obtained by other experiments that demonstrate γ-crystallin as the primary constituent of the insoluble HMW aggregate. The [^{3}H]$NaBH_4$ reduced glycated residues associated with the γ-crystallin comprise 62% of the total radioactivity of the tryptic digest and 57% of the chymotryptic digest. The β-crystallin glycated lysines comprised 21% of the total radioactivity found in the tryptic digest and 24% of the chymotryptic digest radioactivity. The α-crystallin

glycated residues comprised the remainder of the radioactivity. These values support the data obtained on the composition of the insoluble HMW aggregate obtained by HPLC characterization.

FIGURE 36. Separation of glycated peptides isolated by affinity chromatography

Glycated peptides obtained by enzymatic digestion of the insoluble HMW aggregate with either trypsin (A) or chymotrypsin (B) were isolated by affinity chromatography and separated by C-18 reverse phase HPLC. Peak identities are given in Table XI and XII. Tritium borohydride reduced insoluble HMW protein was used for each digestion. One ml fractions were collected with 0.5 ml each used for amino acid analysis and 0.5 ml used for monitoring of radioactivity. Solid line=absorbance at 214 nm. Dashed line=radioactivity in cpm.

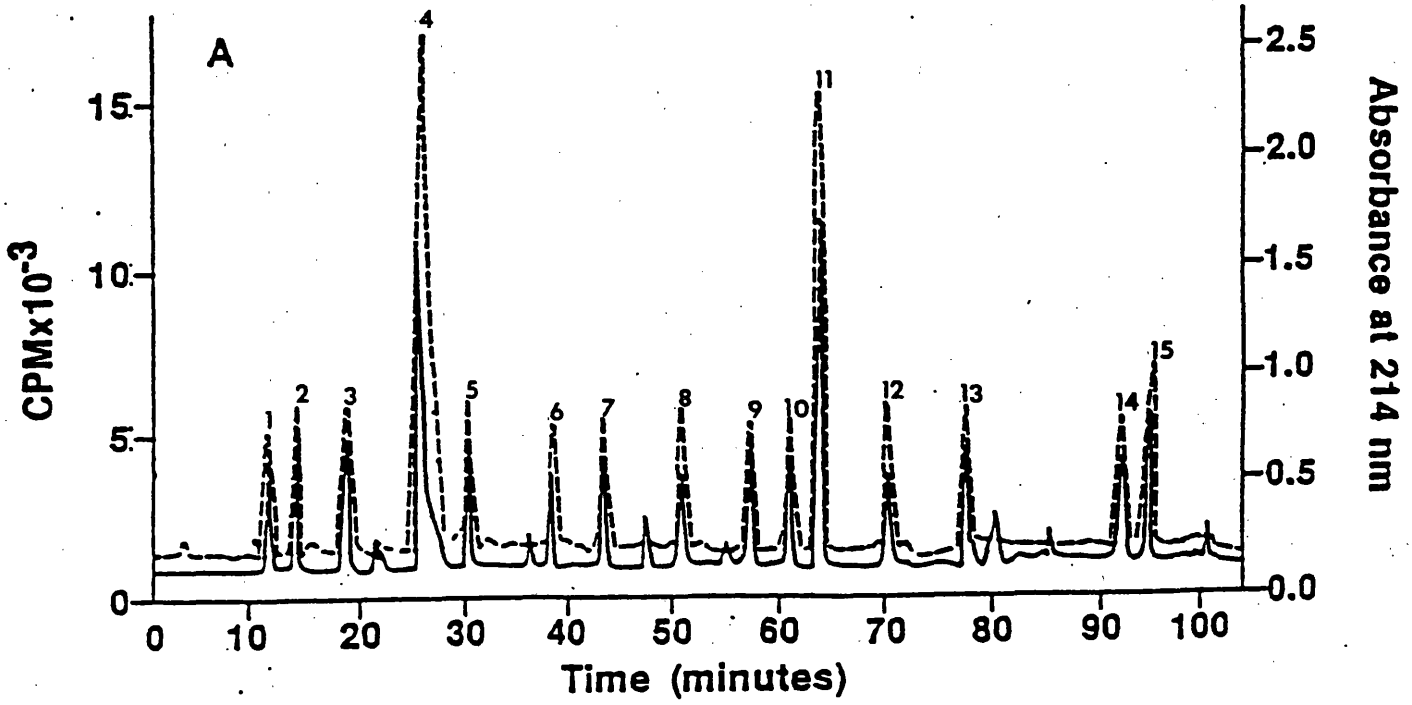
A
CPMx10-3
Absorbance at 214 nm
Time (minutes)
0
5
10
15
0.0
0.5
1.0
1.5
2.0
2.5
0
10
20
30
40
50
60
70
80
90
100
1
2
3
4
5
6
7
8
9
10
11
12
13
14
15

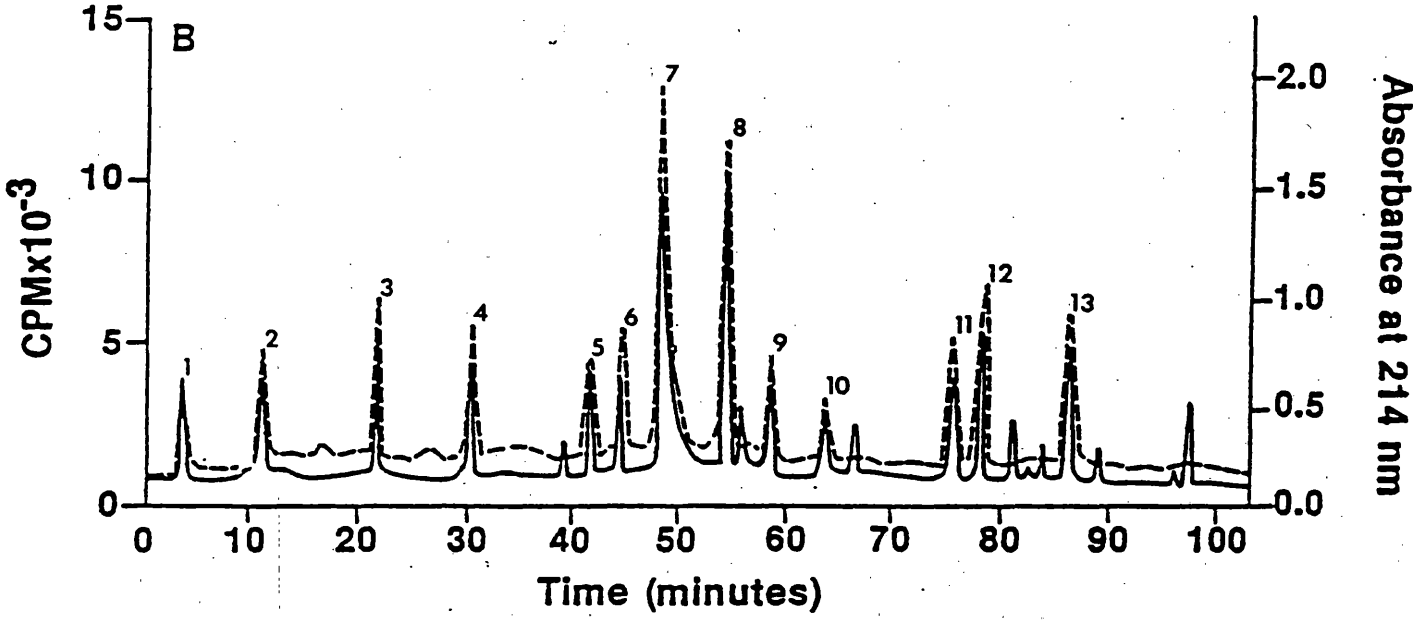
B
CPMx10-3
Absorbance at 214 nm
Time (minutes)
0
5
10
15
0.0
0.5
1.0
1.5
2.0
0
10
20
30
40
50
60
70
80
90
100
1
2
3
4
5
6
7
8
9
10
11
12
13

TABLE XI. Amino acid composition of glycated tryptic peptides isolated by affinity chromatography

Peptides were obtained by tryptic digestion followed by affinity chromatography using Affigel 601. The resulting glycated peptides were separated by C-18 reverse-phase HPLC. Amino acid analysis was performed as described in Methods.

TABLE XI

Amino Acid	Peak 1	Peak 2	Peak 3	Peak 4	Peak 5	Peak 6	Peak 7	Peak 8	Peak 9	Peak 10	Peak 11	Peak 12	Peak 13	Peak 14	Peak 15
Asp		1.01		1.07			3.09	2.02	0.95	1.08	2.06		1.90	1.88	1.88
Thr				1.03		0.88									0.97
Ser			0.88		4.18		1.02				0.97			2.12	1.02
Glu		1.09	1.98	1.05	2.04	2.10			0.87	1.11		3.82	4.12	1.93	1.04
Pro			0.75		1.48	1.26			0.68					0.68	0.71
Gly	0.47			0.79			3.10			2.90	2.04	2.08	1.04		
Ala			1.03	0.93	2.89			1.05		1.88					
Cys															
Val						0.96		1.94			1.01	1.04	1.88	2.04	3.04
Met									0.78		0.86				
Ile				0.98				1.00	2.04				0.95		0.96
Leu		0.98						0.99		3.00	2.03			2.00	2.00
Tyr				0.94			0.89			1.85	0.78	0.90			
Phe				0.89			0.92	1.82	1.01			1.89	0.91	1.77	3.10
His									0.97				1.85	0.91	0.88
Arg		0.97	1.07	1.00			1.04		1.02		1.08	1.02	1.01		
Lys						2.04		0.93		1.09					1.03
Glc Lys															

TABLE XII. Amino acid composition of glycated chymotryptic peptides isolated by affinity chromatography

Peptides were obtained by chymotryptic digestion followed by affinity chromatography using Affigel 601. The resulting glycated peptides were separated by C-18 reverse-phase HPLC. Amino acid analysis was performed as described in Methods.

TABLE XII

Amino Acid	Peak 1	Peak 2	Peak 3	Peak 4	Peak 5	Peak 6	Peak 7	Peak 8	Peak 9	Peak 10	Peak 11	Peak 12	Peak 13
Asp			1.01	1.00	1.09			1.06	0.96	2.83	3.07	1.06	3.18
Thr	0.89					0.91	1.02					0.89	
Ser								0.86		0.78	2.69	0.87	
Glu		2.09		1.03							1.16	3.09	2.93
Pro									0.52			1.29	
Gly		1.03				1.00	0.35	1.01		3.00	0.93	1.07	1.79
Ala								0.96				2.11	
Cys													
Val			1.06		0.93			1.04			0.90		1.12
Met						0.79							
Ile							0.92		3.21		1.09		0.83
Leu	1.01							1.12				1.00	
Tyr		0.82					0.99			0.79			0.98
Phe			0.90	0.88	1.10		1.02		0.82	0.91	0.88		
His			0.82		0.93							0.87	2.68
Arg	1.02			1.11							2.16		0.90
Lys						0.71				0.63			
Glc Lys	1.00	1.00	1.00	1.00	1.00	1.63	1.00	1.00	1.00	1.52	1.00	1.00	1.00

FIGURE 37. Amino acid sequences of the crystallin components of the insoluble HMW aggregate with sites of glycation

The amino acid composition of the glycated polypeptides obtained by affinity chromatography and C-18 reverse phase HPLC were used to determine the sites of glycation within the polypeptide sequences. The dashed lines indicate those peptides obtained by chymotryptic digest. Solid lines indicate peptides obtained by tryptic digest. Numbers correspond to the peaks shown in Figure 36. A) Gamma crystallin. B) Beta crystallin Bp subunit. C) Alpha crystallin A subunit. D) Alpha crystallin B subunit.

A AMINO ACID SEQUENCE WITH SITES OF GLYCATION OF γ-CRYSTALLIN

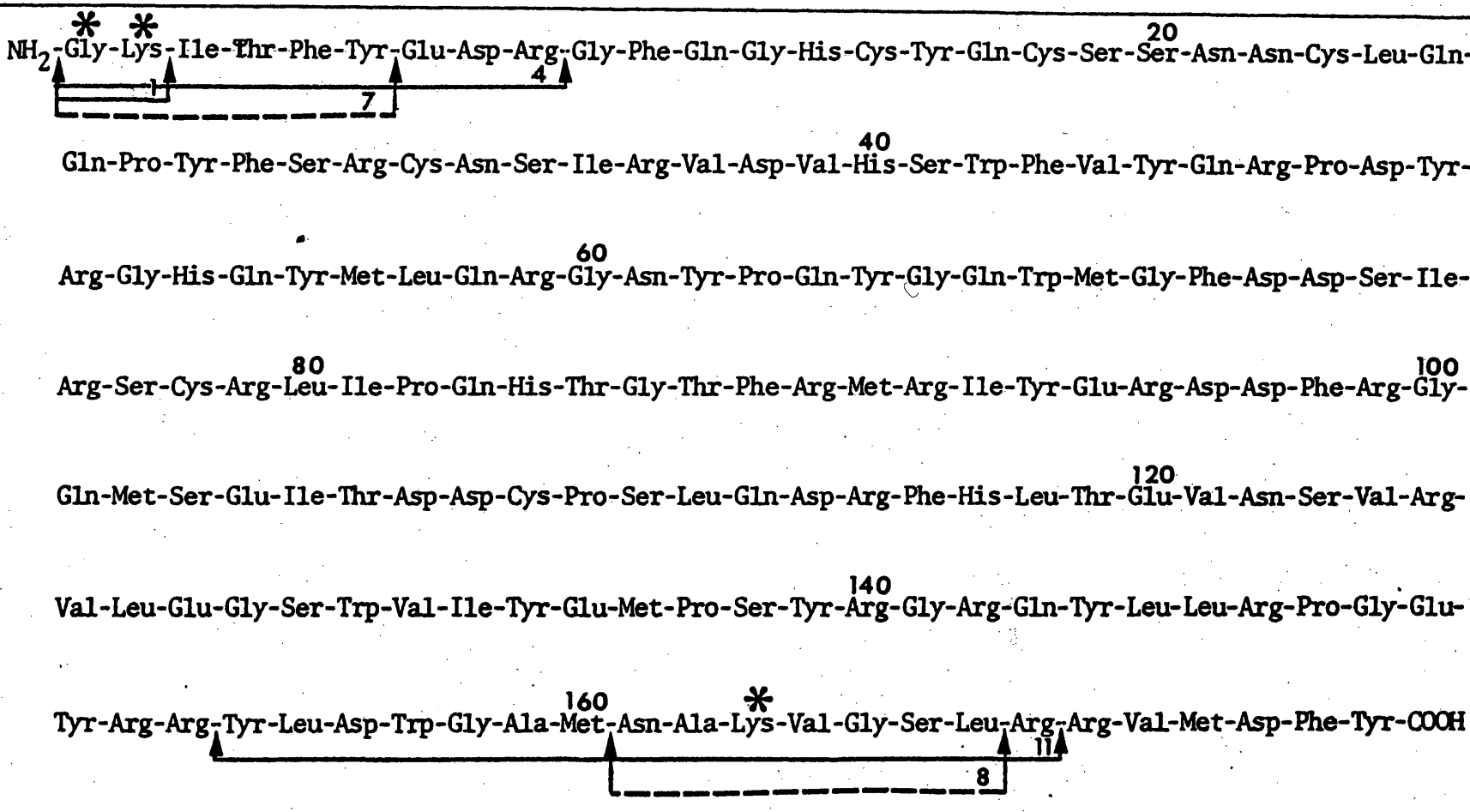

B AMINO ACID SEGUENCE AND SITES OF GLYCATION OF β-CRYSTALLIN Bp SUBUNIT

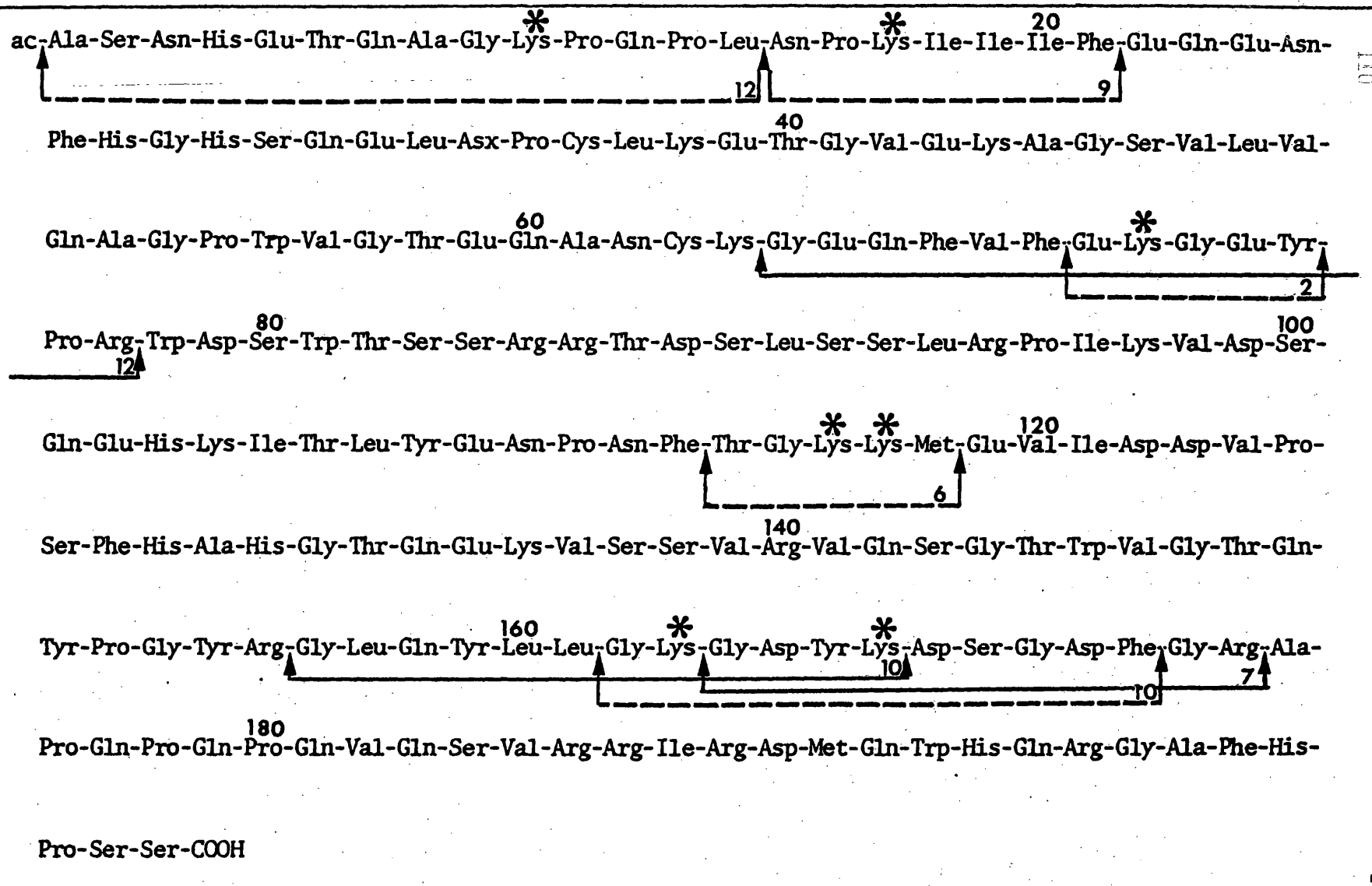

C AMINO ACID SEQUENCE AND SITES OF GLYCATION OF α-CRYSTALLIN A SUBUNIT

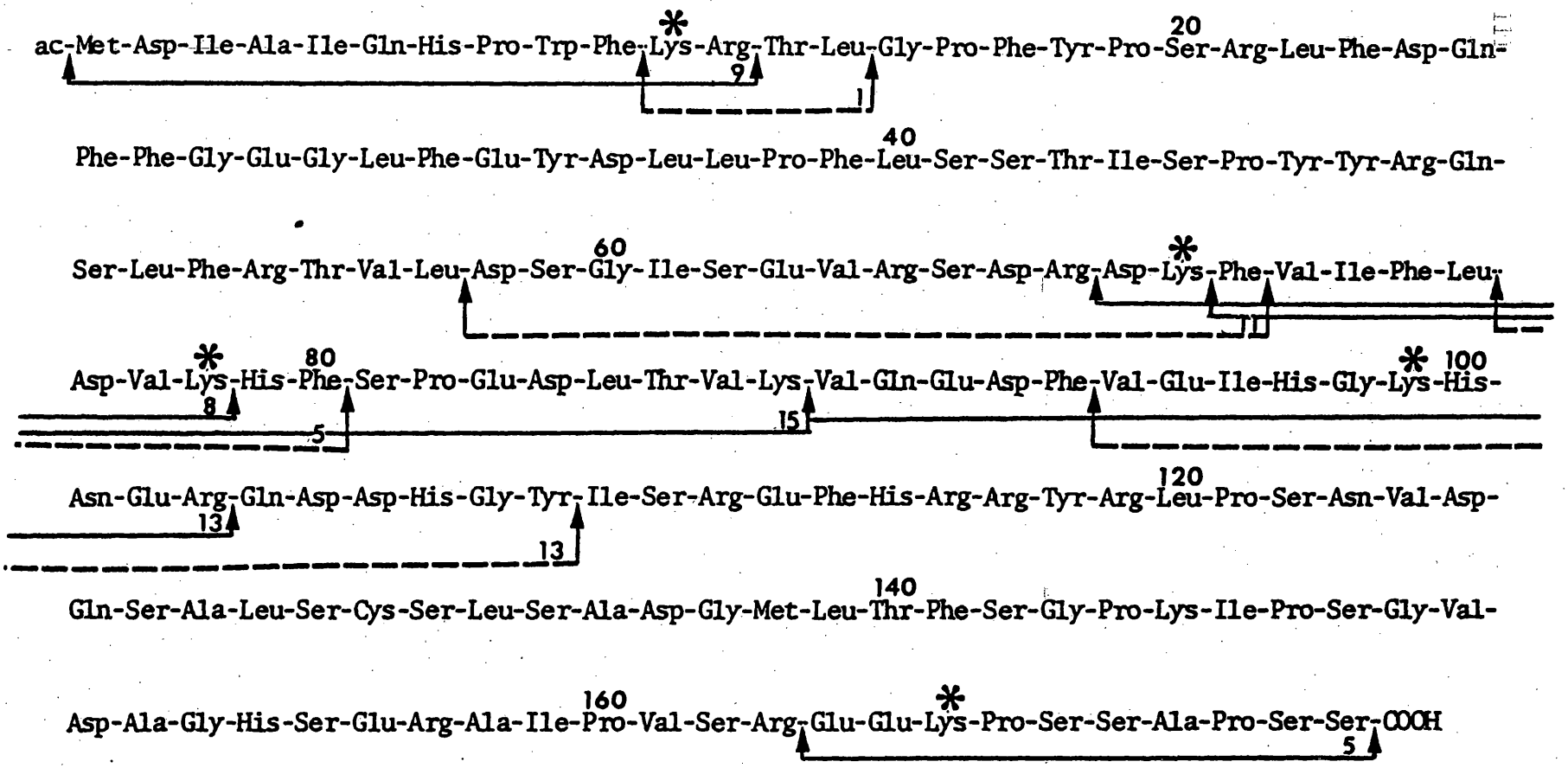

D AMINO ACID SEQUENCE AND SITES OF GLYCATION OF α-CRYSTALLIN B SUBUNIT

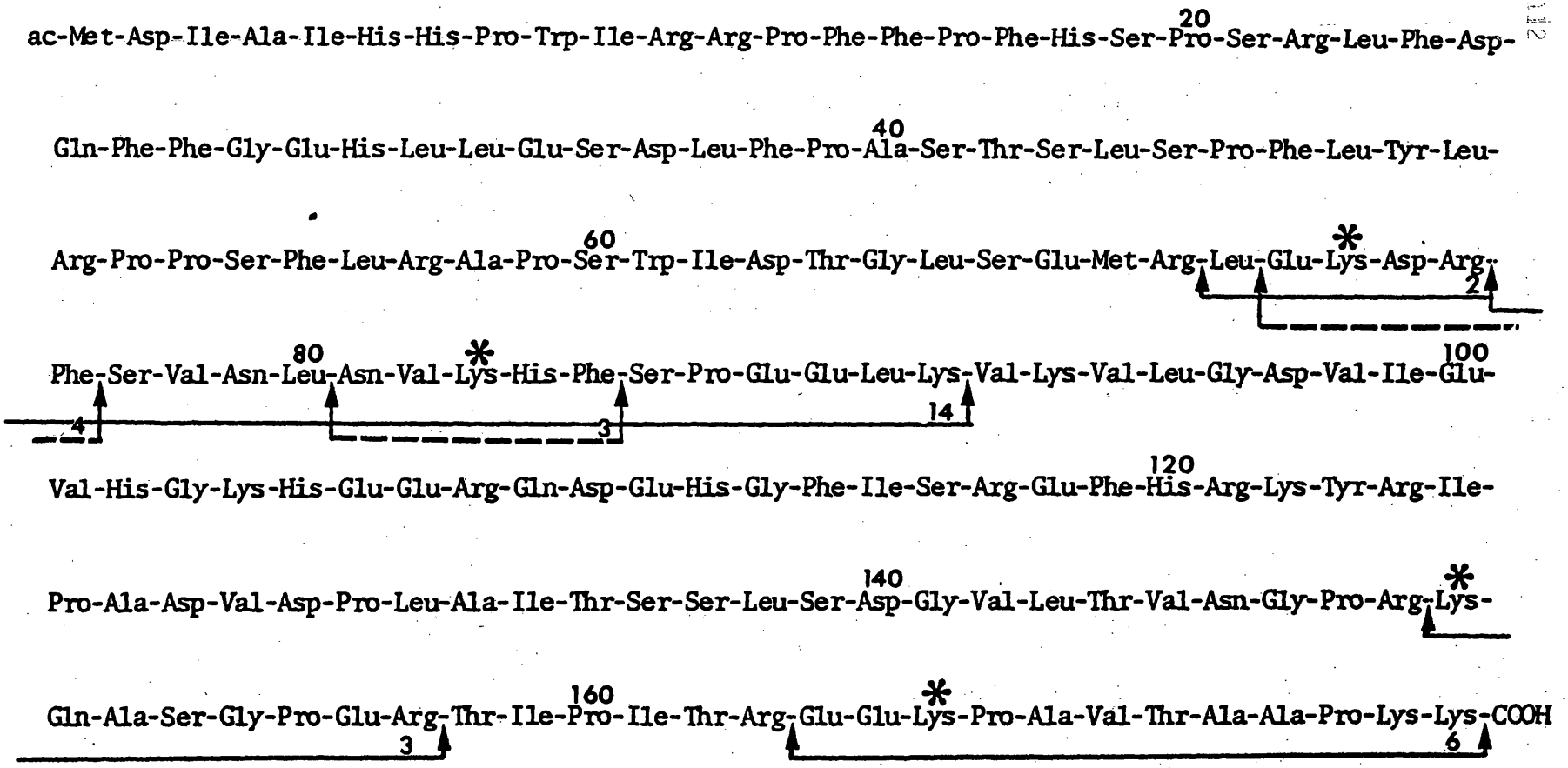

DISCUSSION

I. Progressive Changes

The development of sensitive HPLC techniques was an essential antecedent to the study of progressive changes occurring within the lens leading to diabetic cataract formation. The molecular sieve HPLC methodologies allowed for identification and quantification of the various crystallin proteins from individual animals. These techniques were originally designed to study the high molecular weight proteins from both the soluble and urea-soluble fractions but were subsequently improved to allow for examination of all the crystallin proteins found in each fraction. In conjunction with the HPLC methodologies, various affinity gels were used for the separation and quantification of the glycated lens proteins, glycated peptides, and glycated amino acids. Affinity gels with a phenylboronate ligand attached to an agarose or acrylamide support have been used extensively to quantify glycated hemoglobins in diabetic patients and have been shown to be consistent in their separations.

The use of lenses from individual animals was considered to be the optimum approach to the study of hyperglycemic dependent changes leading to cataract. Rats were chosen as the experimental model for a number of reasons. Diabetic hyperglycemia may be reliably induced by injection of streptozotocin or alloxan which precludes the need for surgical removal of the pancreas. Secondly, characteristic diabetic cataracts develop within 12 to 14 weeks after the onset of diabetes. Finally, rats (as well as mice, rabbits, and other related mammals) possess insulin secreting cells within the parotid gland which are not destroyed by streptozotocin (104). The small amounts of insulin secreted by these cells is not sufficient to lower the plasma glucose levels to normal;

however, it allows the animal to maintain a consistently high plasma glucose level without sudden death by diabetic ketoacidosis.

One of the basic tenets of biochemistry is that the primary structure or amino acid sequence of a protein dictates the secondary and tertiary structure and function. The classical example of how a single change in the primary structure can have dramatic consequences is that of sickle cell anemia. A single modification of the sixth amino acid from glutamate to valine results in dramatic consequences. The non-enzymatic attachment of a carbohydrate residue to the ε-amino group of lysine or the amino-terminus of a protein in effect results in a change in the primary structure. Lysine, a basic hydrophilic polar amino acid, is usually found exposed on the outside of a protein, exposed to the environment. Attachment of a carbohydrate results in an uncharged non-polar 2-deoxyfructolysine residue which would prefer a hydrophobic environment within the interior of the protein.

The proteins of the lens are extremely long-lived and there is virtually no protein turnover. Therefore, most changes observed in protein structure or conformation are due to posttranslational modifications. It has been hypothesized that lens proteins aggregate to form large particles that scatter light-producing lens opacities. Non-enzymatic glycation has been investigated as contributing to the lens proteins becoming water-insoluble and aggregating. However, this research has dealt only with comparisons between normal and mature diabetic cataract lenses using various indirect methods to detect glycated lens crystallins. It is clear that as hyperglycemia continues the lens proteins are increasingly glycated with the insoluble (urea-soluble) fraction demonstrating consistently higher values than the

water-soluble fraction (Figure 11). This linear increase supports earlier work showing an increase in glycation in the diabetic cataract measured by ^{3}H-borohydride reduction (86). Stevens et al. first suggested that non-enzymatic glycation may influence the functional properties of lens crystallin based on the observation of Spector et al. that there was an increase in titratable sulfhydryls of α-crystallin as the ε-amino group of lysines were deionized (85). Stevens and coworkers hypothesized that glycation of the ε-amino groups of lysine may result in a similar structural change potentially leading to insolubilization. The results of the progressive changes in glycation of the soluble and urea-soluble fraction support this contention in several ways. First, it has been well established that there is a significant increase in the insoluble fraction as diabetic cataracts develop. Secondly, not only is there an increase in this insoluble fraction, but the greatest increase in glycation also occurs within this fraction. It was interpreted that as the soluble fraction becomes increasingly glycated, the crystallins become increasingly insoluble or denatured. Once they become denatured and insoluble, they may be subject to even further glycation resulting in the increased levels of glycation found throughout the hyperglycemic duration. Another possibility is that moderate glycation of the lens crystallins does not result in their becoming insoluble but further glycation above a 'threshhold' value results in denaturation and insolubilization. This idea is supported by the increased glycated amino acids found in the diabetic insoluble fractions compared to the diabetic soluble fractions (Figure 15).

Further evidence of a conformational change due to glycation was provided by Liang et al. (90) with their study using circular dichroism

(CD). They demonstrated a change in the near-UV CD spectrum after incubation of purified lens crystallins with glucose-6-phosphate indicating a change in the tertiary structure. Using sulfhydryl titration in the presence and absence of SDS, conformational changes within the lens proteins of the soluble fraction were observed. Sulfhydryl titrations performed in the absence of SDS determine the amount of free reactive sulfhydryls while titrations obtained in the presence of SDS, which denatures the protein, indicate the total sulfhydryls present. A smaller difference between the two values indicates a greater extent of protein denaturation. As hyperglycemia continues, there is a significant level of conformational change occurring which mirrors the increase in glycated lens protein. This conformational change not only supports the findings of Liang et al., but also a depletion of the free sulfhydryls is an indication of disulfide bond formation (Figure 18). Disulfide bond formation has been clearly associated with the lens proteins becoming increasingly insoluble and eventual cataract formation (75).

The increase in insoluble material is by itself not responsible for cataract formation, rather the opacity results from the accumulation of a large disulfide linked high molecular weight (HMW) aggregate. This HMW aggregate, present in the insoluble fraction, disrupts the organized cytoarchitecture of the lens and also acts as scatter points for light. Also present in the soluble fraction is a water-soluble precursor to the insoluble HMW aggregate. Both soluble and insoluble HMW aggregates are found in significant amounts in cataract lenses with the soluble HMW aggregate held together by non-covalent interactions while disulfide linkages are responsible for holding together its

insoluble counterpart. As diabetic hyperglycemia continues there is an increase in both the soluble and insoluble HMW aggregates (Figs. 21 and 22). This increase in the disulfide linked HMW aggregate accompanies the decrease in reactive free and total titratable sulfhydryls. This is in agreement with the proposed disulfide involvement of the insoluble HMW aggregate formation and cataract development. Also, the increases in the soluble and insoluble HMW aggregates during hyperglycemia are mirrored by the increase in glycated protein from both fractions. These relationships were interpreted to be due to non-enzymatic glycation of lens proteins increasing during prolonged hyperglycemia. This glycation results in conformational changes resulting in the lens proteins becoming increasingly water-insoluble and eventually forming disulfide cross-linkages. This conjecture is supported by other research dealing with modification of amino groups and conformational changes of lens proteins. Kern et al. have demonstrated that chronic administration of cyanate, a carbamylating agent, in humans and experimental animals leads to the formation of cataracts which are morphologically similar to diabetic cataracts (105).

The oxidation of sulfhydryls and formation of insoluble proteins and high molecular weight aggregates have been extensively studied. Harding (71) has argued that most of the insoluble protein obtained from rat lenses and human lenses is artifactual, resulting from oxidation of protein sulfhydryl groups during aerobic homogenization. However, in the experiments presented in this paper, all lens protein homogenizations and preparations were done under anaerobic conditions. Also, both control and diabetic lenses were extracted and prepared at the same time under identical conditions. Another observation made by Pirie (106) and

confirmed by Auricchio and Testa (107) was that aerobic homogenization of cataract lenses yields more of the disulfide containing artifact than normal lenses prepared by identical means. This paradox was explained by Harding who demonstrated that human cataracts contain soluble protein in which the reactivity of sulfhydryl groups is increased, presumably by unfolding of the tertiary protein structure (108).

In addition to the increases in HMW aggregates and disulfide content as cataracts develop, other changes within both the soluble and insoluble fractions are occurring. The most prominent change occurs in the γ-crystallin component in both the soluble and insoluble fractions. It has been established that older lenses and cataract lenses have decreased levels of the soluble γ-crystallin (41,116). These age dependent changes were also observed in the control group even though they were only followed for 168 days (Table IV). This decrease was originally attributed to increased proteolysis of γ-crystallin. Both α-crystallins and β-crystallins contain an acetylated amino-terminus which was believed to inhibit proteolysis while γ-crystallin contains a free glycine amino-terminus. However, subsequent work by X-ray crystalography revealed that the amino-terminus of γ-crystallin is folded in such a way as to decrease proteolytic susceptibility. This was later confirmed by in vitro experiments with purified lens crystallins and leucine amino peptidase. Later work revealed that peptidase activity within the lens is extremely low and it is now accepted that the decrease in the γ-crystallin component from the soluble fraction does not result from increased proteolysis. A second theory involves the loss of γ-crystallin from the lens by diffusion into the aqueous humor of the eye. This theory, however, has been thoroughly disputed and for the most part is presently ignored.

The decrease in the γ-crystallin from the soluble fraction corresponds to an increase in the HMW aggregates and the insoluble γ-crystallin component. This γ-crystallin decrease may also play a role in the sulfhydryl oxidation state of the lens; γ-crystallin contains the highest thiol content of any of the other crystallin components. This high cysteine content would play a pivotal role under conditions which would increase sulfhydryl reactivity, i.e. changes in tertiary structure or oxidative stress.

The non-enzymatic glycation of lens proteins is probably only one of several factors involved in cataract formation in diabetes. The ability of the lens to maintain a reducing environment is probably critical for cataract formation and can significantly affect the time of onset of cataract formation. High levels of glutathione maintains a reduced environment in the lens. In almost all forms of cataract the content of reduced glutathione significantly decreases before a mature cataract is formed, resulting in the loss of the reducing atmosphere within the lens. During the hyperglycemia of diabetes, the enzyme aldose reductase is believed to play a key role in the loss of reduced glutathione in the lens. Aldose reductase is a NADPH dependent enzyme which reduces glucose to sorbitol (a polyalcohol). High glucose levels result in the excess production of sorbitol thereby depleting the NADPH pool. This depletion of the NADPH compromises another NADPH dependent enzyme, glutathione reductase, which is responsible for glutathione regeneration and thus maintaining a reduced environment within the lens. The fact that aldose reductase inhibitors can retard but not prevent cataract formation suggest that these agents could retard the fall in glutathione levels. However, the demand for reduced glutathione is eventually so overwhelming

that protein aggregation occurs. Furthermore, the aldose reductase theory does not account for the observed tertiary structure changes associated with the increasing non-enzymatic glycation found in diabetic hyperglycemia. Secondly, data is accumulating that shows that the level of aldose reductase activity in the lens, especially human lenses and rat lenses, is not very high. Paradoxially, aldose reductase may provide some protection from the effects of non-enzymatic glycation by reducing a potential glycating sugar aldehyde (i.e. glucose, galactose, etc.) to the non-reactive polyalcohol, sorbitol.

In summary, the progressive changes within the lens occurring during diabetic hyperglycemia include linear increase in non-enzymatically glycated protein. This increase is greatest within the insoluble fraction. Also ocurring is a corresponding increase in disulfide content apparently resulting from tertiary structure modifications. Concurrent with these changes is a corresponding increase in both a soluble HMW aggregate and an insoluble HMW aggregate. These progressive changes are in agreement with the conjecture that non-enzymatic glycation leads to tertiary structure changes resulting in aggregation, insolubilization, and disulfide formation.

II. Glycation and the HMW Aggregates

A description of the progressive changes occurring in the diabetic lens during cataract development is an essential prelude to the study of diabetic cataracts. However, such terms as water-soluble, urea-soluble and HMW aggregates are vague and their nature must be elucidated to complete the picture of cataract formation. In addition, the glycation of the various components which comprise the soluble and insoluble

fractions as well as the corresponding HMW aggregates was studied to determine any correlation with the proposed mechanisms for cataractogenesis. As described in the methods section, sensitive HPLC methodologies were developed to separate the lens crystallins from the soluble and urea-soluble fractions. Also developed was an analytical C-4 reverse phase HPLC system which allowed one-step separation of the crystallin subunits. In the later system the low pH of the trifluoroacetic acid mobile phase dissociates the crystallins into their component subunits without the use of disaggregation compounds such as urea, SDS, or guanidine HCl. The system is similar to that developed in Schroeder's laboratory for the separation of the hemoglobin chains (109). Since these HPLC methodologies are relatively new, a great deal of effort was undertaken to assure the identity of each component. Initially, the identities of the molecular sieve peaks were determined by comparison to molecular weight standards followed by amino acid analysis and by comparisons of those established in the literature. Subsequently, C-4 reverse phase HPLC subunit peak identities were obtained by amino acid analysis followed by separation of purified crystallins. The results of the reverse phase separations of the crystallin subunits were in agreement with predictions made from amino acid composition. The purity of these subunits is questionable because no additional analysis was performed to determine their purity (i.e. isoelectric focusing or rechromatographing on another HPLC system). However, the results obtained by amino acid analysis are in excellent agreement with published values. The minor discrepancies in the amino acid composition of some of the subunits which were attributed to species differences as well as slight inaccuracies in my procedures. However, these minor differences did not interfere with the identification of the subunit peaks.

The lens fiber proteins (crystallins) exist in two major groups, those which are water-soluble and those that are water-insoluble. The latter have been referred to as the "albuminoid" fraction. "Albuminoid" is no longer considered a meaningful term, and is now preferable to refer to this as the "water-insoluble fraction." The water-insoluble protein has been of interest for many years especially because of the increased amounts found in cataract lenses. However, the exact nature of this fraction has been difficult to elucidate. Early work showed that the water-insoluble protein could be fractionated by treatment with a concentrated urea solution into a urea-soluble and urea-insoluble fraction. For a while it was assumed that urea-soluble protein isolated from lenses was derived from α-crystallin. The assumption was later invalidated when it was reported that the insoluble protein from rat lens and dogfish lens are closely similar to γ-crystallin (110), although later results showed that the insoluble fractions are composed of a mixture of all three groups of crystallins (111). The results of C-4 reverse phase HPLC separation of the urea-soluble fraction confirm this report as well as offer some insight as to changes occurring within this fraction in the cataract state (Figures 25 and 26).

The actual formation of the insoluble fraction appears to be a natural process as was shown by Folhost et al. with experiments showing 40% of labeled soluble proteins becoming incorporated into the insoluble fraction within seven weeks (73). Those proteins that are initially in the water-soluble fraction eventually become part of the insoluble fraction. However, there is no evidence of insoluble proteins reverting to the soluble fraction. Lens proteins are subject to a number of post-translational modifications such as deamidation, oxidation,

c-terminal degradation, and non-enzymatic glycation which could result in protein structural unfolding and the protein becoming water-insoluble. The process of insolubilization albeit a natural process may be accelerated or occur to excess in certain cataractous states. During diabetic hyperglycemia non-enzymatic glycation of the lens crystallins is dramatically increased over the normal lenses. In the diabetic cataract condition there is a considerable increase in several of the crystallin components within the insoluble fraction indicating an increased denaturation and insolubilization of these components. By comparison to the control insoluble fraction there is a significant increase in insolubilization of the γ-crystallin component as well as the β-crystallin primary βBp subunit. Interestingly, the γ-crystallin and the β-crystallins are high in thiol content, therefore denaturation of these components would increase the potential for disulfide cross-linking, a factor associated with cataract formation.

Lens protein denaturation and insolubilization by itself does not result in lens opacification. Rather the denatured lens proteins aggregate to form large (m.w. 2×10^6 daltons) disulfide-linked aggregate proteins which are believed to cause opacification in two ways. First, these high molecular weight (HMW) aggregates disrupt the higly ordered cytoarchitecture of the lens fibers which is essential for lens transparency. Secondly, the HMW aggregates are believed to be large enough to actually act as scatterpoints for light (9). It is currently believed that this HMW aggregate is formed by aggregation of soluble lens crystallins resulting in a soluble HMW precursor. This precursor aggregates further and forms disulfide crosslinkages resulting in the insoluble disulfide-linked HMW aggregate associated with cataracts. The

exact nature of this aggregate and its soluble precursor is relatively unknown. In the bovine lens the soluble precursor is composed primarly of α-crystallin; however, in the human lens and rat lens the components of the aggregates are still in debate. In the diabetic cataract lens the soluble HMW precursor is composed primarily of γ-crystallin with moderate amounts of α-crystallin held together by non-covalent crosslinkages. The addition of β-crystallins results in the insolubilization of the aggregate and the development of covalent disulfide crosslinkages (Figure 25). This finding is in agreement with the results obtained in the characterization of the diabetic insoluble fraction components in which the γ-crystallin and β-crystallins demonstrated the greatest increase within the insoluble fraction. Secondly, work done by Awasthi et al. showed that the initial aggregation of the crystallins occurs by a mechanism other than sulfhydryl crosslinking (88). These findings support the proposed theory of the soluble HMW precursor formation as well as the results of the characterization of the HMW aggregate components.

III. Characterization of the Non-enzymatic Glycation of Lens Proteins

Reduction of the aldimine and ketoamine linkages with tritiated sodium borohydride has been the primary measure of non-enzymatic glycation of proteins. This reduction results in one non-exchangable tritium molecule for each glycated residue. Borohydride reduction has been used for decades in organic and carbohydrate chemistry and has been a reliable tool for the analysis of carbohydrates. Spector has challenged the use of ^{3}H-$NaBH_4$ as a measure of glycation because of suspected side reactions. The incidental side reactions of borohydride reduction include cleavage of peptide bonds, reduction of indole groups of tryptophan, and

reduction of carboxyl groups. However, Bunn and coworkers (87) have described conditions which avoid these side reactions. These conditions were used in this study and provided a reliable tool for the study of non-enzymatic glycation. The results obtained by tritiated borohydride reduction were also in agreement with results obtained by affinity chromatographic procedures. This correlation supports the reliability of this reduction as a measure of non-enzymatic glycation.

As mentioned earlier, the extremely long life span of the lens proteins provides great opportunities for posttranslational modifications. Under normal conditions posttranslational events occur only to a small degree resulting in a minimal amount of insoluble protein. However, as the lens ages the modified proteins continue to accumulate resulting in protein denaturation and formation of more insoluble material. Within this insoluble fraction the HMW aggregates also accumulates in a linear fashion until a level is reached which sufficiently disrupts the lens architecture and cataracts develop. One such posttranslational modification which occurs during lens aging is non-enzymatic glycation. Stevens et al. (84) first provided evidence of this by the demonstration that within the soluble fraction, the soluble HMW aggregate from 4-year-old bovine lenses had the largest amount of glycation compared to the soluble crystallins. By the use of molecular sieve HPLC and tritium borohydride label this was extended to the diabetic cataract showing that both the soluble and insoluble HMW aggregates are heavily glycated (Figures 26 and 28). The theory of non-enzymatic glycation-dependent formation of these aggregates is supported by the finding that the most glycation found in the normal lens is found in the HMW aggregates. Furthermore, in both normal and diabetic lenses the specific activity of the HMW aggregates remains constant as compared to the normal lenses.

The consistent level of glycation of the HMW species indicates that perhaps those crystallins with the greatest amount of glycation contribute to HMW aggregate formation more readily. Similarly, intermediate levels of glycation or perhaps non-critical sites of glycation merely leads to the lens proteins becoming water-insoluble but not yet forming the HMW aggregate responsible for cataracts.

This conjecture is supported by the finding that the components which comprise the HMW aggregates contain a large amount of glycated residues (Figure 30). Secondly, those components which show the greatest increases in glycation during the diabetic hyperglycemia demonstrate the greatest increases within the insoluble fraction (Figure 29). These same components are also the ones which compose the HMW aggregates. This aggregation is then stabilized by covalent disulfide linkages which results in the formation of the insoluble HMW aggregate associated with cataracts. The results of my experiments support and extend this conjecture to the following sequence of events: Initially, glycation of the γ-crystallin and α-crystallin lead to their forming the soluble HMW aggregates (Fig. 30A). This aggregate is held together by non-covalent bonds and is not yet large enough to become insoluble. As the glycation process continues and with the addition of glycated β-crystallin the aggregate increases in size to become insoluble. Subsequent disulfide crosslinking results in the characteristic disulfide linked HMW aggregate responsible for the opacities of cataracts. This hypothesis is supported by several findings by other researchers. First, Bloemendal et al. has found that under certain conditions γ-crystallin can form aggregates with α-crystallin (112). Secondly, the high thiol content of β-crystallin and γ-crystallin allow for the formation of covalent crosslinking when the β-crystallin becomes incorporated into the aggregate.

The final characterization of non-enzymatic glycation of the lens proteins by localizing the sites of glycation within the HMW constituent polypeptides involved in a combination of techniques. Recently, cataract research has focused upon the formation of the insoluble HMW aggregate, therefore this protein was chosen as the focus for this final characterization. Shapiro et al. first located the glycated residues of glycated hemoglobin by enzymatic digestion of glycated hemoglobin followed by cation exchange chromatography and amino acid analysis (113). However, this method involved extremely large quantities of protein and was not suitable for quantifying the glycated residues in the lens crystallins. This problem was circumvented by the use of the newly developed glycoaffinity gel and Affigel 601. The phenylboronate-acrylamide gel (Affigel 601) has a higher ligand concentration than the affinity gels used to quantify the glycoprotein levels and is thereby suitable to selectively bind glycated-amino acids and small glycated polypeptides obtained by enzymatic digestion.

Enzymatic digest of trypsin and chymotrypsin were used for two primary reasons: First, to provide overlapping peptides to ensure accurate location of the glycated residue. Secondly, trypsin may not cleave at a glycated lysine residue therefore the possibility existed for multiple glycated lysines within a single polypeptide. Chymotryptic digestion would be relatively unaffected by glycated lysines and would provide potentially deciding information in case of equivocable results obtained by the tryptic digest. However, multiple glycated residues within a single polypeptide did not prove to be a problem since for the most part the amino acid sequences of the lens crystallins have alternating arginine and lysine residues. For those sequences with two or more lysine residues (α-crystallin) the chymotryptic digestion provided

segments with single glycated lysine residues which were used to confirm the location of the glycated residues.

This study not only located the sites of glycation, but also allowed quantification of the modified residues present in the HMW aggregate. As expected, the γ-crystallin residues represent the majority of the glycated residues as measured by tritium incorporation. Secondly, the γ-crystallin has only three potential sites for glycation of which all are found to be glycated. By contrast, the β-crystallin has thirteen lysine residues and only seven glycation sites. Similarly, the α-crystallin A and B subunits have seven and ten lysines, respectively, of which only five lysines are glycated within the A subunit and four in the B subunit. Lastly, as mentioned earlier, there is a great deal of sequence homology between the three crystallin classes. Therefore, it was not surprising to see that most of the glycated lysines were located at relatively similar regions within the different crystallin subunits (Fig. 37). This is indicative of a somewhat specific pattern of glycation with some residues reactive to glycation while other are not. This specificity may result from the location of the lysine residues within the tertiary structure of the protein molecule. Lysines exposed on the outside of the protein would be more susceptible to glycation than those within the interior of the protein due to steric hindrances. Another possible contributing factor is the pK of the ε-amino group of lysine. The presence of an acidic residue near the ε-amino group of lysine within the tertiary structure will lower the apparent pK of the lysine (115). This lower pK would be more favorable to glycation. This concept is represented by glycation of hemoglobin and albumin where hemoglobin in βLys-66 and αLys-61, and serum albumin Lys-523 are the principle lysine residues modified (114).

SUMMARY

Because of their remarkable longevity, lens crystallins undergo a substantial amount of non-enzymatic glycation during diabetic hyperglycemia. These posttranslational modifications have the potential to disrupt the structural and functional properties of the lens crystallins and contribute to the formation of cataracts.

Streptozotocin induced diabetic rats were used to study the relationship between glycation of lens proteins and the formation of insoluble high molecular weight (HMW) aggregates believed to be responsible for cataract formation. After the onset of diabetes, cataracts developed in about 12 to 13 weeks. Five control and five diabetic rats were sacrificed every three weeks and lenses removed. Levels of glycated protein and glycated amino acids in lenses from each animal were examined by affinity chromatography. In addition, the changes in crystallin composition and development of HMW aggregates were monitored by sensitive HPLC techniques. The animals were followed in this manner until cataracts developed (105 days) and for an additional 63 days. Secondly, the non-enzymatic glycation of both the soluble and insoluble lens proteins was characterized in control and diabetic cataract lenses. This characterization included identification of the protein components of the insoluble fraction as well as their level of glycation. Lastly, the crystallin components which comprise the HMW aggregate were identified and the extent of glycation was determined. The characterization of the glycation of the HMW components was extended to locating the actual sites of glycation within the crystallin polypeptide sequence.

As diabetic hyperglycemia continues there is a linear increase in glycated protein in both the soluble and insoluble fractions. This

increase is paralleled by an increase in the soluble HMW and insoluble HMW aggregates. Other changes include a decrease in reactive sulfhydryls which indicates an increase in disulfide bond formation. Within the soluble fraction there was a steady decrease in the γ-crystallin component as well as a consistent increase in the insoluble γ-crystallin. Characterization of the soluble HMW aggregate and the insoluble HMW aggregate revealed that they are composed primarily of γ-crystallin with a small amount of α-crystallin. In addition, the insoluble HMW aggregate contains a moderate amount of β-crystallin subunits. Further analysis demonstrated that these HMW components are also heavily glycated. Secondly, the components of the insoluble fraction from both control and diabetic cataract lenses were all glycated more extensively than their soluble counterparts with insoluble γ-crystallin showing the most glycation.

This study has demonstrated that as diabetic hyperglycemia continues there is a relationship between the increasing levels of glycated proteins and the formation of HMW aggregates. This relationship also extends to the increased glycation of those components which comprise the HMW aggregates. There appears to be a causal relationship between glycation of lens crystallins and their unfolding. As this glycation increases, so does the protein denaturation and eventually aggregation to form large insoluble protein aggregates responsible for cataracts.

BIBLIOGRAPHY

1. West, K. M. (1978) The Epidemiology of Diabetes, p. 94, Elsevier Press, New York.
2. Gottschalk, A. (1972) Glycoproteins, Part A, pp. 141-157, Elsevier Press, New York.
3. Bloemendal, H. (1981) In: Molecular and Cellular Biology of the Eye Lens (Bloemendal, H., ed.), pp. 1-47, Wiley and Sons, New York.
4. de Jong, W. W., van Kleef, F. S., and Bloemendal, H. (1974) Intracellular carboxy terminal degradation of the A chain of α-crystallin. Eur. J. Biochem. 48: 271-276.
5. Van Venrooij, W. J., de Jong, W. W., Janssen, A., and Bloemendal, H. (1974) In vitro formation of αA_1 from αA_2 chains of α-crystallin. Exp. Eye Res. 19: 157.
6. Borkman, R. F., and Lerman, S. (1977) Evidence for a free radical mechanism in aging and U.V. irradiated ocular lenses. Exp. Eye Res. 25: 303-309.
7. Masters, P. M., Bada, J. L., and Zigler, J. S. Jr. (1978) Aspartic acid racemization in heavy molecular weight crystallins and water-soluble protein from normal human lenses and cataract. Proc. Natl. Acad. Sci., USA 75: 1204-208.
8. Stevens, V. J., Rouzer, C. A., Monnier, V. M., and Cerami, A. (1978) Diabetic cataract formation: Potential role of glycosylation of lens crystallins. Proc. Natl. Acad. Sci., USA 75: 2918-2922.
9. Benedek, G. B. (1971) Theory of transparency of the eye. Appl. Optics 10: 459-473.
10. Kozak, G. P. (1979) Why treat diabetes? In: Individualizing Therapy in Maturity Onset Diabetes (Levine, R., ed.), New York Science and Medicine Publishing Co., Inc.

11. Kohner, E. M., Fraser, T. R., Joplin, G. F., Dollery, C. T., and Henkind, P. (1968) The effect of diabetic control on diabetic retinopathy. in Treatment of Diabetic Retinopathy (PHS Publication #1890) (Goldberg, M. F. and Fine, S. L., eds.), pp. 119-128, Washington D.C., U.S. Government Printing Office.

12. West, K. M. (1978) Epidimiology of Diabetes and Its Vascular Lesions, Chap. 6, pp. 45-82, Elsevier, New York.

13. Spiro, R. G. (1973) Biochemistry of the renal glomerular basement membrane and its alterations in diabetes mellitus. N. Engl. J. Med. 288: 1337.

14. Moorhouse, J. A. (1976) Diabetes Mellitis (Fajans, S. S., ed.), pp. 243-255, National Institutes of Health, Bethesda, Md.

15. Grave, G. D. (ed.) (1979) Early Detection of Potential Diabetes: The Problems and the Promise. Raven Press, New York.

16. Spiro, R. G. (1973) Biochemistry of the renal glomerular basement membrane and its alterations in diabetes mellitus. N. Engl. J. Med. 288: 1337.

17. Adcock, L. H., and Gray, C. H. (1957) The metabolism of sorbitol in the human subject. Biochem. J. 65: 554.

18. Gabbay, K. H., and O'Sullivan, J. B. (1968) The sorbitol pathway, enzyme localization and content in normal and diabetic nerve and cord. Diabetes 17: 239.

19. Weingrad, H., and Clements, R. S. (1979) Diabetic neuropathy - new concepts of its etiology. Diabetes 28: 604.

20. Gabbay, K. H. (1973) The sorbitol pathway and the complications of diabetes. N. Engl. J. Med. 16: 831-836.

21. Kinoshita, J. H., Dvornik, D., and Kraml, M. (1968) The effect of an aldose reductase inhibitor. Biochim. Biophys. Acta 158: 472.

22. Takazajura, E., Nakamoto, Y., and Hayakawa, H. (1975) Onset and progression of diabetic glomerulosclerosis: A prospective study based on serial renal biopsies. Diabetes 24: 1.

23. Bloodworth, J. M. B., Engerman, R. L., and Powers, K. L. (1969) Experimental diabetic microangiopathy: 1. Basement membrane statistics in the dog. Diabetes 18: 455.

24. Spiro, R. G. (1969) Glycoproteins: Their biochemistry, biology, and role in human disease. N. Engl. J. Med. 281: 991, 1969.

25. Abraham, E. C. (1985) Glycosylated Hemoglobins. Marcel Dekker, Inc., New York.

26. Koenig, R. J., Peterson, C. M., Kilo, C., Cerami, A., and Williamson, J. R. (1976) Hemoglobin A_{Ic} as indicator of the degree of glucose intolerance in diabetes. Diabetes 25: 230.

27. Peterson, C. M., and Jones, R. L. (1977) Minor hemoglobins, diabetic "control," and diseases of postsynthetic protein modification. Ann. Intern. Med. 87: 489.

28. Bunn, H. F., and Brieht, R. W. (1970) Nonenzymatic glycosylation of Hb A_{Ic} and its effect on 2,3-DPG binding. J. Clin. Invest. 49: 1088-1095.

29. Koenig, R. J., and Cerami, A. (1975) Synthesis of hemoglobin A_{Ic} in normal and diabetic mice: Potential model of basement membrane thickening. Proc. Natl. Acad. Sci., USA 72: 3687-3691.

30. Sasaki, J., Arora, V., and Cottam, G. L. (1982) Nonenzymatic glycosylation of human LDL decreases its metabolism by human skin fibroblasts. Biochem. Biophys. Res. Comm. 108: 791-796.

31. Witztum, J. L., Fisher, M., Pietro, T., Steinbrecher, U. P., and Elam, R. L. (1982) Nonenzymatic glycosylation of high-density lipoproteins accelerates its cataolism in guinea pigs. Diabetes 31: 1029-1032.

32. Witztum, J. L., Mahoney, M., Branks, M. J., Fisher, M., Elam, R. L., and Steinberg, D. (1982) Nonenzymatic glucosylation of low-density lipoprotein alters its biologic activity. Diabetes 31: 283-291.

33. Vlassara, H., Brownlee, M., and Cerami, A. (1981) Nonenzymatic glycosylation of peripheral nerve protein in diabetes millitus. Proc. Natl. Acad. Sci., USA 78: 5190-5192.

34. Bell, E. T. (1972) Renal lesions in diabetes mellitus. Am. J. Med. Pathol. 18: 744.

35. Scarborough, N. L., and Carrier, G. O. (1983) Increased contractile response of aortas from diabetic rats to alpha-2 adrenergic receptor stimulation. Proc. Soc. Exp. Biol. Med. 172: 127.

36. Jose, J. G. (1970) The lens. In: Biochemistry of the Eye (Anderson, R. E., ed.), Academic Press, New York.

37. Young, R. W., and Ocumpaugh, D. E. (1960) Autoradiographic studies on growth and development of lens capsules in rat. Invest. Ophthalmol. 5: 583.

38. Peczon, B. D., Peczon, J. D., Cintron, C., and Hudson, B. G. (1980) Changes in chemical composition of anterior lens capsules of cataractous human eye as a function of age. Exp. Eye Rs. 30: 155-165.

39. Dische, Z., Zelmanis, G., and Rothschild, C. (1967) The hexosaminohexuronide of the bovine lens capsule. Arch. Biochem. Biophys. 721: 685-694.

40. Kuwabara, T. (1975) The maturation of the lens cell: A morphologic study. Exp. Eye Res. 20: 427-443.

41. Bloemendal, H. (1982) Lens proteins. CRC Critical Reviews in Biochemistry 82: 1-38.

42. Chylack, L. T. Jr. (1980) The crystallin lens: An overview. In: Red Blood Cell and Lens Metabolism (Srivastava, S. K., ed.), Elsevier Press, New York.

43. Kuck, J. F. (1970) In: Biochemistry of the Eye (Graymore, C. N., ed.), pp. 203-21, Academic Press, New York.

44. Chylack, L. T. Jr. (1975) Mechanism of 'hypoglycemic' cataract formation in the rat lens. I. The role of hexokinase instability. Invest. Ophthalmol. 14: 746-755.

45. Hockwin, O., Blum, G., Korte, I., Murata, T., Radetzki, W., and Rast, F. (1971) Studies on the citric acid cycle and its portion of glucose breakdown by calf and bovine lenses in vitro. Ophthalmic Res. 2: 143-148.

46. Korte, I., and Hockwin, O. (1972) Studies on the citric acid cycle and its portion of glucose breakdown by calf and bovine lenses in vitro. Ophthalmic Res. 3: 13.

47. Kuck, J. F. (1962) Glucose and fructose synthesis in the diabetic rat lens. Invest. Ophthalmol. 1: 390-395.

48. Bindels, J. G., Siezen, R. J., and Hoenders, J. J. (1979) A model for the architecture of α-crystallin. Ophthalmic Res. 11: 441-452.

49. Carlisle, C. H., Lindley, P. F., Moss, D. S., and Slingsby, C. (1977) Preliminary bovine lens proteins, γ-crystallin fraction II. J. Mol. Biol. 110: 417-419.

50. Chirgadze, Y. N., Nikonov, S. V., Garber, M. D., and Reshetnikova, L. S. (1977) Crystallographic study of γ-crystallins from calf lens. J. Mol. Biol. 110: 619-624.

51. De Jong, W. W., Van der Ouderaa, J., Versteeg, M., Groenewood, G., van Amelsvoort, J. M., and Bloemendal, H. (1975) Primary structure of the alpha crystallin A chains of seven mammalian species. Eur. J. Biochem. 53: 237-242.

52. Schoenmakers, J. J. G., and Bloemendal, H. (1968) Subunits of α-crystallin from adult and embryonic cattle lens. Nature (Lond.) 220: 790.

53. Delacour, J., and Papaconstinou, J. (1970) A change in α-crystallin subunit composition in relation to cellular differentiation in adult bovine lens. Biochem. Biophys. Res. Comm. 41: 401-406.

54. Siezen, R. J., and Hoenders, H. J. (1979) The quaternary structure of bovine α-crystallin. Surface probing by limited proteolysis in vitro. Eur. J. Biochem. 96: 431.

55. Francois, J., and Rabaey, M. (1959) Agar microelectrophoresis at high tension of soluble lens proteins. Arch. Ophthalmol. 61: 351-360.

56. Bloemendal, H., and Herbink, P. (1974) Growing insight into the structure of β-crystallin. A review. Ophthalmol. Res. 6: 81.

57. Herbink, P., and Bloemendal, H. (1974) Studies on β-crystallin. I. Isolation and partial characterization of the principle polypeptide chain. Biochim. Biophys. Acta 336: 370.

58. Zigler, J. S., and Sidbury, J. B. Jr. (1976) A comparative study of β-crystallin from six mammals. Comp. Biochem. Physiol. 53: 349-355.

59. Driessen, H. P. C., Herbink, P., Bloemendal, H., and de Jong, W. W. (1981) The β-crystallin Bp chain is internally duplicated and homologous with γ-crystallin. Exp. Eye Res. 31: 243.

60. Zigler, J. S. Jr., and Sidbury, J. B. Jr. (1973) Structure of calf lens β-crystallins. Exp. Eye Res. 16: 207.

61. Bjork, I. (1961) Studies on γ-crystallin from calf lens. I. Isolation by gel filtration. Exp. Eye Res. 1: 145-154.

62. Croft, L. R. (1972) The amino acid sequence of γ-crystallin (fraction II) from calf lens. Biochem. 128: 961-970.

63. McAvoy, J. W. (1978) Cell division, cell elongation and distribution of α-, β-, and γ-crystallins in the rat lens. J. Embryol. Exp. Morph. 44: 149-165.

64. Lerman, S., and Zigman, S. (1967) Metabolic studies on the cold precipitable protein of the lens. Acta Ophthalmol. 45: 193-198.

65. Spector, A., Li, L. K., Augusteyn, R. C., Schneider, A., and Freund, T. (1971) α-Crystallin. The isolation and characterization of distinct macromolecular fractions. Biochem. J. 124: 337.

66. Harding, J. J., and Dilley, K. J. (1976) Structural proteins of the mammalian lens: A review with emphasis on changes in development, aging, and cataract. Exp. Eye Res. 22: 1.

67. Barber, W. (1973) Human cataractogenesis: A review. Exp. Eye Res. 16: 85.

68. van Kamp, G. J., Schats, L. H. M., and Hoenders, H. J. (1973) Caracteristics of α-crystallins related to fiber cell development in calf lenses. Biochim. Biophys. Acta 295: 166-173.

69. Morner, C. T. (1894) Untersuchung der proteinsubstanten in den leichtbrechenden medien des auges. Z. Physiol. Chem. 18: 61-106.

70. Dische, Z. (1965) The glycoproteins and glycolipoproteins of the bovine lens and their relation to albuminoid. Invest. Ophthalmol. 4: 759-778.

71. Harding, J. J. (1972a) The nature and origin of the urea-insoluble protein of human lens. Exp. Eye Res. 13: 33-40.

72. Jedziniak, J. A., Kinoshita, J. H., Yates, E. M., Hocker, L. O., and Benedek, G. B. (1973) On the presence and mechanism of formation of heavy molecular weight aggregates in human normal and cataractous lenses. Exp. Eye Res. 15: 185-192.

73. Fulhorst, H. W., and Young, R. (1966) Conversion of soluble lens protein to albuminoid. Invest. Ophthalmol. 5: 298-303.

74. Kibbelaar, M. A., Ramaekers, F. C. S., Ringens, P. J., Selten-Versteegen, A.M.E., Poels, L. G., Jap, P.H.K., van Rassum, A. L., Feltkamp, T.E.W, and Bloemendal, H. (1980) Is actin in eye lens a possible factor in visual accommodation? Nature 285: 506-508.

75. Anderson, E. I., and Spector, A. (1978) The state of sulfhydryl groups in normal and cataractous human lens proteins. I. Nuclear region. Exp. Eye Res. 26: 407-417.

76. Spector, A., and Debdutta, R. (1978) Disulfide-linked high molecular weight protein associated with human cataract. Proc. Natl. Acad. Sci., USA 75: 3244.

77. Roy, D., and Spector, A. (1976) High molecular weight protein from human lenses. Exp. Eye Res. 22: 273.

78. Itoh, R., Ozaki, Y., Mizuno, A., and Iriyama, K. (1983) Structural changes in the lens proteins of hereditary cataracts monitored by Raman spectroscopy. Biochemistry 22: 1773.

79. Hockwin, O., and Koch, H. R. (1975) In: Cataract and Abnormalities of the Lens (Bellows, J. G., ed.), pp. 243-254, Grune & Stratton, New York.

80. Ohrloff, C., Holstege, A., and Hockwin, O. (1976) Enzymes involved in the glycogen metabolism of the lens in relation to age, topographic distribution and association with water-soluble proteins. Ophthalmic Res. 8: 227-232.

81. Zigman, S., and Vaughn, T. (1974) Near UV light effects on the lenses and retinas of mice. Invest. Ophthalmol. 13: 462-464.

82. Zigman, S., Datiles, M., and Torczynski, E. (1979) Sunlight and human cataracts. Invest. Ophthalmol. 18: 462-467.

83. Flückiger, R., and Winterhalter, K. H. (1978) Glycosylated hemoglobins. In: Biochemical and Clinical Aspects of Hemoglobin Abnormalities (Caughey, W. S., ed.), pp. 205-214, Academic Press, New York.

84. Stevens, V. J., Rouzer, C. A., Monnier, V. M., and Cerami, A. (1978) Diabetic cataract fromation: role of glycosylation of lens crystallins. Proc. Natl. Acad. Sci., USA 75: 2918.

85. Spector, A., and Zorn, M. (1967) Studies upon the sulfhydryl groups of calf lens α-crystallins. J. Biol. Chem. 242: 3594-3600.

86. Monnier, V. M., Stevens, V. J., and Cerami, A. (1979) Nonenzymatic glycosylation, sulfhydryl oxidation and aggregation of lens protein in experimental sugar cataracts. J. Exp. Med. 50: 1098-1107.

87. Chiou, S. H., Chylack, L. T., Tung, W. H., and Bunn, H. F. (1981) Nonenzymatic glucosylation of bovine lens crystallins. J. Biol. Chem. 256: 5176-5180.

88. Awasthi, Y. C., Ansari, N. H., and Srivastava, S. K. (1980) Glycosylation of the lens crystallins in cataractogenesis. In: Red Blood Cell and Lens Metabolism (Srivastava, S. K., ed.), Elsevier Press, New York.

89. Ansari, N. H., Awasthi, Y. L., and Srivastava, S. K. (1980) Role of glycosylation in protein disulfide formation and cataractogenesis. Exp. Eye Res. 31: 9-19.

90. Liang, J. N., and Chikrabarti, B. (1981) Glycosylation-induced structural changes in bovine lens crystallins. Invest. Ophthalmol. 20 (Supp.): 129.

91. Pande, A., Garner, W. H., and Spector, A. (1979) Glycosylation of human lens protein and cataractogenesis. Biochem. Biophys. Res. Comm. 89: 1260-1266.

92. Monnier, V., and Cerami, A. (1982) Nonenzymatic glycosylation and browning in diabetes and aging: Studies on lens proteins. Diabetes 31: 58.

93. Gopolakrishna, K., Srinivasa Rao, P. N., Ramakrishna, B., and Pattabiraman, T. N. (1983) Nonenzymatic glycosylation of lens proteins in different types of cataracts. Indian J. Med. Res. 78: 426.

94. Kasai, K., Nakamura, T., Kase, N., Hiraoka, T., Suzuki, R., Kogure, F., and Shimoda, S. I. (1983) Increased glycosylation of proteins from cataractous lenses in diabetes. Diabetologia 25: 36-38.

95. Lee, J. H., Shin, D. H., Lupovitek, A., and Shi, D. X. (1984) Glycosylation of lens proteins in senile cataract and diabetes mellitus. Biochem. Biophys. Res. Comm. 123: 888.

96. Garlick, R. L., Mazer, J. S., Chylack, L. T., Jr., Tung, W. H., and Bunn, H. F. (1984) Nonenzymatic glycation of human lens crystallins. J. Clin. Invest. 74: 1742.

97. Isolab Inc., Drawer 4350, Akron, Ohil, 44321.

98. Heinrikson, R., Heinrikson, R. L., and Meridith, S. C. (1984) Amino acid analysis by pre-column derivitization by PITC. Anal. Biochem. 136: 65.

99. Moore, S., and Stein, W. H. (1949) Photometric ninhydrin method for use in the chromatography of amino acids. J. Biol. Chem. 176: 367.

100. Raabo, E., and Terkildsen, T. C. (1960) In the enzymatic determination of blood glucose. Scand. J. Clin. Lab. Invest. 12: 402.

101. Bradford, M. (1976) Anal. Biochem. 72: 248.

102. Lowry, O. H., Rosebrough, N. J., Farr, A. L., and Randall, R. J. (1951) Protein measurement with the foline phenol reagent. J. Biol. Chem. 193: 265.

103. Boyer, P. D. (1957) Meth. Enzymol. XXV: 388.

104. Rosenquist, T. Personal communication.

105. Kern, H. L., Belhorn, R. W., and Peterson, C. M. (1976) Sodium cyanate-induced ocular lesions in the beagle. J. Pharmacol. Exp. Ther. 195: 333.

106. Pirie, A. (1968) Color and solubility of the proteins of human cataracts. Invest. Ophthalmol. 7: 634.

107. Auricchio, G., and Testa, M. (1972) Ophthalmology 164: 228.

108. Harding, J. J. (1972c) Conformational changes in human lens proteins in cataract. Biochem. J. 129: 97-100.

109. Shelton, J. B., Shelton, R. J., and Schroeder, W. A. (1984) High performance liquid chromatographic separation of globin chains in a large pore C-4 column. J. Liquid Chrom. 7: 1969.

110. Lerman, S., Zigman, S., and Forbes, W. F. (1968) Insoluble protein fraction of the lens. Exp. Eye Res. 7: 444-448.

111. Harding, J. J. (1969) The nature and origin of the insoluble protein of rat lens. Exp. Eye Res. 8: 147-156.

112. Bloemendal, H., Zweers, A., Benedetti, E. L., and Walters, H. (1975) Selective reassociation of the crystallins. Exp. Eye Res. 20: 463-478.

113. Shapiro, R., McManus, M. J., Zalut, C., and Bunn, H. F. (1980) Sites of nonenzymatic glycosylation of human hemoglobin A. J. Biol. Chem. 255: 3120-3127.

114. Garlick, R. L., and Mazer, J. S. (1983) The principal site of nonenzymatic glycosylation of human serum albumin in vivo. J. Biol. Chem. 258: 6142.

115. Dickerson, R. E. and Geis (1969) The Structure and Action of Proteins. Harper & Row, New York.

116. Perry, R. E. and Abraham, E. C. (1986) High performance liquid chromatographic separation of lens crystallins and their subunits. J. Chromatog. 351: 103.

117. Rasch, R. (1979) Conrol of blood glucose levels in the streptozotocin diabetic rat using long-acting heart-treated insulin. Diabetologia 16: 185.

118. Mallia, A. K., Hermanson, G. T., Krohn, R. J., Fujimoto, E. K., and Smith, P. K. (1981) Preparation and use of a boronic acid affinity support for separation and quantitation of glycosylated hemoglobins. Anal. Lett. 14: 649.

119. Brownlee, M., Vlassara, H., and Cerami, A. (1980) Measurement of glycosylated amino acids and peptides from urine of diabetic patients using affinity chromatography. Diabetes 29: 1044.

120. Allen, G. (1981) Sequencing of Proteins and Peptides, Chapter 3, pp. 53-59, Elsevier, New York.

121. Kato, Y., Komiya, K., Sasaki, H., and Hashimoto, T. (1980) Separation range and separation efficiency in high speed gel filtration on TSK-gel SW columns. J. Chromatog. 190: 297.

122. Schroeder, W. A., Shelton, J. B., and Shelton, J. R. (1980) Separation of hemoglobin peptides by high performance liquid chromatography (HPLC). Hemoglobin 4: 551.